UNIVERSITY OF EDINBURGH

THE CHEMICAL EFFECTS OF ULTRASONIC WAVES

by

WILLIAM A. J. BRYCE, A.H.-W.C., A.R.I.C.

THESIS

submitted for the degree of

DOCTOR OF PHILOSOPHY.

October, 1958.

Preface

I wish to thank Dr. C. T. Greenwood and Dr. D. Taylor for their unfailing help and encouragement during the period of this research. Some of the results in section 5 have already been published in conjunction with Dr. C. T. Greenwood and reprints are inserted at the end of the thesis.

I wish to thank Professors E. L. Hirst and J. P. Kendall for the provision of equipment and laboratory facilities.

I would also like to thank Dr. J. M. G. Cowie for his collaboration in certain aspects of this work.

The University Chemistry Department,
The King's Buildings,
Edinburgh, 9.

CONTENTS

INTRODUCTION.

Certain types of high polymer molecules are frequently susceptible to degradation by purely mechanical forces. In the solid state, degradation may occur on milling or grinding, whilst in solution, the polymer may be degraded by shearing forces during ultrasonic irradiation (1), shaking (2), high speed stirring (3), beating (4), or turbulent flow through a capillary (5). Of the above methods, ultrasonic irradiation is one in which a number of the variables can be satisfactorily controlled.

If a polymer has a mechanically weak link then this will break preferentially. By employing any of the above methods therefore it should be possible to determine whether a certain polymer (susceptible to degradation) has a weak link in its chain.

Some of the naturally-occurring polymers (starch (1), dextran (2) or their derivatives (cellulose nitrate (7)) have been degraded by ultrasonic irradiation. In the case of starch, the action of ultrasonic irradiation on its components has not been studied previously.

A complete treatment of the kinetics of degradation has

For definition see page 22

two aspects. (1) a determination of the distribution of chain lengths in the reaction mixture at different stages: and (2) an investigation of the change of the physical properties of the system (e.g. number and weight average molecular weight, hydrodynamic behaviour) with time.

In this thesis, the components of starch (amylose and amylopectin) and glycogen have been subjected to ultrasonic irradiation. In order to investigate whether there were any mechanically-weak bonds in these polymers, rates of degradation have been studied by following changes in molecular weight distribution, in number and weight average molecular weights, and in hydrodynamic behaviour.

SECTION I

Theory

1. ULTRASONICS.

Ultrasonic waves produce physical, chemical and biological changes. Although the mechanism by which these changes occur has not been fully explained, much relevant information has been obtained.

Most of the investigations have been in liquid media and among the reported chemical effects of intense ultrasonic irradiation are reactions of hydrolysis, addition, oxidation, polymerization, degradation of polymers and molecular rearrangement.

Hydrogen peroxide, nitrous and nitric oxide are produced slowly by irradiation of water containing dissolved air (8-11), if carbon tetrachloride is present then free chlorine is generated. Alkyl and aryl halides in aqueous suspension are hydrolysed (12-14) to produce a halide ion presumably the corresponding hydroxyl compound or ether. Esters such as dimethyl sulphate are hydrolysed five times faster in the presence of ultrasound than in its absence(15.16).

o-,p-,and m-hydroxy benzoic acid are obtained on irradiating a solution of benzoic acid (11).

The hydration of acetylene to acetaldehyde is accelerated by ultrasonic waves (17), as is the addition of oxygen to the olefinic linkage of oleic acid and certain oils (16).

If one of the products of a reaction is a gas then the acceleration due to ultrasonic waves may be large. Examples of this are the evolution of nitrogen from the decomposition of benzazide (18, 19), diazobenzene and diazotoluene chlorides (20); and also the decomposition of potassium persulphate (21).

Ultrasonic waves of sufficient intensity kill and then disintegrate a great variety of cells including protozoa, yeast, erythrocytis, green algae and bacteria such as E. coli. Viruses such as cowpox, poliomyelitis, and staphylococcus-bacteriophage have their infectivity destroyed in some cases. In a recent study on bacteriophages, morphology was found to be a determining factor: those strains which are small spheres were resistant, but the large viruses with complex structures were inactivated by ultrasonic waves (22).

Polymerization by ultrasound has been studied in the cases of carbon suboxide (23) and emulsions of styrene and styrene-butadiene in water (24). Ultrasonic degradation of polymers in solution is also well known (25), e.g. polystyrene (26-30), polvinyl acetate polyacrylates, nitrocellulose (31), proteins (23), starch, agar, gelatin and gum arabic (1.32-34).

Cavitation.

Practically all of the observed effects of ultrasonics in liquid systems have been attributed to cavitation, which is the formation and violent collapse of small bubbles or cavities in the liquid as a result of pressure changes (35-38).

For the full development of cavitation by ultrasonic energy it is necessary to fulfil certain initial and subsequent conditions (39). The liquid conditions and the three phases of cavitation are (1) the preinitiation condition of the liquid, (2) the initiation phase of cavitation, (3) the catastrophic phase of cavitation, (4) the bubble phase of cavitation.

The precondition of the liquid determines whether the initiation phase can take place. The initiation phase must reach completion before the catastrophic phase can start. Both the initiation and catastrophic phase are fundamental and are common to aerated and degassed water. The bubble phase is only produced in aerated water. The three phases of cavitation are produced within a combined interval of several milliseconds.

The mechanism of this cavitation phenomena is as follows:- (1) The preinitiation condition required the presence in the water of weak spots, or nuclei . The strength of these nuclei must be small compared to the strength of the water itself since the energy available from ultrasonically induced tensions are far below the theoretical level required to rupture the water material.

Regarding the actual nature of these nuclei or weak spots and their effect on cavitation, much has been written in the literature (35.40.41). It is believed that the strengths of the

nuclei have a wide but not necessarily continuous distribution and that the weaker (or larger) nuclei are fewer in number than the stronger (or smaller) nuclei. Many different models have been proposed to explain the initiation of the various phenomena (boiling, freezing and crystallisation) dependent on nucleation. That the nuclei are simple spherical cavities can be ruled out because if the cavities were empty, they would collapse. If furthermore the spherical cavities were stabilised by a gas-content under pressure such as to overcome the surface tension trying to collapse them, then the gas-content would soon decrease due to diffusion into the surrounding liquid which is saturated with the gas at only one atmosphere and hence the cavity would collapse. The above explanation does not hold for gas trapped in pores or faults in solid-liquid interfaces as surface tension cannot compress the gas trapped in a pore or fault. In opening up such pockets of gas by tension in the liquid, surface tension forces only gradually increase to oppose the expansion. Thus, gas entrapped on very small solid particles may serve as nuclei for cavitation. However, Fox and Herzfeld (42) have put forward the hypothesis that the nuclei are very small bubbles, stabilised by an organic "skin", which mechanically prevents loss of gas by diffusion. The cavitation occurs when the skin breaks and the cavitation threshold is determined by the breaking strength of the film and the size of the bubble.

The initiation phase may be started whenever a sufficiently weak nucleus enters the high intensity area of the ultrasonic field. Thus as a single nucleus approaches the maxima, its volume oscillates with the sonic frequency and gradually but continuously grows larger. If the slowly growing cavity reaches its resonant size, then the second or catastrophic phase begins. If however due to turbulence in the liquid the oscillating cavity streams out of the above region then it will again collapse and produce no further effect.

The catastrophic phase will not develop unless and until the initiation phase has reached completion. This occurs when the growing vibrating cavity of the initiation phase reaches the size at which it is resonant with the ultrasonic frequency. At this size the cavity quite suddenly begins to vibrate with immensely increased amplitude, growing large and collapsing and rebounding in time with the tension and compression of the ultrasonic field. The above vibrating cavity cannot collapse to zero volume because of its small but definite gas content. This violent vibration of the cavity now radiates periodic shock waves of an amplitude largely exceeding the amplitude of the driving sonic waves. It is the new periodically radiated spherical shock wave which makes this second phase of the cavitation burst catastrophic. These shock waves (combined with the already pre-

sent ultrasonic waves) are of sufficient magnitude to open up myriads of microcavities in the very nearby water volume, this rupture may be of unnucleated water. As long as the cavity is in the high intensity region the shock waves are produced and hence the microcavities also. This continues until the vibrating cavity passes out of the high intensity region.

The bubble phase only occurs in aerated systems (39) and only after the catastrophic phase has reached completion (shock wave emission). Only a relatively few bubbles are generated during a cavitation burst. Just why this violently vibrating cavity can generate only a few noncollapsing gas bubbles while it is producing hosts of collapsing microcavities is unknown. The bubbles may originate from occasional stray nuclei which endow them with an initial gas content.

The above picture of cavitation is true if high ultrasonic intensities are available. If water is fully freed from dissolved gases and suspended particles, its apparent cohesive strength is much greater than usual; negative pressures of the order of 100 atmospheres are required to produce cavitation (35. 44). Ultrasonic intensities sufficient to give pressure amplitudes in the region of $\pm$ 100 atmospheres are possible if a barium titanate spherically focusing radiator is employed. Most of the work in this field has been accomplished using flat transducers (low degree of focusing) and the maximum sonic intensities are considerably below that required for cavitation of degassed water.

The postcavitation condition of the liquid is very important as far as chemical effects are concerned since it is the by-products of cavitation that cause the chemical effects.

When a microcavity collapses there are a number of related physical phenomena that may occur. It may collapse with a violent hammering action which may generate local pressures of thousands of atmospheres and local temperatures of several hundred degrees (45). Electrical discharges also occur as the result of the electric potential built up between opposite walls of the cavity (46-48).

At present it is not known which of the above is of fundamental importance in producing chemical reactions. Some investigators have emphasised the temperature effect (49-51), others have considered the pressure increase (37), some suggest that water is mechanically separated into H^+ and OH^- ions (52. 53) whilst many believe that electrical discharge is the essential step (12 47 48 54), possibly through the intermediation of luminescence and the resulting decomposition of water into reactive H and OH radicals (55). Another significant factor is the shock wave itself (1.39)

Most of the reactions in aqueous solutions can be attributed to the presence of OH and H radicals. The formation of hydrogen peroxide, hydroxylation of benzoic acid and hydration of acetylene are all in agreement with this. The acceleration of

reactions which result in a gaseous product is due to the degassing effect of ultrasonics.

However the breakdown of certain viruses, bacteria and polymers would not seem to fall into the above category. In this group, it would seem from the results that the size and shape of the irradiated substance is of prime importance.

Anderson et al (22) irradiated certain viruses and found that those which were spherical in shape were inactivated very much more slowly than those that had spherical heads with flagella. As will be shown later, glycogen, which is thought to have a spherical configuration is degraded very slowly with ultrasonics.

The role of cavitation in the destruction of micro-organisms and polymers must therefore be of a dual nature. If the destruction was due to a micro-organism or polymer being very near or in the edge of a cavity then the effect due to the temperature increase or the light and electrical energy emitted would be the same for all shapes. If however it is either the shock wave or the pressure change due to cavity collapse that is the main scource of destruction then the dependance on shape may be accounted for. It should be noted that the two modes of action will coexist in non-degassed solutions.

The above description has been almost entirely devoted to aqueous solutions. There is ample evidence that cavitation occurs in pure organic liquids. Chambers (55) reported cavitation in som 14 organic liquids. He reported

sonoluminescence in 14 polar organic liquids but no luminescence in certain nonpolar liquids. As his measurement of sonoluminescence was by eye, his readings are open to doubt, especially as other workers have reported no sonoluminescence.

Most of the work reported in the literature on the degradation of high polymers has been accomplished employing organic media.

The mechanism of ultrasonic degradation of high polymers in solution has been discussed in the literature from two partically differing viewpoints. Schmid (56-58) developed his theory that frictional forces are created between solvent and solute by the ultrasonic waves. If the chain molecules were long enough and other conditions suitable, he said, these forces could exceed the C-C bond strength and break the polymer chains into smaller but not arbitrarily short segments. A definite limit existed below which no further degradation occurred. Schmid investigated the effects of numerous process variables and explained them according to his theory. In some of his later work, he suggested that cavitation bubbles might act as resonators, locally amplifying the sound but he did not believe cavitation was required for degradation.

Other workers (26·29.54.) have produced data in support of cavitation as an essential initiator of ultrasonic degradation of polymers. This evidence was obtained from variations in the ultrasonic power level, pressure and nature

of gas in equilibrium with the test solution. If the power was below a certain value, or if a solution was thoroughly degassed or saturated with a highly soluble gas, they claimed that cavitation did not occur and that there was no degradation.

The interpretation of the above results with regard to the cavitation process is that when the power level was low, the power was insufficient to start the initiation phase. This limit will be termed the cavitation threshold power. When the liquid was degassed, the maximum power employed was below the cavitation threshold power for a degassed system. That a small quantity of a highly soluble gas or volatile liquid such as ether may suppress cavitation has been known for some time but a full and satisfactory explanation has not been put forward.

That cavitation is necessary and that frictional forces are the main agency in the degradation of polymers is now generally accepted. It is only in the generation of the flow of solvent that opinions are divided; whether it is generated by the collapse of the microcavities or the shock wave is still an unanswered question.

All the work reported in the literature agrees that there appears to be a limit to the extent of ultrasonic degradation of polymers. This is in agreement with Schmids original work and is to be expected from the mode of degradation if it is purely mechanical. On the basis of this Schmid, Jellinek and White and Mostafa (27.29.56-58) have published theoretical solutions for the kinetics of degradation of polymers by ultrasonic waves.

2. STARCH.

Although the chemical constitution and fine structure of starch have been the subject of many researches in the past, it is only within recent years that major advances have been made.

In 1940, it was proved conclusively that the starch granule contained two major components (60) - amylose and amylopectin- both glucose polymers. This was followed by the first successful quantitative separation by Schoch (60) using a polar organic molecule (e.g. butanol) as a complexing agent for the amylose. These results meant that some of the previous work had to be repeated using the pure components. As a glucose determination in itself was no longer a criterion of purity, new methods of analysis had to be developed based on the interaction of the components with iodine - the optical density measurements of Hassid and McCready (61) and the potentiometric iodine titration method of Bates, French and Rundle (62).

Early investigations on whole starch established the presence of α 1-4 D linkages. Two chemical methods proved particularly useful in elucidating the structure. These are, (1) the Haworth technique of methylation followed by acid hydrolysis and separation of the component sugars (63), and (2) the quantitative estimation of the reaction products after the action of periodic acid first introduced Hudson and Jackson (64).

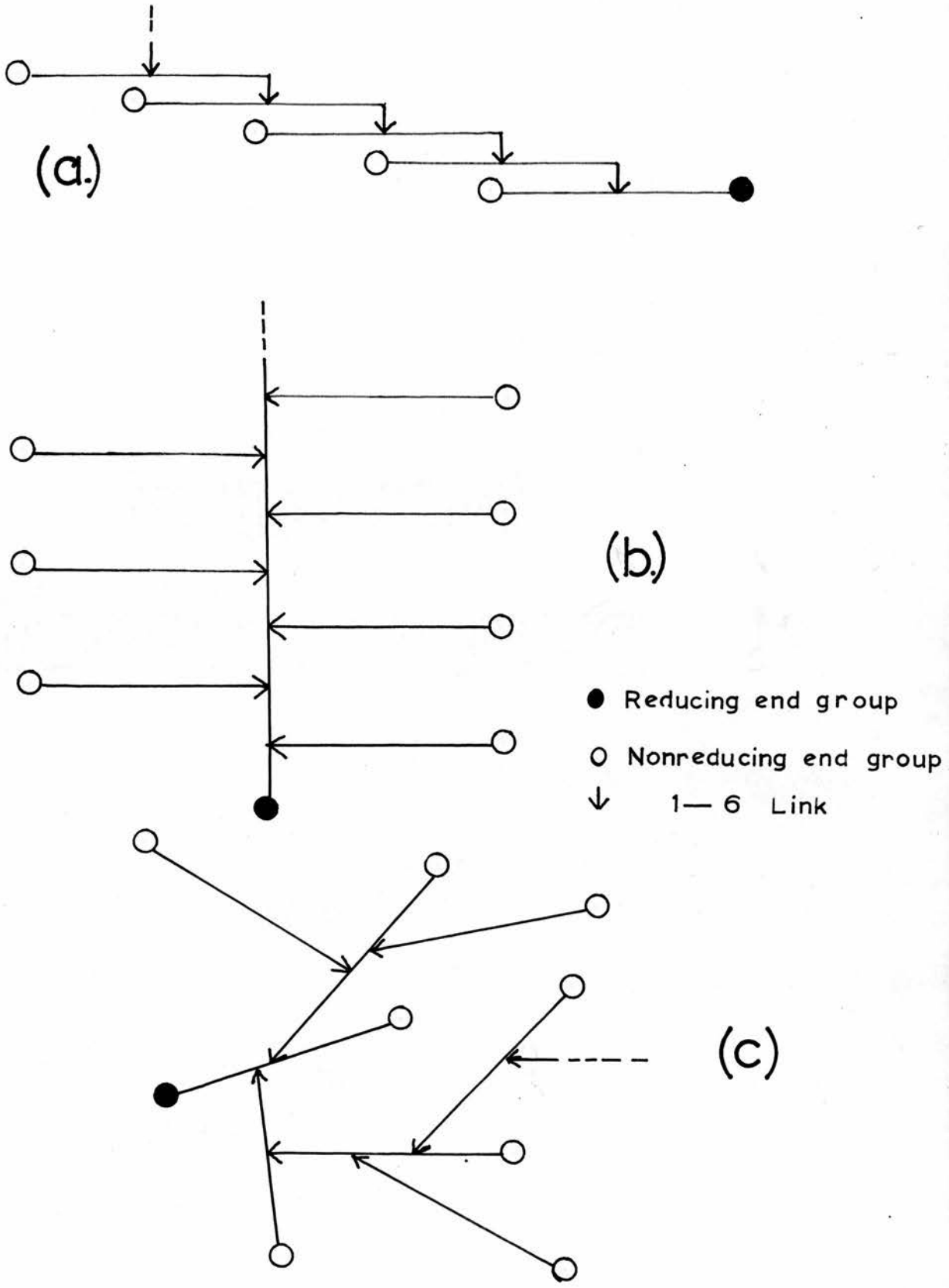

Fig. 1. 1.

These methods have been applied to the pure starch components, and in conjunction with molecular weight determinations have enabled both the configuration and the degree of branching to be estimated.

The Structure of Amylopectin:-

That amylopectin contained α 1-4 D and probably 1-6 D linkages had been known for some time (it was not until 1951 that Wolfram and co-workers (65) proved 1-6 linkages were present). The results of the determination of average length of unit chain from methylation and periodate oxidation studies, in conjunction with molecular weight determinations suggest a branched molecule. Three different structures have been proposed for amylopectin.

(1) The laminated structure proposed by Haworth, Hirst and Isherwood (66). Fig. 1. 1a.

(2) The herringbone structure proposed by Huseman and Staudinger (67). Fig. 1. 1b.

(3) The ramified structure proposed by Bemfield and Meyer (68). Fig. 1. 1c.

Recent enzymic studies (69) have supported the ramified structure. Very little work has been carried out on the hydrodynamic behaviour of amylopectin and its configuration in solution is still in doubt.

The structure of Amylose:-

The very small percentage (0.2 - 0.4%) of nonreducing end-groups, the very low reducing power of amylose, in conjunction with molecular weight determinations suggested that amylose is a linear molecule (17). Later investigations confirmed these results (18). However, more recent enzymic experiments suggest that such a simple concept is not quite correct. Hydrolysis with β-amylose (which will convert a linear α 1-4 glucan completely into maltose) has shown some amyloses may be converted only 75% into maltose. In fact, recent work by Cowie and Greenwood (70) has shown that it is possible to isolate from potato starch two amylose fractions one of which has a low D.P. (approx 2000) and a β-limit of 100%, the other has a much higher D.P. (approx 4000) and a lower β-limit. The nature of the link that forms the barrier to amylolsis has not been determined.

A helical configuration for amylose was proposed by Freudenberg (71). Xray diffraction studies of the solid amylose-iodine complex by French and Rundle (72) have supported this proposal. The results indicated that amylose consists of long chains of glucose units arranged in the form of helices, each turn of the helix consisting of about 6 glucose residues.

When starch is fractionated by the thymol/butanol complex method (see experimental methods - "Isolation") the purified products have a rather wide molecular weight distribution. As the above method is very mild and degradative effects are kept to a minimum, it seems reasonable to assume that the distribution has not been altered by fractionation. The subfractionation of the pure components has never been satisfactorily accomplished. This is due mainly to the lack of good solvents and the lability of the molecules. The lability of the components will be discussed in the experimental methods section under heading "Preparation of Solutions".

3. GLYCOGEN.

Glycogen is found in the cells of most animals and many micro-organisms. In these organisms, glycogen is important as the storage form of carbohydrate, and hence as a scource of energy.

Chemical studies by Karrer (73) indicated that glycogen and starch have closely related structures. Measurement of the osmotic pressure exerted by certain glycogen derivatives led Carter and Record (74) to suggest that glycogens have a molecular weight of the order of 10^6 . In 1937 two different molecular structures were postulated by Haworth and Hirst (66) and by Staudinger (67), respectively. Haworth and Hirst suggested the laminated structure (see fig. 1 1a) and Staudinger the herringbone structure (see fig. 1 1b). Results of the methylation assay of glycogen and of the limit dextrin remaining after β amylolysis led Meyer (75) to propose the ramified structure (see fig. 1 1c). Enzymic studies (76) have supported Meyers proposal.

It is now generally accepted that glycogen is a highly branched macromolecule composed of several thousand chains; on the average, each chain contains 10-14 α 1-4 linked D glucose residues and is joined to an adjacent chain by a 1-6 glucosidic linkage.

Comparision of glycogen and amylopectin:- Both are glucose polymers with so far as is known the same type of structure.

Table 1. 1.

Physical property.	Glycogen.	Amylopectin.
Solubility in water.	very soluble	dif. soluble
Average length of unit chain	10-14	20-24
So.	150-300 $x10^{-13}$	100-500 $x10^{-13}$
Do.	1.1 $x10^{-7}$	
[3]	7	70
Mol. wt.	60 $x10^{6}$	? $x10^{6}$
Iodine stain.	Brown	Red

From the above it may be seen that although the only difference in structure is in the length of the α 1-4 chain, the physical characters of the two polysaccharides are vastly different. The cause of this vast difference is thought to be due to the difference in molecular shape (77).

4. MOLECULAR WEIGHTS OF POLYMERS.

In this thesis the term monomolecular is used to describe chemically homogeneous system with no variation in molecular weight (e.g. polystyrene x mer), the term polymolecular denotes a chemically homogeneous system having a variation in molecular weight (e.g. polystyrene A mer.....Z mer) and the term polydisperse is used to describe a system containing more than one component (e.g. polystyrene and polyvinyl acetate).

The measurement of the molecular weight of a polymolecular polymer results in an average value being obtained. The particular average obtained depends upon the method of determination and in some cases on the shape of the molecule.

Methods based on colligative properties such as osmotic pressure, freezing point lowering or the determination of the end groups by either chemical or physical means give the number average molecular weight Mn.

$$Mn = \sum_i n_i M_i / \sum n_i = \sum c_i / \sum c_i M_i \qquad 1.\ 1.$$

Methods depending on the weight of the particle present such as light scattering give a weight average molecular weight Mw.

$$Mw = \sum_i n_i M_i^2 / \sum n_i M_i = \sum c_i M_i / \sum c_i \qquad 1.\ 2.$$

There are another two averages met in practice, the viscosity and Z averages. The viscosity average (Mv) is obtained from viscosity measurements and was defined by Flory (77) as

$$Mv = \left[\sum n_i M_i^{1+\alpha} / \sum n_i M_i\right]^{\frac{1}{\alpha}} \qquad 1.\ 3.$$

where α is a constant and Mv = Mw when = 1.

The Z average is obtained from equilibrium centrifugation experiments and is defined as

$$Mz = \sum n_i M_i^3 / \sum n_i M_i^2 = \sum c_i M_i^2 / \sum c_i M_i \qquad 1.\ 4.$$

For polymolecular systems $Mn \leqslant Mv \leqslant Mw \leqslant Mz$

When molecular weights are determined by sedimentation velocity experiments combined with independent diffusion measurements the average molecular weight obtained is in some cases not a simple average. If the system is polymolecular, then both the sedimentation coefficient (S) and the diffusion coefficient (D) are average values. Therefore the average molecular weight obtained depends on the method of calculating S and D.

In the evaluation of D it is usual to apply the moments method (see diffusion), this gives a weight average D. The number average D is at present not securable and Dz is very sensitive to experimental errors.

It is possible to obtain Sn, Sw and Sz depending on the method of evaluation.

As the above quantities are both functions of the frictional coefficient then the type of average obtained will vary with the shape of the molecule. Table 1. 2. gives a list of the averages obtained by combining S and D measurements for molecules of different shapes. This table is an excerpt from a table published by S. Singer (78).

TABLE 1. 2.

Type of Average.	Free draining coil Value.	Matted Coil Value.	Sphere Value.
WW.	Mn.	$\Sigma n M^{3/2} / \Sigma n M^{1/2}$	$\Sigma n M^{5/3} / \Sigma n M^{2/3}$
NW.	Mn.	$\left[\Sigma n M / \Sigma n M^{1/2}\right]^2$	$(\Sigma n M)^2 / \Sigma n M^{1/3} \Sigma n M^{2/3}$
ZW.	Mn.	$\frac{\Sigma n M^{3/2} \Sigma n M^{1/2}}{\Sigma n \Sigma n M}$	$\frac{\Sigma n M^{5/3} \Sigma n M^{2/3}}{\Sigma n M^{1/3} \Sigma n M}$

Where NW represents a number average S combined with a weight average D.

As may be seen from the above only the free draining coil gives a simple average.

5. THEORETICAL KINETICS OF DEGRADATION.

In this work, degradation of a polymer will be defined as the breakdown of a polymer with little or no monomer or dimer production, and depolymerization will be breakdown of a polymer molecule with monomer or dimer as the main product.

Degradation as measured by changes in viscosity.

The most convenient method of following the degradation of a polymer in solution is to measure the decrease in intrinsic viscosity $[\eta]$* of the system with time of reaction. In many instances throughout the literature, viscosity measurements $[\eta]$ or $\left[\frac{\eta_{sp}}{c}\right]$ have been employed to characterise the polymer degradation products, the rate of degradation then being expressed simply as the change of viscosity with time.

Changes in intrinsic viscosity are not themselves directly a true measure of the degradation rate and any apparent limit in intrinsic viscosity v. time curves may be fallacious. This can be shown as follows. The correct method of interpreting changes in intrinsic viscosity was published by Ekenstam (79) and Schuby and Huseman (80).

Consider a polymer system containing n gram moles of equally strong and accessible cleavable bonds/litre, then for a zero order degradation reaction

$$dn/dt = -k_0 \qquad 1.\ 5.$$

and for a first order degradation reaction

$$dn/dt = k\,n \qquad 1.\ 6.$$

* for definition see page 84

If there were W grams of polymer composed of repeating units of molecular weight M and having a number average degree of polymerization P then the overall condition must hold that

$$\frac{dp}{dt} = \left[\frac{dp}{dn}\right]\left[\frac{dn}{dt}\right] \qquad 1.\ 7.$$

but $n = W(p-1)/PM_o$ 1. 8.

hence $dp/dn = M_oP^2/W$ 1. 9.

and for a zero order reaction

$$k_o = W\left[\underline{P_t^{-1} - P_o^{-1}}\right]/Mot \qquad 1.\ 10.$$

where P_t and P_o are the values for the number average degree of polymerization at times t and o respectively. Similarly, for a first order reaction

$$k_1 = \frac{1}{t} \ln \frac{\left[1-P_o^{-1}\right]}{\left[1-P_t^{-1}\right]} \qquad 1.\ 11.$$

or $$k_1 = \frac{1}{t}\left[P_t^{-1} - P_o^{-1}\right] \qquad 1.\ 12.$$

on expansion of the logarithm and ignoring terms higher than the first.

Hence for either a zero or first order reaction the degradation rate constant in the initial stages is proportional not to P but to P^{-1}, and P^{-1} versus t will be linear. For large amounts of degradation this relationship will still hold for a zero order reaction but $\ln\left[1-P^{-1}\right]$ versus t is necessary for a first order reaction as higher terms in the expansion are then required.

Thus if degradation is followed viscometrically and $[\eta] = KP$, the degradation rate constant is obtained from

Fig. 1. 2.

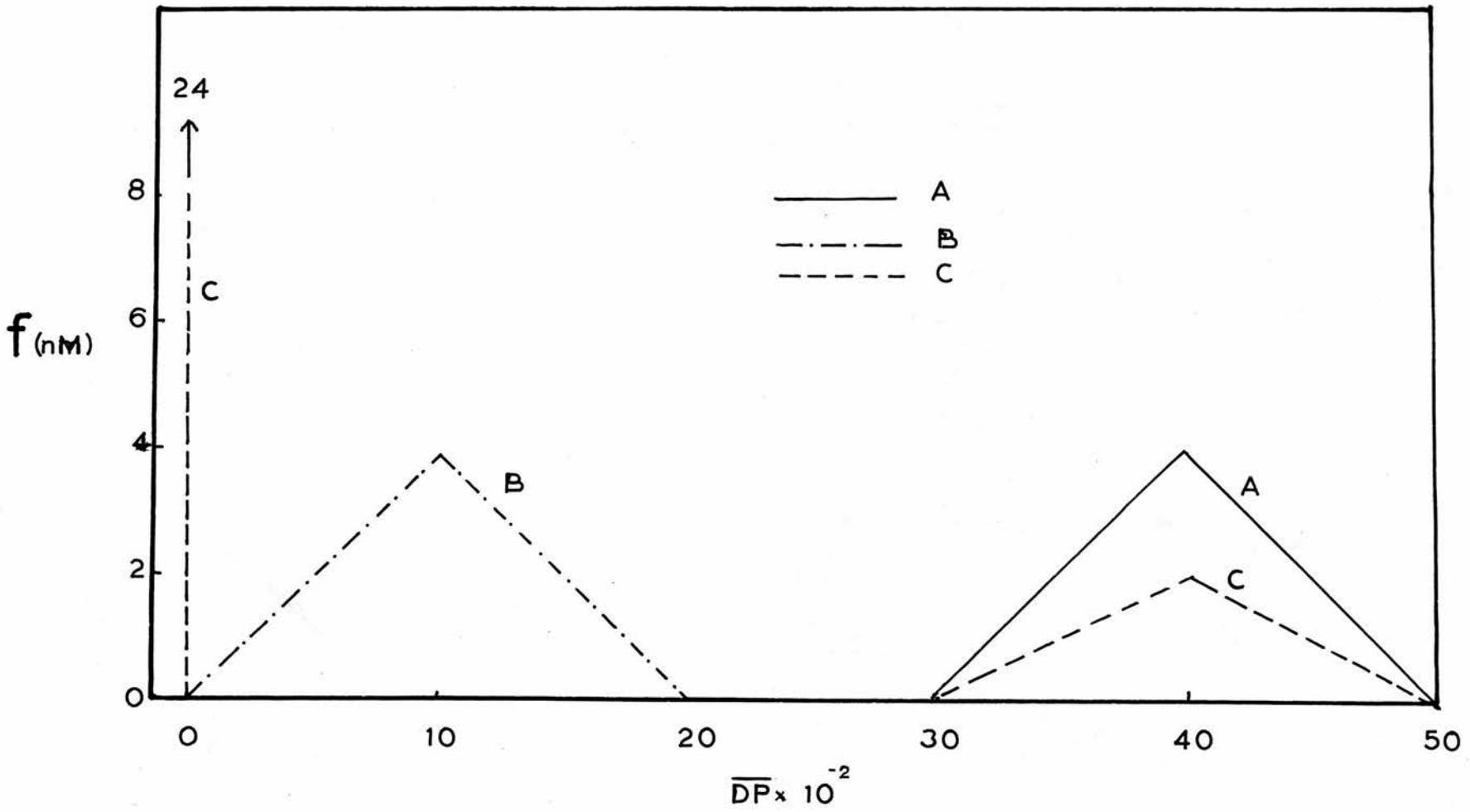

the graph of $[\eta]^{-1}$ v.t. and not $[\eta]$ v.t. in agreement with McBurney (81). The presence of some rapidly degraded weak linkages will then be shown by $\lim_{t \to 0} [\eta] \neq$ that for the original polymer.

Although viscosity measurements give a rapid but accurate estimate of the amount and rate of degradation they give very little information about the changes in molecular weight distribution. This is a very serious disadvantage as may be seen from a study of the curves opposite (fig. 1. 2). Curve A shows the theoretical distribution for a polymolecular polymer of D.P. = 4000, after X% degradation the resultant distribution will be as shown in B. However, a distribution of the form shown in curve C would have the same weight average and hence approx. the same limiting viscosity number as the polymer in B. Although, therefore, the mechanism of transforming A to B and C respectively is obviously totally different, this could not be deduced from the viscosity measurements alone.

As stated in the "Introduction", it is necessary to follow the change in molecular weight distribution with time and compare theoretical and experimental results for different times of reaction. Molecular weight distributions can be obtained from both velocity and equilibrium ultracentrifugation experiments. However, there are major difficulties in both the theoretical and experimental fields. The mathematics involved in interpreting

the kinetics of the degradation of even a monomolecular polymer is rather complex unless a few simplifying assumptions are made. Further, experimentally it is almost impossible to obtain a monomolecular polymer, and hence the molecular weight distributions met with in practice can only be interpreted by dividing the distribution into a number of increments and treating each of these kinetically as though it were monomolecular and then compounding the results.

General theory of polymer degradation:- Montroll and Simha (82) have given a complete statistical treatment of the random breaking of a polymer molecule. Simha (83) has developed this and obtained equations for the molecular weight distribution of degradation products with time of reaction. His derivation is outlined below.

Consider a system where at time $t = o$ there are $N_j(0)$ molecules consisting of j monomers and having j-1 links, where $n \geqq j \geqq z$. If these molecules are then exposed to a degradation process in which any bond in a molecule breaks at a rate characteristic of both its position in the molecule and the molecular size ie. rate constants of the type $k_i^{(j)}$, where the lower index gives the ordinal number of the respective bond and the upper one the degree of polymerization of the corresponding molecule, then the following set of differential equations hold :-

$$\frac{dn}{dt} = \sum_{i=1}^{n-1} k^{(n)} N_n$$

$$\frac{dn_{(n-1)}}{dt} = \left[k_1^n + k_{n-1}^n\right] N_n - \sum_{i=1}^{n-2} k_1^{n-1} \quad N_{(n-1)}$$

$$\frac{dn_j}{dt} = \left[k_{n-j}^n + k_j^n\right] N_n + \left[k_{n-j-1}^{n-1} + k_j^{n-1}\right] N_{n-1} \qquad \text{1. 13.}$$

$$+ \left[k_i^{j+1} + k_j^{j+1}\right] N \quad - \sum_{i=1}^{j-1} k_i^j \quad N_j$$

$$\frac{dn_2}{dt} = \left[k_{n-2}^n + k_2^n\right] N_n + \left[k_2^{n-1} + k_{n-3}^{n-1}\right] N_{n-1.} \quad \ldots\ldots$$

$$\ldots\ldots \quad \ldots - k_1^2 N_2.$$

These equations express the fact that a particular chain can be generated by disintegration of any of the larger ones and is in turn itself destroyed by degradation.

If both ends of the molecule are equal then because of symmetry $k_i^j = k_{(j-i)}^j$

The solutions of equations 1. 13. can be written in the form

$$Nj = \sum_{\ell=1}^{n} h_\ell a_{j\ell} e^{\lambda_\ell t} \qquad \text{1. 14.}$$

where (1) h_ℓ are integration constants determined by the initial conditions (2) $\lambda_\ell = - \sum_{i=1}^{\ell-1} k_i^\ell$ for $1 = 1\ 2\ 3 \ldots n$

(3) $a_{j\ell}$ are solutions of the following system of linear equations

$$-\lambda_\ell a_{i\ell} + 2k_i^2 a_{2\ell} \ldots\ldots\ldots 2k_i^j a_{j\ell} + \ldots\ldots\ldots 2k_i^n a_{n\ell} = 0$$

$$(-k_i^2 - \lambda_\ell) a_{2\ell} + \ldots\ldots\ldots 2k_2^j a_{j\ell} + 2k_2^n a_{n\ell} = 0 \qquad \text{1. 15.}$$

$$\left(-\sum_{i=1}^{n-1} k_i^n - \lambda_\ell\right) a_{n\ell} = 0$$

If $j > 1$ then $a_{j\ell} = 0$ and the remaining $a_{j\ell}$ obey the relation $-\lambda_1 a_{1\ell} + 2k^2 a_{2\ell} \ldots\ldots\ldots 2k_1^\ell a_{\ell\ell} = 0$

$$(-k_1^2 \quad -\lambda_\ell)\, a_{2\ell} \quad + \quad \ldots\ldots \quad 2k_2^\ell\, a_{\ell\ell} \quad = \quad 0$$

$\ldots\ldots\ldots\ldots\ldots\ldots\ldots\ldots\ldots\ldots\ldots\ldots\ldots\ldots$ 1. 16.

$$\left(-\sum_{i=1}^{\ell-2} k_i^{\ell-1} \quad -\lambda_\ell\right) \quad + \quad 2k_{\ell-1}^{\ell}\, a_{\ell\ell} \quad = \quad 0$$

In this way by successive solution, the coefficients $a_{j\ell}$ for $j > 1$ can be expressed in terms of the rate constants and of the quantities $a_{j\ell}$.

The final result for the Nj(t) appears in the form

$$N_j(t) = h_j a_{jj}\, e^{-\sum_{i=1}^{j-1} k_i^j t} + h_{j+1} a_{j+1\,j}\, e^{-\sum_{i=1}^{j} k_i^{j+1} t} \ldots\ldots + h_m a_{jm}\, e^{-\sum_{i=1}^{m-1} k_i^m t} \qquad 1.\ 17.$$

$$N_i(t) = \sum_{i=1}^{n} i\, N_i\,(0) - \sum_{i=2}^{n} i\, N_i(t) \qquad 1.\ 18.$$

If Ni(0) = the number of i mers initially present, equations 1. 17. and 1. 18. represent the most general solution of the rate equations.

Random degradation:- If all linkages are broken at random then $k_i^j = k$, independent of i and j and the rate equations reduce to

$$\frac{dNj}{dt} = 2k \sum_{\ell=j+1}^{n} N_i \quad -k(j-1)\, Nj \qquad 1.\ 19.$$

hence on integration and substitution of the appropriate equations 1. 16, 1. 17 and 1. 18 the solution is

$$N_j(t) = e^{-k(j-1)t}\left[h_j a_{jj} - 2h_{j+1} a_{j+1}\, e^{-kt} + h_{j+2} a_{j+2}\, e^{-2kt}\right] \qquad 1.\ 20.$$

for $n \geqq j \geqq 2$.

If the material at t = o is monomolecular, then Nj(0) = 0

for $j \neq n$, and the integration constants $h_j a_{jj} = (n-j+1)N_m(0)$

Introducing, for simplification $\alpha = 1 - \exp\left[-kt\right]$ 1. 21.

the solution can be written as :-

$$Nj = N_m(0)\ (1-\alpha)^{j-1}\ \alpha\left[2+(n-j+1)\alpha\right] \qquad 1.\ 22.$$

$$1 \leq j \leq n-1$$

and $$N_m = N_m(0)\ (1-\alpha)^{n-1} \qquad 1.\ 23.$$

This result is identical with that previously found from statistical considerations by Montroll and Simha (82). In their work α denoted the average degree of degradation, defined as $\frac{R}{P}$ where R = the average number of cuts per molecule and P+1 = number of monomeric units in a molecule. In the above derivation α is expressed as a function of the time elapsed since the start of reaction.

The decrease of the weight average (Mw) and number average (Mn) molecular weights with time is found from 1. 21 and the following equations derived by Montroll and Simha

$$\frac{Mw}{Mo} = \frac{n\alpha^2 + 2(1-\alpha)\left[(1-\alpha)^n + n\alpha - 1\right]}{n\alpha^2} \qquad 1.\ 24.$$

$$\frac{Mn}{Mo} = \frac{n}{1+\alpha(n-1)} \qquad 1.\ 25.$$

where Mo = monomer molecular weight.

Using these equations, the weight average and number average as a function of the reduced time $\lambda = kt$ have been calculated here for a linear polymer of 4000 D.P.

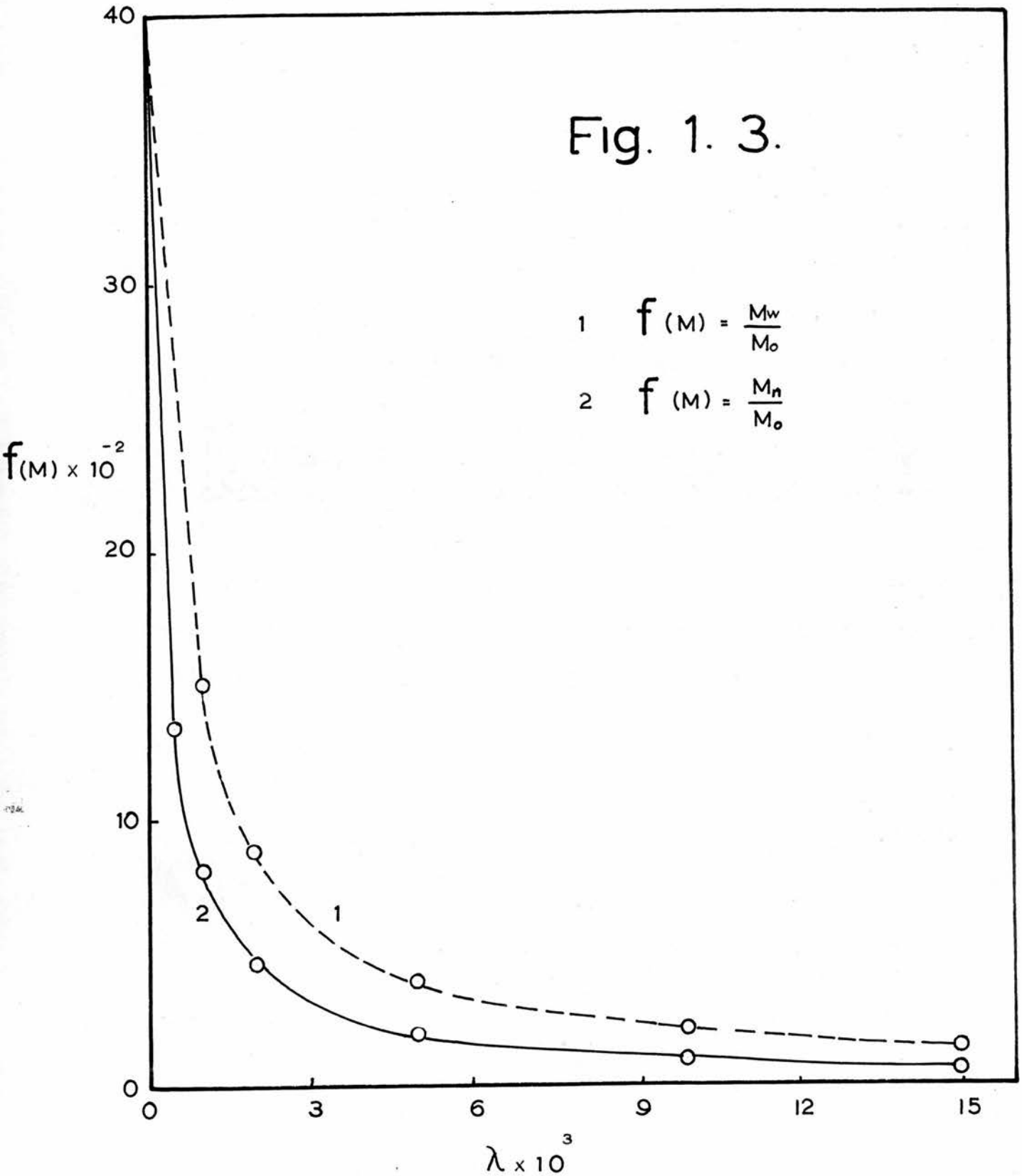
Fig. 1. 3.
1 $f_{(M)} = \frac{M_w}{M_o}$
2 $f_{(M)} = \frac{M_n}{M_o}$
$f_{(M)} \times 10^{-2}$
40
30
20
10
0
0
3
6
9
12
15
$\lambda \times 10^{3}$
1
2

The results are shown in fig. 1. 3.

The above kinetic scheme for a totally random breakdown may or may not be applicable to ultrasonic degradation. As stated in section I, it has been suggested by Schmid (56-8), Jellinek (29) and others (27) that there is a limit to the degradation which may take place under ultrasonic irradiation.

Random degradation with a limiting molecular weight:- Schmid proposed that the rate of bond scission due to ultrasonic irradiation is expressed by the equation

$$dx/dt = k\,N(P - Pf) \qquad \text{I. 26.}$$

where k = a constant, N is avogadro's number, P is the average chain-length (D.P.) at time t and Pf is the ultimate chain-length to which the system tends on long exposure.

Jellinek and White (29) on the basis of a "limit" made the simplifying assumptions that the rate constants for the breaking of all links are equal in all molecules that have a DP above a minimum Pe and that for all molecules with a DP less than Pe the rate constants are zero.

$$\frac{d\,Nn}{dt} = -\sum_{1}^{P_{n-1}} Kn\,Nn$$

$$\frac{d\,Nn-}{dt} = 2\,Kn\,Nn - \sum_{1}^{P_{n-2}} Kn-1\;\;Nn-1 \qquad \text{I. 27.}$$

$$\frac{d\,Nx}{dt} = 2\,Kn\,Nn + 2K_{n-1}\,N_{n-1} \ldots\ldots 2K_{x+1}N_{x+1} - \sum_{1}^{P_{x-1}} k_x N_x$$

Where Nx is the number of chains Px at time t.

For all chains of length Pe and smaller

$$K_e = 0$$

$$K_{e-1} = 0 \qquad 1.\ 28.$$

$$K_2 = 0$$

assuming that bonds are broken at random and that the initial sample is monomolecular then the number-average chain-length Pn is given by

$$P_N = \frac{P_n}{\left[2P_e\left\{\frac{P_n-P_e-1}{P_e+1}\left((1-\alpha)^{P_e+1}-1\right)-\frac{P_n-P_e}{P_e}\left((1-\alpha)^{P_e}-1\right)\right\}-\alpha(1-\alpha)^{P_n-2}+(1-\alpha)^{P_e}\left(1+\alpha(P_n-P_e-2)\right)\right]} \qquad 1.\ 29.$$

Where Pn = the original chain-length, Pe = the largest chain-length not further broken down, and $\alpha = 1 - \exp(-kt)$, k is the rate constant for the breaking of all links in molecules larger than Pe.

At $t = \infty$ ie. when $\alpha = 1$ equation 1. 29. becomes $P_n = \frac{P_e + 1}{2}$ 1. 30.

The corresponding expression for the weight average chain length is

$$P_W = \frac{2P_e^3}{3P_n}\left[\frac{P_n-P_e-1}{P_e+1}\left\{(1-\alpha)^{P_e+1}\right\}-\frac{P_n-P_e}{P_e}\left\{(1-\alpha)^{P_e}-1\right\}\right]$$

$$+\frac{(1-\alpha)^{P_n-2}}{P_n}\left[\frac{2}{\alpha^2}-(P_n-1)^2\right]-\frac{(1-\alpha)^{P_e}}{P_n}\left[\frac{2}{\alpha^2}-(P_n-P_e-2)\right] \qquad 1.\ 31.$$

$$\left(\frac{2}{\alpha}+\alpha(P_e+1)^2\right)-(2P_n-P_e-3)(P_e+1)\Big]+P_n(1-\alpha)^{P_n-1}$$

In this case the ultimate molecular weight is

$$Pw = \frac{2\,Pe}{3} \qquad 1.\ 32.$$

On the above assumptions, the ultimate molecular weight is obtainable from experiment, and hence it is possible to calculate k.

Again on this theory the number distribution for original chains

$$Nn = \frac{1}{Pn}(1-\alpha)^{Pn-1} \qquad 1.\ 33.$$

and for chains between Pn-1 and Pe

$$Nx = \frac{\alpha}{Pn}(1-\alpha)^{Px-1}\ (2 + (Pn-Px-1)\alpha) \qquad 1.\ 34.$$

and for chains smaller than Pe + 1

$$Nx = \frac{2}{Pn}\left[\frac{Pn-Pe-1}{Pe+1}(1-\alpha)^{Pe+1} - \frac{Pn-Pe}{Pe}\left[(1-\alpha)^{Pe}-1\right]\right] \qquad 1.\ 35.$$

Where Nn and Nx are the number of moles of material with chain-lengths n and x respectively when the whole system contains one base mole of polymer.

The weight-distribution, representing the amount of polymer in grams, with chain-lengths n and x contained in one gram of material is obtained by multiplying the first of these equations 1. 33 by Pn and the second and third by Px.

Behaviour on ultrasonic irradiation of a polymer containing a mechanical weak link. If there is no weak link in the molecule then the second type of kinetic treatment (with a limit) may be applicable to ultrasonic degradation but if there is a weak

link then upon the relative strength of the weak link will depend whether there is superimposed on the limit type of kinetics a totally randon degradation.

SECTION II

Experimental Methods

EXPERIMENTAL METHODS.

1. ISOLATION OF STARCH.

Starch was isolated from two varieties of patatoes (Arran Banner and Majestic).

Potatoes were peeled, sliced and then minced into ethanol to inhibit enzymic activity. The ethanol/pulp mixture was extracted in an Atomix blendor for 2 mins, the slurry was filtered through muslin, and the filtrate immediately centrifuged (M.S.E. "Major" 1800 r.p.m.). The supernatant liquid was discarded, the starch product was washed with 0.1M sodium chloride and re-centrifuged. The washing process was carried out 4 times. The pulp retained by the muslin was re-extracted with 0.1M sodium chloride (3 times) in the blendor. Starch from the different extractions was combined. The resultant product was suspended in 0.1M sodium chloride, a layer of toluene added and shaken overnight to denature protein. The denatured protein imparted a brown colour to the toluene layer. The mixture was allowed to settle and the protein/toluene layer was discarded. This process was carried out until the toluene layer remained colourless. The pure starch was then stored under toluene at $0^{\circ}C$, rather than under methanol.

Preliminary results with methanol-stored starch indicated variations in leaching properties which were thought to be due to dehydration. It was found that removal of samples from the storage container always left some starch above the liquid level on the side of the container which if the solvent was methanol, dried. If the dried starch was dispersed in water the granules burst. Therefore repeated extraction of starch samples (stored under methanol) results in a variation from sample to sample.

2. ISOLATION OF AMYLOSE AND AMYLOPECTIN.

By dispersion at 98° C: Distilled water was de-aerated at room temperature by stirring vigourously and passing a stream of oxygen free nitrogen for 30 mins. Sufficient starch to make a 0.5% dispersion was added and the temperature increased to 98° C (Isomantle), it was held at that temperature for 1 hour (with a continuous stream of oxygen-free nitrogen passing and mechanical stirring). The solution was then cooled to 60° C (under a N atmosphere), and powered thymol (1g./1.) added. After dispersion of the thymol by stirring, the mixture was allowed to cool to room temperature and set aside for 3 days. The amylose/thymol complex which settled out was removed by centrifugation in a constant-feed Sharples supercentrifuge, and immersed immediately in water/excess butanol before recrystallisation.

The supernatant, which contained the amylopectin, was freeze dried, refluxed with methanol, redissolved in water, and freeze dried.

For recrystallisation, 1 litre of water/excess redistilled butanol was de-aerated at room temperature in the manner described above, the thymol/amylose complex added and the temperature increased to 98°C (nitrogen atmosphere), held at 98°C for 10 mins, allowed to cool to room temperature and set aside for 24 hours.

The amylose/butanol complex precipitate was removed by centrifugation (M.S.E. "Major" 1800 r.p.m.). The resultant complex was then redispersed and reprecipitated a further 3 times. The resultant amylose/butanol complex was dehydrated by repeated stirring with pure butanol and was dried under vacuum.

The purity of the product obtained by the above method was determined as described in detail later in this section.

By Aqueous Leaching at 58°C:- A de-aerated starch suspension (see above) was maintained at 58°C for 3 mins., allowed to cool to room temperature and then kept at 0°C for 4 hours. The gelatinised granules then settled as an opaque bottom layer with a clear supernatant liquid. The latter was then decanted, filtered through a G.4 sintered glass filter excess butanol was added, the mixture shaken and left at room temperature for 24 hours. The amylose/butanol was then reprecipitated and dried as in the preceding section to yield amylose A58.

The opaque-layer was again extracted at 58°C, but this time the clear layer was discarded. The twice 58°C-extracted opaque layer was then dispersed at 98°C as above and the amylose remaining after leaching, isolated by precipitation as a complex designated A98-58.

3. ISOLATION OF GLYCOGEN.

The livers of freshly-killed rabbits were minced, divided into two portions and extracted by (1) the classical Pfluger method of extraction with 30% sodium hydroxide and subsequent purification by reprecipitation with ethanol and 80% acetic acid. (2) extracted with trichloroacetic acid at 2°C and the glycogen product purified by reprecipitation with ethanol until a trace of ammonium acetate was required to cause coagulation as described by Stetten, Katzen and Stetten (84) The glycogens isolated by the above methods are designated OH- and TCA-glycogen respectively. The purity of the products determined as outlined later in this section.

4. ISOLATION OF β-AMYLASE.

β-amylase was isolated by the method of Peat, Pirt and Whelan (85).

Ether defatted soya flour was shaken with water (5 ml/g of flour) for 2 hours, octyl alcohol (0.1 ml/l) being added to prevent foaming. The suspension was centrifuged and to the supernatant solution was added N sulphuric acid to bring the pH to 4.8. The precipitate was removed on the centrifuge and the solution heated at 60-61°C for 30 minutes. After cooling, the precipitate was centrifuged and rejected. Ammonium sulphate ("Anala R" 41.8 g/100 ml) was added slowly with stirring. The precipitate was centrifuged and dissolved, 10 ml of water being used for each 250 ml of original ammonium sulphate solution. The enzyme solution was dialysed against distilled water for 36-48 hours, and then stored under toluene in the refrigerator. All operations, except where otherwise stated, were carried out at room temperature.

The final purification of the enzyme was fractional precipitation. A solution of pH 3.7 was prepared containing ammonium sulphate (490g), hydrated sodium acetate (9.86 g) and glacial acetic acid (29.2 ml) per litre. To the enzyme solution was added ammonium sulphate solution until the ammonium sulphate

concentration was 16.5 g/100 ml., the precipitate discarded and the ammonium sulphate concentration increased to 27.0 g/100 ml. the precipitate was centrifuged and dissolved immediately in ice cold water. The above procedure was repeated but the ammonium sulphate concentration was increased to 17.0 and decreased to 24.0 g/100 ml. Finally the lower ammonium sulphate concentration was increased to 17.5 g/100 ml. and the upper remained at 24.0 g/100 ml. .

The final precipitate was dissolved in 10 mls of ice cold distilled water and stored under toluene in the refrigerator. All operations in the final purification were carried out at 0°C.

5. ESTIMATION OF GLUCOSE AND MALTOSE.

Glucose was estimated by the method of Lampitt, Fuller and Cotton (86) using alkaline ferricyanide.

A glucose solution was prepared by dissolving approx. 10 gms of glucose in 100 mls. of distilled water and adding 1 drop of conc. ammonia. When equilibrium had been attained, the optical rotation of the solution was measured and hence the concentration of glucose in solution determined. A diluted solution of the glucose (approx. 1 mg/ml) was used to calibrate an approx. 0.01 N ceric sulphate solution.

Aliquots (0.5 - 4.0 mls) of the dilute glucose solution were acidified with 1 ml. of 3N sulphuric acid and "hydrolysed" (reproducing the conditions under which glucose would be estimated) on a boiling water-bath for 2 hours. The solutions were cooled and 1.0 N followed by 0.1 N potassium hydroxide added until a blue end point with bromocresol green was obtained. The volume of each solution was made up to 10 mls, 5 mls of a solution of equal parts sodium carbonate (10.6 gms in 500 mls) and potassium ferricyanide (8.25 gms in 500 mls) added to each solution. The solutions were then heated on a boiling water bath for 15 mins, cooled and 5 mls. of 5N sulphuric acid added to each and the resultant solutions titrated with 0.01 N ceric sulphate using xylene cyanol F.F. as indicator

When the above procedure was carried out with dried "analar" starch, no significant difference was apparent in the calibration.

A standard solution of maltose (crystallised 3 times) was prepared and used to calibrate the ceric sulphate with respect to maltose. The initial 2 hours hydrolysis was omitted in this case.

The percentage anhydroglucose in the amylose, amylopectin and glycogen after hydrolysis was estimated by the method detailed above.

6. POTENTIOMETRIC IODINE TITRATION.

A quantitative estimate of the amount of iodine bound by the starch components was obtained by the potentiometric-titration method introduced by Bates, French and Randle (62) using the apparatus designed and built by Anderson and Greenwood (87).

In this method a polysacchoride-iodide solution and blank-iodine iodide solution are contained in two opposing half cells connected by a salt-bridge. The equilibrium free iodine concentration is measured by means of a null deflection method. This differential method is most sensitive at low free iodine concentrations.

The apparatus had an electrometer (88) of high sensitivity with the necessary zero stability required for null point determinations. The electrometer circuit was connected to the sample half cell via a two-way "make before break" switch, so that the electrometer grid was never in open circuit.

Solutions were continuously stirred in the titration cells (1 l. 4 necked "Pyrex" flasks). The necks were fitted with ground glass "Quickfit" joints, three of these accomodated the stirrer, platinum electrode, and salt-bridge while the fourth was for the addition of iodine. The electrodes were made of platinum foil (2cm x 2cm) fused to platinum wire which was sealed through glass tubing which contained a pool of mercury. No potential difference existed between the two electrodes when they were in contact with the same electrolyte.

Approximately 3-5 mg. amylose or 25-30 mg. amylopectin was placed in a weighing stick, inserted in a vacuum drier (80°C) and left overnight. The weighing stick was then removed, stoppered and allowed to cool for 10 mins. in a dessicator. The sample was then weighed, transferred to a flask, and dissolved in 0.2M potassium hydroxide (10 ml.). Before addition to the half cell, the colution was brought to pH 5.85 by adding a predetermined volume of 0.4 phosphoric acid. A blank was made consisting of the same volumes of potassium hydroxide and phosphoric acid.

The titration conditions were: iodide 0.01 M pH5.58 and temperature 20°C. The electrolyte solution contained 0.1 M potassium iodide (210 ml), 0.066 M. phosphate buffer (15 ml pH5.85) and was made up to 2 litres with distilled water. 800 ml. were placed in each half cell and left to come to temperature equilibrium.

The sample solution and blank were added to their respective half cells and the flasks rinsed with electrolyte (40 ml) so that final volumes were 840 ml. The circuit was then checked for balance (galvonometer).

Small volumes (0.1 ml) of 0.01 M iodine-potassium iodide solution were added to the half cell which contained the sample by means of an "Agla" microsyringe. Approximately 4 mins was

allowed for equilibration after each addition before an attempt at balancing was made. A balance was accomplished by adding the same iodine solution to the other half cell until the galvonometer deflection was zero.

The difference in the volume of iodine added to the two half cells gave the amount of iodine bound by the sample.

A plot of iodine bound (mg/100mg. polysaccharide) v. total free iodine was constructed and the iodine affinity found by extrapolating the linear portion of the curve to zero free iodine concentration.

7. β - AMYLOLSIS.

15 mg. of amylose were dessolved in 10 ml. of 0.2N potassium hydroxide and the solution neutralised with hydrochloric acid. Because glycogen and amylopectin are soluble in water, the alkali treatment was omitted. To the neutral solution, 3 ml. of sodium acetate/acetic acid buffer (pH 4.8) and 0.1mls of β-amylase solution were added. The solution was made up to 25ml. and incubated at 35°C for 36 hours. 5 ml. samples were withdrawn after 8, 12, 24 and 36 hours incubation; and the percentage conversion to maltose determined by the method outlined above. β-amylolysis limits of amylose, amylopectin and glycogen were determined.

8. OPTICAL ROTATION.

The optical rotation of glycogen in water was measured (conc. 1%) in a Hilger polarimeter.

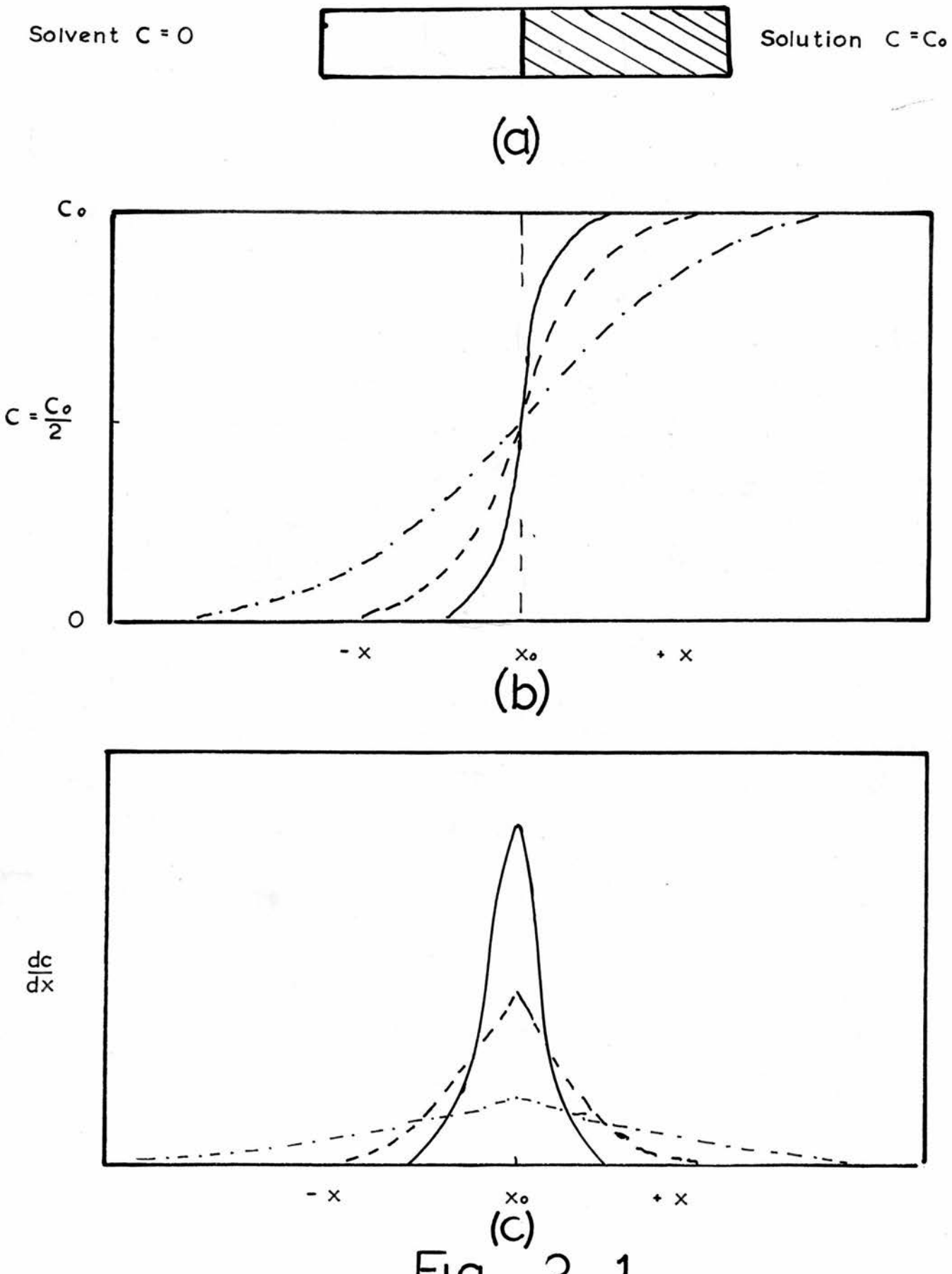

Fig. 2. 1.

9. DIFFUSION.

Theoretical. Consider a system in which a solution (concentration Co) is in contact with its solvent as shown in fig. 2. 1A (~~timed through 90 clockwise~~). The boundary between solvent and solution is at a point $x = o$. It is assumed that the only external forces acting on the system are osmotic and gravitational. If the system is in the vertical position then the gravitational force maintains the concentration constant within a horizontal plane. Under these conditions the rate of diffusion is according to Fick (89)

$$\frac{dm}{dt} = -DA \frac{dc}{dx} \qquad 2.\ 1.$$

where dm is the quantity of solute which in time dt diffuses across a boundary of cross sectional area A under the influence of a concentration gradient dc/dx. D is the diffusion constant of the solute molecules. Expressing mass in terms of concentration equation 1 becomes

$$\frac{\partial c}{\partial t} = D \frac{\partial^2 c}{\partial x^2} \qquad 2.\ 2.$$

The solution of the above equation must satisfy the following conditions at $t = o$; $c = o$ for $x < o$; $c = c_o$ for $x > o$, where Co is the initial concentration.

If there is no change in concentration at either end of the cell then a solution to 2. 2. is

$$C_x = \frac{C_0}{2}\left\{1 - \frac{2}{\sqrt{\pi}}\int_0^Y e^{-Y^2} dy\right\} \quad \text{where} \quad y^2 = \frac{x^2}{4Dt} \qquad 2.\ 3.$$

In fig. 2. 18. the relation are shown between c and x for various values of t.

If an interferometric optical method is employed for scanning the system, then the curves in fig. 2. 18. are obtained. These may be changed into dc/dx v x curves by arithmetical differentiation. If Schlieren optics are employed then the differential curves are obtained directly (as in fig. 2. 1c). In the ideal case, these curves have the shapes of Gaussian distribution curves and are equal with respect to area. These curves follow the equation;

$$dc/dx = c \exp\left(-x^2/4Dt\right) / 2\sqrt{\pi\ Dt} \qquad 2.\ 4.$$

Most methods of calculating the diffusion constant are based on the assumption that in the ideal case the curves have the properties of a Gaussian distribution.

Although D may be calculated by 4 different methods, only two of these have been quoted extensively. These are (1) Maximum Ordinate-Area Method, Da and (2) the Statistical or Moments method, Dm,

$$Da = A^2 / 4\ \pi\ t\ (Hm)^2 \qquad 2.\ 5.$$

where A is the area with x measured in cms. and y measured in arbitrary units. Hm is the height of maximum ordinate in y units.

$$Dm = \sigma^2/2t \qquad 2.\ 6.$$

where σ is the standard deviation.

For a monomolecular system then Dm = Da, but for a polymolecular system Dm $\neq$ Da. The ratio Dm/Da has been quoted by Gralen (90) as being a measure of the polymolecularity of the system. Gralen has proved that Dm is a weight-average diffusion constant, the actual significance of Da for a polymolecular system still awaits elucidation.

In the past, several attempts have been made to measure diffusion constants by indirect methods. Noteworthy in this field is the measurement of diffusion constants from the boundary spreading during sedimentation-velocity experiments. Until recently this method suffered from the disadvantage that Faxens (91) equation (from which D was calculated) did not take into account that the sedimentation constant (S) was dependent on concentration. The development of the method awaited a solution of the equation (2. 7.) when S was dependent on C.

$$\frac{\partial c}{\partial t} = \frac{\partial}{r\partial r}\left\{r\left(D\frac{\partial c}{\partial r} - S\omega^2 r c\right)\right\} \qquad 2.\ 7.$$

where c is concentration of solute, t is time, r is distance from centre of rotation, ω is angular velocity, D is the diffusion coeff. and S is the sedimentation coeff.

In 1956 Fujita (92) solved the above equation and obtained an equation for the boundary gradient curves observed when there is a single monomolecular solute with D constant and S a linear function of C.

Baldwin (93) stated that Fujita's equation (47) may be written as

$$\left(AF(\varepsilon_m)/H\right)^2 = 2D(e^{\gamma}-1)\left\{1+(1-\lambda)^{\frac{1}{2}}\right\}/\omega^2 S_0 \qquad 2.\ 8.$$

where $A/H = \int_{x_0}^{x_w}(dc/dx)\,dx/(dc/dx)max. = \int_{x_0}^{x_w}(dnc/dx)dx/(dnc/dx)\ max$

$$\varepsilon_m = (\omega^2 S_0 x_0^2 k C_0/2D)^{\frac{1}{2}}\left\{\lambda^{\frac{1}{2}}/(1+(1-\lambda)^{\frac{1}{2}})\right\}$$

$$F(\varepsilon_m) = \frac{\Phi'(\varepsilon_m)}{1+\Phi(\varepsilon_m)} + 2\varepsilon_m$$

$$\Phi(\varepsilon_m) = \frac{2}{\pi}\int_0^{\varepsilon_m} e^{-y^2}dy$$

This function can be obtained from tables.

Φ' = differential of above from above tables.

$$\lambda = kC_0(1-e^{-\gamma})$$

$$\gamma = 2\omega^2 S_0 t$$

$$S = S_0(1-kc)$$

$S_0 = S$ at $c=0$ at $20^\circ C$.

$C_0 = C$ at $t=0$

ω is angular velocity.

Although the above equation holds only for a monomolecular substance, Baldwin (93) obtained results 10% high for a hetereogeneous sample of bovine plasma albumin.

Baldwin (94) also considered the case of a polymolecular system in which both S and D of the individual species are functions only of the concentration, Employing a statistical approach he derived the following formula:-

$$P = \left\{ B/\omega^4 x_0^2 \; F(t) \right\}^{\frac{1}{2}} \qquad 2.\ 9.$$

where P is the standard deviation of the sedimentation coeff and

$$B = \sigma^2 - \sigma_0^2 - 2\omega^2 \bar{S}^+ \int_{t_0}^{t} \sigma^2 dt - 2\left(\bar{D}_0 - \frac{k n_c^0}{2}\right)(t - t_0) \qquad 2.\ 10.$$

$$+ 2\omega^2 \int_{t_0}^{t} \bar{x}\,(2a_1 q_1 + 3a_2 q_2)\, dt$$

$$F(t) = (t^2 - t_0^2) + 4(\omega^2 \bar{S}^+)(t^3 - t_0^3)/3 \qquad 2.\ 11.$$

where x_0 is distance of meniscus from centre of rotation.

ω = angular velocity 2. 11a.

$\bar{S}^+ = \bar{S}_0 - a_1 n_c^0 - a_2 (n_c^0)^2$

$S_0 = \sum_i \alpha S_{i0}$, $n_c^0 = \sum_i R c_i^0$ R is a constant.

$\sigma^2 = \mu_2 - (\mu_1)^2$ μ_1 is the first moment = $\bar{x}$

α = is fractional amount of solute i

$S_i = S_{i0} - a_1 n_c - a_2 n_c^2$

$D_i = D_{i_0} - k n_c$

$$\bar{x} = \int_{x_0}^{x_\omega} x \left(\frac{dc_i}{dx}\right) \frac{dx}{c_1^\beta}$$

$$Q_1 = \int_{x_0}^{x_w} (x - \bar{x})\, n_c\, (dn_c/dx)\, dx \,/\, n_c^{\beta}$$

$$Q_2 = \int_{x_0}^{x_w} (x - \bar{x})\, n_c^2\, (dn_c/dx)\, dx \,/\, n_c^{\beta}$$

x_w is a position in the plateau region (β) where $dc/dx = 0$.

This theory presumes a knowledge of the diffusion constant but when it is not possible to make independent diffusion measurements, in which case (D-km/C) is unknown, then the above equation may be used in another way (94). If $\sigma^2_{corr.}$ is defined by

$$\sigma^2_{corr.} = \sigma^2 - 2\omega^2 \bar{s}^{+} \int_{t_0}^{t} \sigma^2 dt \pm 2\omega^2 \int_{t_0}^{t} \bar{x}\,(2a_1Q_1 + 3a_2Q_2)dt \quad 2.\ I2.$$

$\sigma^2_{corr.}$ can be plotted against $t-t_0$. If the solute is monomolecular, the plot will be a straight line with slope 2(D-mk/2) whereas for a polymolecular solute, the plot will have upward curvature.

The above theory, however has the following limitations (94.). (1) For systems which are both strongly concentration dependent and markedly polymolecular, the representation of the depenence of Si on Nc in equation 2. 11a. will be inadequate when the initial concentration is more than a certain value. (2) For the purpose of calculation, equation 2. 11a. will be considered satisfactory only if any error introduced into B by the use of this

Antweiller Diffusion Cell

Filling Position

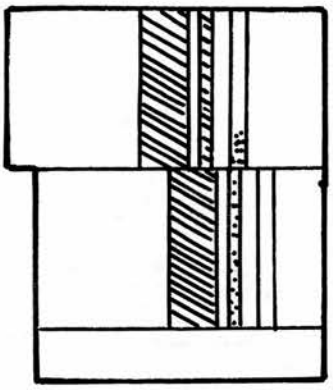

Measuring Position

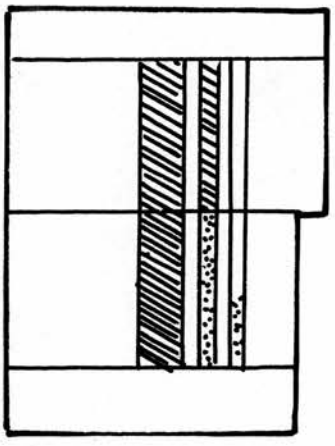

Solvent

Solution

equation is less than the experimental uncertainty of σ^2. Provided that $\bar{s}^+/\bar{s}_0 > 0.9$ this should not be a serious source of error.

The above limitations necessitate that experimental work is made in the very dilute range. As will be shown later, the system under consideration restricts the concentration range to 0.01 - 0.1 gms/100 ml. This is 1/20th of the concentration Baldwin employed to confirm the theory using protein solutions.

Experimental. Diffusion measurements were carried out in an Antweiler micro-electrophoresis and diffusion apparatus at 20°C. The measurement of the change in refractive index or refractive index gradient with respect to position in the cell is measured by a Jamim interferometer or by a Philpott-Svennson Shlieren system.

Using the interferometer the measurement of the relative refractive index and the raising or lowering of the cell (in 0.1 mm. intervals) is done manually. Facilities are available for taking a photographic record of the schlieren diagram.

The standard cell for the apparatus is illustrated opposite. In this cell the solvent/solute boundary is formed by sliding one compartment over the other. Facilities are available for doing this slowly and accurately. The optical path length of the solution is 0.5 cms.

From the initial runs (amylose A98 1% solution in KOH), it was obvious that there were going to be many complicating factors. The following results were obtained employing the interferometric system.

Temp. 20°C. concentration 1% solvent 0.2MKOH. substance A98.

TABLE. 2. 1.

Run.	Da.x 10^{7}	Dm. x 10^{7}
1	2.8	16.57
2	2.12	16.82
3	2.84	15.87
4	1.98	14.62

$Da = 2.44 \times 10^{-7}$

$Dm = 15.47 \times 10^{-7}$

$Dm/Da = 6.34$

The high Dm/Da ratio and the obviously too high value for Dm(Glucose at 20°C $D \simeq 6.0 \times 10^{-7}$) raised the question whether any small sugars were present. The amylose samples were examined chromatographically (various solvents) for low molecular weight constituents. In every case no material left the starting line, and hence no oligosaccharides were present.

When the sedimentation constant of the above sample was determined, it was found to have a large concentration dependence. As a consequence of the above it was thought that D was probably concentration dependent. The diffusion constant was measured at 0.1% concentration, the results are listed below.

Substance A98 concentration 0.1% Solvent 0.2MKOH. temp. 20°C.

TABLE. 2. 2.

Run.	Da. x 10^7	Dm. x 10^7	Da x 10^7 corr.	Dm x 10^7 corr.
1	6.88	4.71	0.78	0.98
2	0.94	0.94	0.94	0.94
3	0.75	0.88	0.76	0.92
4	0.29	0.22	0.81	1.30
5	0.12	0.11	0.60	0.86
6	0.23	0.13	0.83	1.00

At such a low concentration it is impossible to utilise the Schlieren system, because of the glass/grease/glass interface and hence the Jamin interferometer was employed.

After the results in table 2. 2. columns 2 and 3 had been obtained, the method was examined critically. Even with the interferometric system it is impossible to take readings at the glass/grease/glass interface. This results in no readings for approx. 0.4 mm. This in itself would not be disastrous, but it occurs at the maximum in the dn/dx v x curve. The manufacturers suggest that the position of the missing points may be found by linear interpolation . This was the method employed in calculating the results in columns 2 and 3 of table 2. 2.

Fig. 2.2.

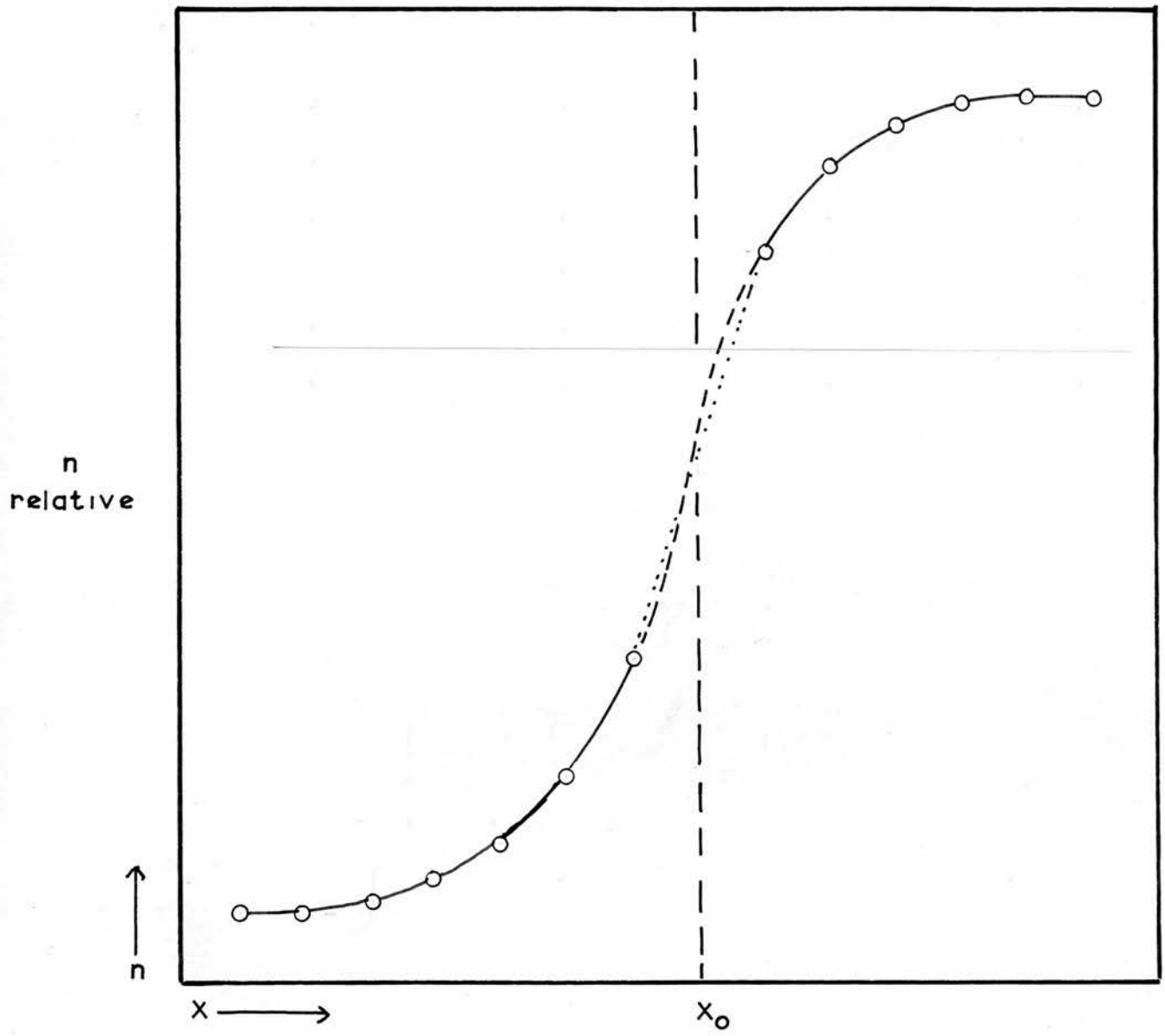

The relative refractive index v. x results were plotted and a curve drawn through the missing point positions subject to the following conditions. (1) The curve must be smooth and continuous (2) at x_o the refractive index has a constant value ($c_o/2$ at boundary position). Taking the values of the missing points from the curve so formed, the results in columns 4 and 5 of table 2. 2. were obtained. In fig. 2. 2. is shown a curve with the two types of interpolation. Though the difference looks small, the actual effect is large as may be seen from the results. That the second method gives more consistent results is obvious but the validity of these results is very doubtful.

The conclusion drawn from the above was that employing the standard cell it was impossible to measure the diffusion constant at low concentrations with accuracy.

In an effort to find an answer to the problem, two different approaches were tried. (1) An analysis of the indirect methods of measuring diffusion constants (2) design of a new cell.

The design of a new type diffusion cell is a problem which has been attempted by many investigators with varying degrees of success.

In this case, the normal restrictions on the design of a diffusion cell were applicable, but at the same time there was the additional restriction that the new cell must fit the Antweiler apparatus.

No previously designed cell could either fulfil the requirements (ie. increased path length through solution, boundary not at junction of half cells when measuring, same or smaller external dimensions as standard), or be easily modified to fulfil them. As the design and building of a new cell was going to be time-consuming, if not impossible, and analysis of the indirect methods was undertaken.

The best hope of success lay in determining the diffusion constant from the boundary spreading during sedimentation velocity experiments. It was realised that only a partial success could be obtained as the theories were going to be applied at or near their limits. At this stage in the work only 12 mm. Kel F sedimentation cells were available which curtailed the concentration to above 0.15%.

As the theoretical work discussed above had only been recently published no work other than Baldwins original (94) was available. Baldwin had applied the theory to β-lactoglobulin (no measurable heterogeneity) and bovine plasma albumin (moderate heterogeneity $P_{2sw} = 1.05$ and $P_{2sw} = 0.69$ S) In view of this it was decided to test the theory employing the water soluble polysaccharide from Zea mays and glycogen. The fractions employed had a large positive skew distribution, S was dependent on C (95, 96), and the diffusion constant had already been measured by direct means (95, 96).

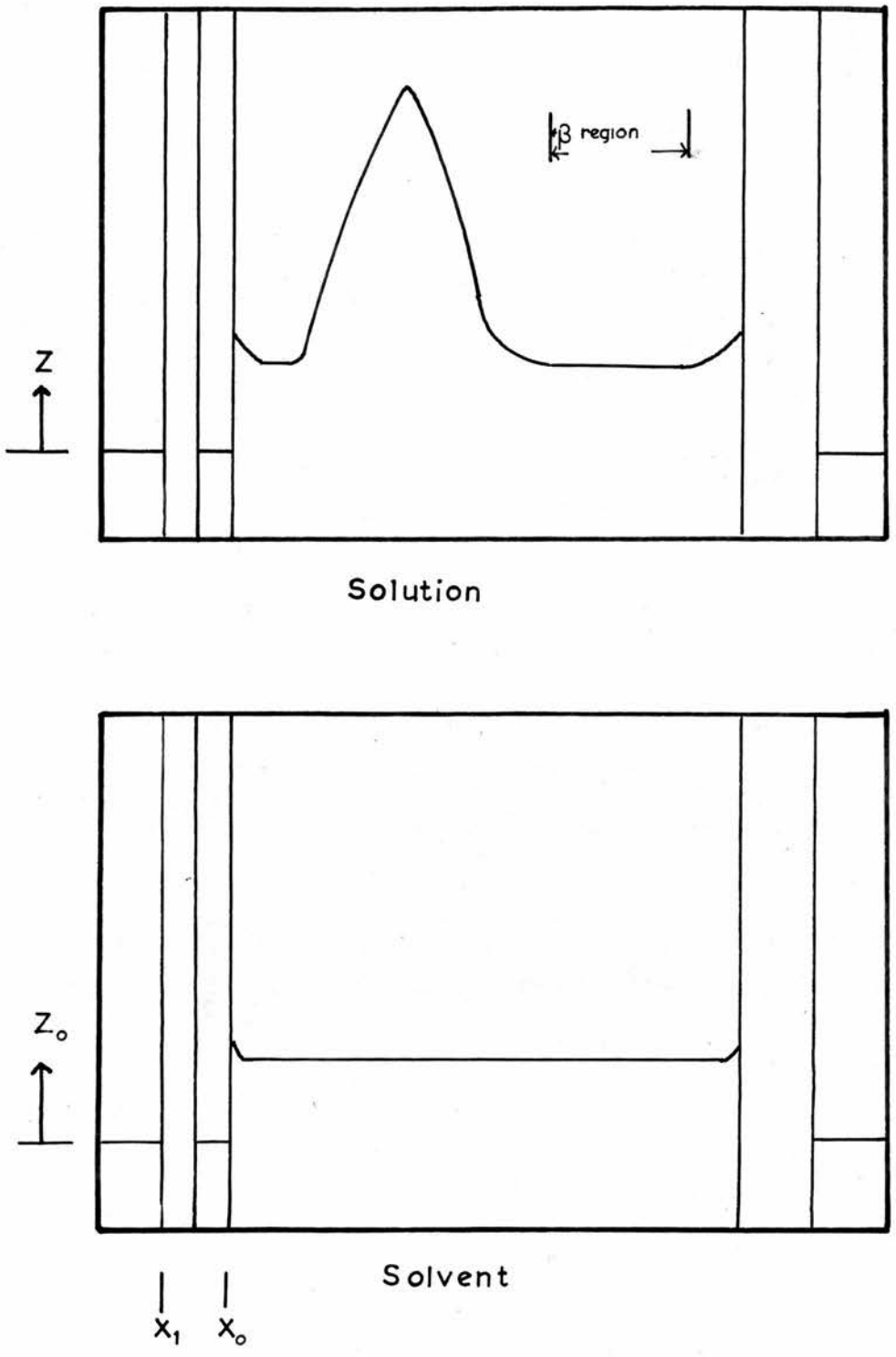

Fig. 2. 3.

In order to calculate ρ from a given sedimentation experiment, the following groups of quantities are required.

(1) Those which are computed from each schlieren photograph by numerical integration: $\bar{x}$, σ^2, Q_1, Q_2, and n_c^0

(2) Those which must be found from additional experiments: a_1, a_2, and $(\bar{D}_0 - k\frac{n_c^0}{2})$

(3) others, the anqular speed of rotation, ω and the time from the first photograph.

Numerical values for the above quantities are determined as outlined below.

In fig. 2. 3. are two schlieren diagrams, one is the diagram of a solution containing a species which is sedimenting and the other is the diagram of pure solvent.

The distance between two points in the cell, x_1 and x_2 is magnified on the schlieren curve by a factor F.(2.215). $X_2 - X_1 = F(x_2 - x_1)$ where X is the co-ordinate axis on the photographic plate which corresponds to the direction of sedimentation in the cell. The other co-ordinate Z is linearly related to $\partial n/\partial x$. $Z = G.AB\cot\psi(\partial n/\partial x + f(x))$ denoting Z in the reference baseline experiment (pure solvent) by Zo then $Zo = GAB\cot\psi(\partial n_0/\partial x + f_0(x))$, if $f(x) = f_0(x)$ then

$Zc = Z - Zo = GAB\cot\psi\ \partial n/\partial x$ 2. 13.

where G is the magnification due to cylindrical lens, A is the optical path length through solution, B is the optical lever arm and ψ is the angle of the schlieren diaphragm.

By means of a comparator (2 dimensional) ~~then~~ Zc may be measured at fixed intervals of X.

If X' is an arbitrary origin from one of the set of readings (X. **Z.**) and by writing $X - X'$ as $h\Delta X$. Thus h takes values of 1. 2. 3..... to the right of X and -1 -2 -3..... to the left of X then $x' = x_1 + (X - X_1)/F$

where x_1 is the distance from the centre of rotation to an edge of an index hole in the counterbalance cell and X_1 marks this edge on the photographic plate and

$$\bar{x} = x' + \Delta X \sum h Z_c / F \sum Z_c$$
$$\sigma^2 = (\Delta X/F)^2 \sum h^2 Z_c / \sum Z_c - (x' - \bar{x})^2$$
$$Q_1 = \Delta X \sum h n_c Z_c / F \sum Z_c + (x' - \bar{x}) n_c^{\beta}/2.$$
$$Q_2 = \Delta X \sum h n_c^2 Z_c / F \sum Z_c + (x' - \bar{x})(n_c^{\beta})^2/3$$

Where $n_c^{\beta} = \Delta X \sum Z_c / FG.AB \cot\psi$ and

$$(n_c)_j = \frac{\Delta X}{FGAB\cot\psi}\left\{\sum_{i=2}^{j-2}(Z_c)_i + (Z_{c_i} + Z_{c_j})/2\right\}$$

as a check on the accuracy of the $\partial n/\partial x$ measurements

$n_c^0 = n_c^{\beta}(\mu_2/x_0^2) = n_c^{\beta}(\bar{x}^2 + \sigma^2)/x_0^2$ and n_c^0 may be found using a differential refractometer.

Also $Ln(\mu_2/x_0^2)^{\frac{1}{2}} - (\omega^2 t)^2 \bar{S}^+\left\{a_1 n_c^0 + 2a_2(n_c^0)^2 - P^2/S^+\right\} = \bar{S}^+\omega^2 t$ 2. 14.

Thus to calculate $\bar{S}^+$ from a given experiment, one needs preliminary estimates of a_1, a_2, P and t_0 . Since for dilute solutions the $(\omega^2 t)^2$ term is usually not very large then the estimated values need not be accurate.

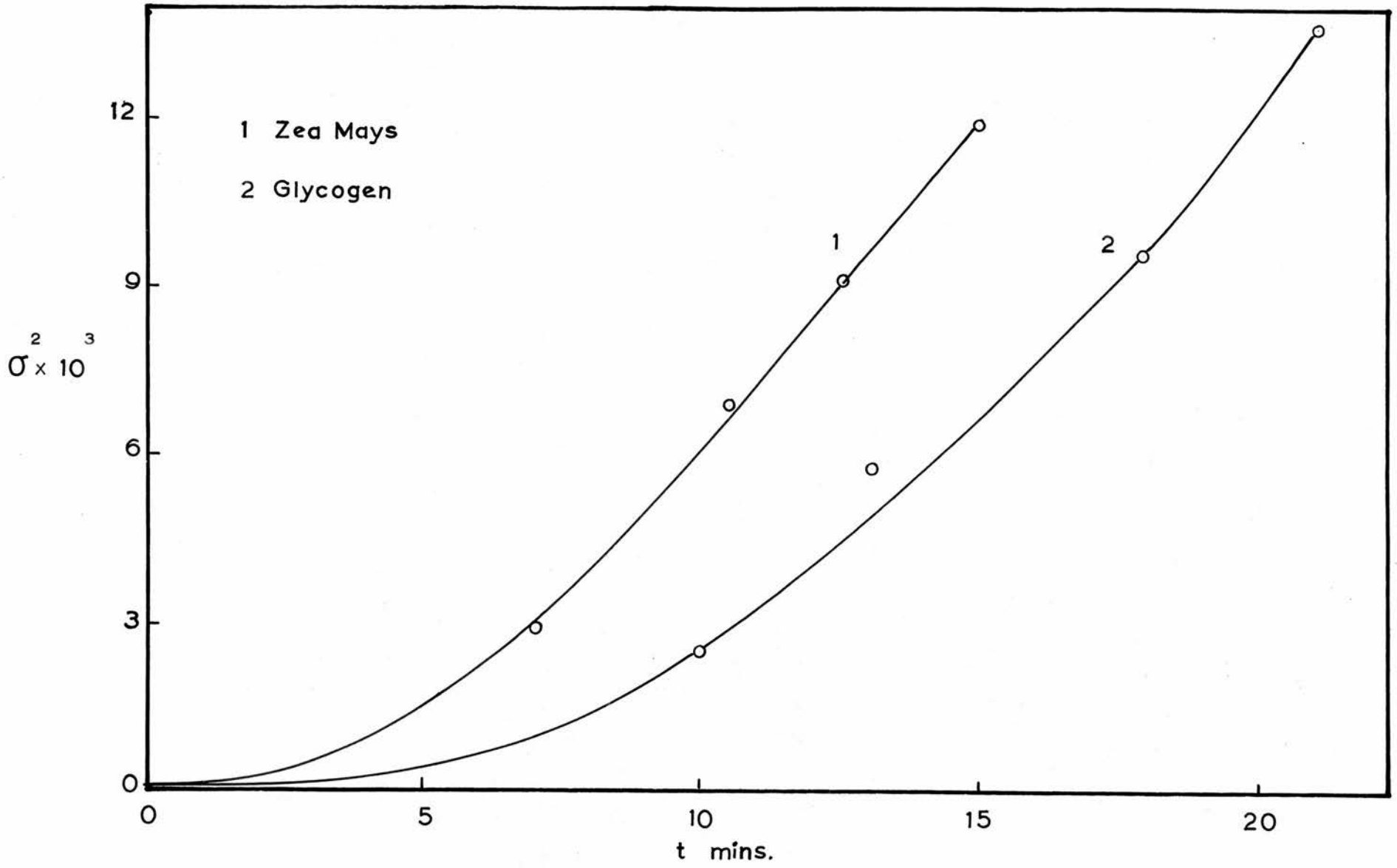
1 Zea Mays
2 Glycogen
1
2
12
9
6
3
0
$\sigma^2 \times 10^3$
0
5
10
15
20
t mins.

Fig. 2. 4.

Due to the polymolecularity of the two samples it was impossible to measure the schlieren diagrams after 17 mins ultracentrifugation (20,000 r.p.m.). This curtailed the experiment, so that only five schlieren diagrams were available for computation.

The method of finding numerical values for the following integrals $\int_{t_0}^{t} \sigma^2 dt$ and $\int_{t_0}^{t} \bar{x} q_1 dt$ is by trapezoidal integration. $\int_{t_0}^{t} \sigma^2 dt = \Delta t \left\{ \sum_{i=2}^{i=n-1} \sigma_i^2 + (\sigma_1^2 + \sigma_n^2)/2 \right\}$ This method is accurate if n is a large number. In the above case $n = 5$ which is not enough to employ the above method, but by plotting σ^2 v. t it was possible to obtain a better approximation. This method was employed for both integrals.

When $\sigma^2_{corr.}$ v. t was plotted for glycogen and Zea mays both curves had upward curvature (fig. 2. 4.), and hence it was impossible to obtain Do directly. Do had therefore to be obtained by inserting the information obtained from experiment into equation 2. 9. and solving the simultaneous equations so formed for the unknowns, ρ and Do. Previous experiments had shown that in both cases (glycogen and zea mays) -k was very small. The values obtained are listed in table 2. 3.

TABLE. 2. 3.

Substance.	Classical.		Indirect.	P-indirect.	P-distribution.
	$\times 10^7$ Da.	$\times 10^7$ Dm.	$\times 10^7$ Do.	S	S.
Zea mays.	0.41	0.53	0.53	82.9	
Glycogen.	1.23	1.60	1.22	34.55	36.5

P-distribution was obtained from a determination of the molecular weight distribution of the above glycogen sample by the method in section 4. 4 b.

Although the above results substantiate Baldwins method, it is doubtful whether the above application results in an accurate value of Do being obtained.

If equation 2. 9. is written in the form

$$\sigma_x^2 - \rho^2 x_0^2 \omega^4 F(t) = 2(t - t_0)(D_0 - k m_c^0/2)$$

where

$$\sigma_{xc}^2 = \sigma^2 - \sigma_0^2 - 2\omega^2 \bar{s}^2 + \int_{t_0}^{t} \sigma^2 dt + 2\omega^2 \int_{t_0}^{t} \bar{x}(2a_1 Q_1 + 3a_2 Q_2)\, dt.$$

and it assumed that $k \simeq o$ (from experimental evidence in the above cases) then $\Delta f(z) = 2(t - t_0) D_0$. So that $\Delta f(z)$ increases with t and D and decreases in P . However all the above terms are interdependent. Obviously if $\Delta f(z)$ is small then the errors in Do will be large. The method will be accurate for either (1) a polymer with a broad distribution ($P^2 = 10 \times 10^{-23}$) and a high D ($D = 1 \times 10^{-6}$) or (2) a polymer with a narrow distribution ($P^2 = 1 \times 10^{-26}$) and a low D ($D = 1 \times 10^{-7}$).

The samples of Zea mays and glycogen studied here would appear to be the lower limit for samples of such wide monomolecularity and diffusion coefficient.

As amylose would be investigated under similar conditions (P^2 large, $D = 1 \times 10^{-7}$) and as S is strongly concentration dependent it was decided not to pursue the matter any further.

The above method is obviously going to be of great value in the measurement of the molecular weights and polydispersity of proteins and enzymes where only milligrams of material are available and it is preferable to obtain a molecular weight without destroying or degrading the material.

By employing an interference optical system rather than the Philpotts-Svenson Schlieren optics it should be possible to increase the accuracy of the method, but whether this would increase the range of applicability is an open question. This hypothesis was not tested due to interference optics being unavailable.

After the above attempts, it was decided to design and build a new cell. It was thought that the best chance of success lay in combining the boundary-formation-by-sliding type cell (Antweiler) with the boundary-raising type cell (Lamm).

The main problem at this stage was of making a diffusion compartment which had a constant cross-sectional area and two opposite faces optically plane and parallel. It was found that two 1 cm. "Unicam" cells could be aligned such that the necessary conditions were fulfilled.

Diffusion Cell

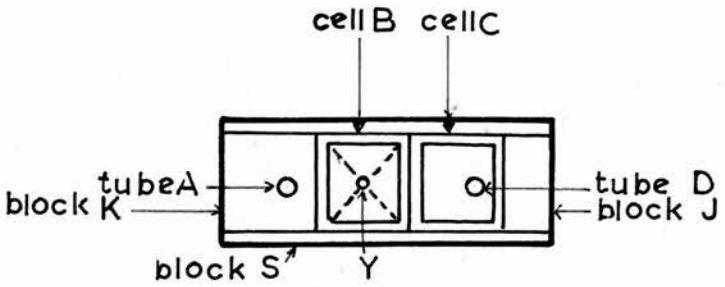

TOP VIEW

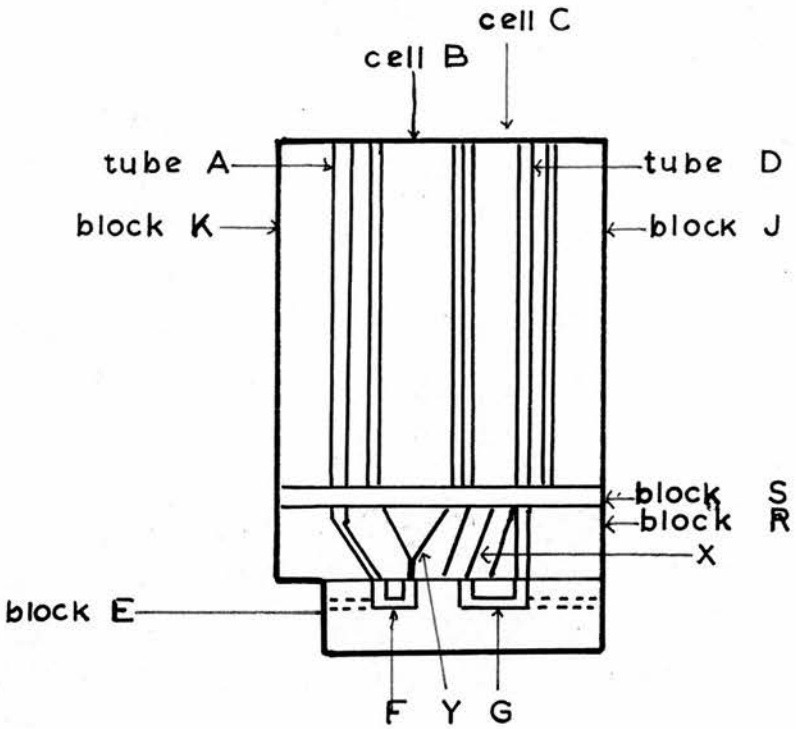

FRONT VIEW

Fig. 2. 5.

Two "Unicam" cells (1 cm.) which could be aligned such that the faces were optically plane and parallel (checked using Jamin interferometer) had their bases removed and were sealed together with "Araldite" cold-setting resin. The sealing was carried out with the cells in the light path of the Jamin interferometer in order that any disturbance caused by the drying of the resin could be corrected immediately. A block of Perspex was heated in an oven until it became soft and then an accurately made pyramidal brass die was pressed into it and held in the press until the Perspex was hard. The block was then removed, machined to the required dimensions and the holes for tubes A, D and X drilled (see fig. 2. 4.). The block E was also made of Perspex, machined to the correct size and drilled. The ends of the horizontal drilling were then sealed as in fig. 2. 5. Blocks J. K. and S were machined to size and drilled. A piece of capillary tubing (0·5 mm.) was ground to the required angle at each end and sealed into block R (Araldite). The two cells were then sealed onto block R and inside block S (Araldite). The fit of cell B over was the critical alignment at this stage, a bad fit at this junction would cause turbulence when the boundary was raised. The tube D, blocks Jand K and tube A were sealed in position (Araldite) and the cell set aside for 3 days. The faces of blocks R and E were then ground together (jewellers rouge) until a perfect fit was obtained. During the experimental

a watertight seal at the E/R interface was formed by employing a small amount of silicone grease. As an added precaution against leakage, a spring loaded top was built for the cell. The completed cell is shown in fig. 2. 5.

The cell manipulation is as follows. Solvent is inserted down tube A (hypodermic) and via F and Y fills cell B. By this mehtod no air bubbles occur at the interface of F and Y. Cell B is filled to approx. 1.5 cms above the top of block R. Solution is inserted down tube D (hypodermic) and allowed to fill cell C via the capillary X, and tube G to the same level as cell B. This results in no air bubbles in G or X. The cell is now put into the Antweiler apparatus and allowed to come to temperature equilibrium. Block E is then moved (mechanically) until G connects the ends of X and Y. A small amount of solution (0.1 ml.) is added to cell C every 5 mins. The level in B rises but due to the fine capillary there is no sudden change in liquid levels. Y which has an inverted pyramidal shape allows the boundary to expand in the X and Z planes from 1 mm. diameter to 1 cm. square without causing any turbulence. When the level of the boundary (as seen by the schlieren system) is in a suitable position for taking readings the addition of further solution is discontinued.

The experiments were timed from the instant that X and Y were connected. This procedure should result in the time of diffusion being less than the measured time. As will be seen from the results

Fig. 2.6.

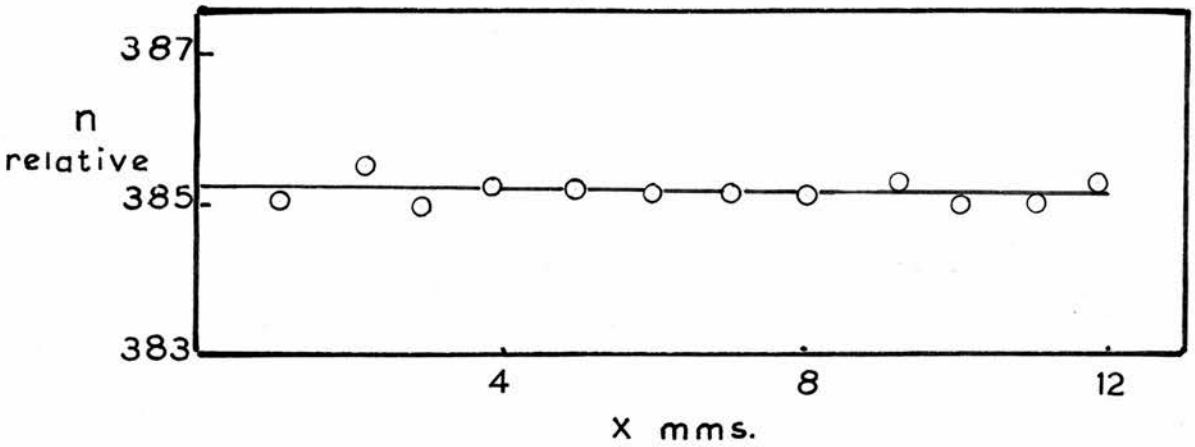

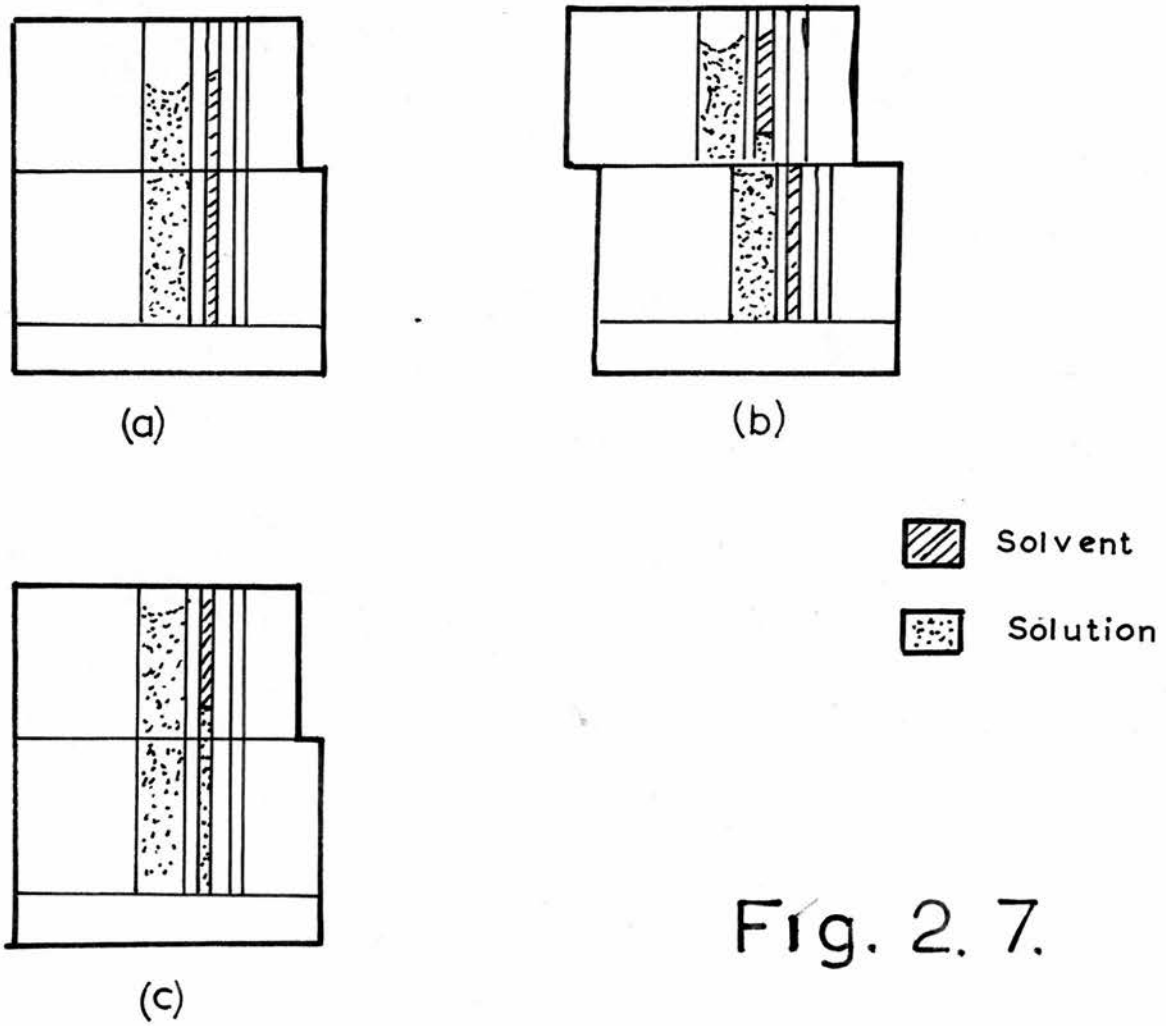

Fig. 2. 7.

of experiments on substances with known diffusion coefficients the error due to the latter is small (table 2. 4.).

The alignment of the two "Unicam" cells was checked by inserting water in both and measuring the relative refractive index with distance and it was found to be satisfactory fig. 2. 6.

The results in table 2. 4. were obtained employing the above cell.

TABLE. 2. 4.

Substance.	$D \times 10^7$ measured.	$D \times 10^7$ literature value.
Glucose	0.50	0.53
	0.52	
Maltose.	0.39	0.41
	0.40	

Most of the D's quoted in the "Results section" were obtained using the above cell. However the use of alkaline solutions resulted in the soft glass of the "Unicam" cells being eventually attacked and hence benefiting from experience with the above cell new method of making use of the Antweiler silica cell was evolved.

The new movements and positions of the Antweiler cell are shown in fig. 2. 7. The cell is filled as in fig. 2. 7(a). The upper compartment is then moved to the position shown in fig. 2. 7(b) careful addition of more solution to the

comparison compartment (by means of a micrometer syringe) will raise the boundary from its interfacial position. The cell is then moved into position C fig. 2. 7, after removal of the residual solvent and its replacement by solution. In this manner extremely sharp boundaries were formed.

10. PREPARATION OF SOLUTIONS.

Amylose is soluble in potassium hydroxide solution but since on standing retrogradation takes place with the formation of a precipitate, all work on the solution should be completed within 24 hours. Since the presence of oxygen in the alkaline solution results in degradation of the amylose, an inert atmosphere is necessary.

Again, if an aqueous solution containing dissolved oxygen is irradiated with ultrasonic waves hydrogen peroxide is formed, which would lead to oxidative breakdown.

As the above effects would be superimposed on any mechanical degradation it was necessary to eliminate them.

A survey of the literature (97) led to the conclusion that if the solution was saturated with hydrogen before and during irradiation the formation of hydrogen peroxide would be suppressed and probably eliminated. This hypothesis was tested using hydrogen saturated distilled water: no hydrogen peroxide could be detected even after 6 hrs. irradiation (see estimation of hydrogen peroxide).

Cylinder hydrogen after passage through a glass wool pad to remove dust particles was employed without further purification.

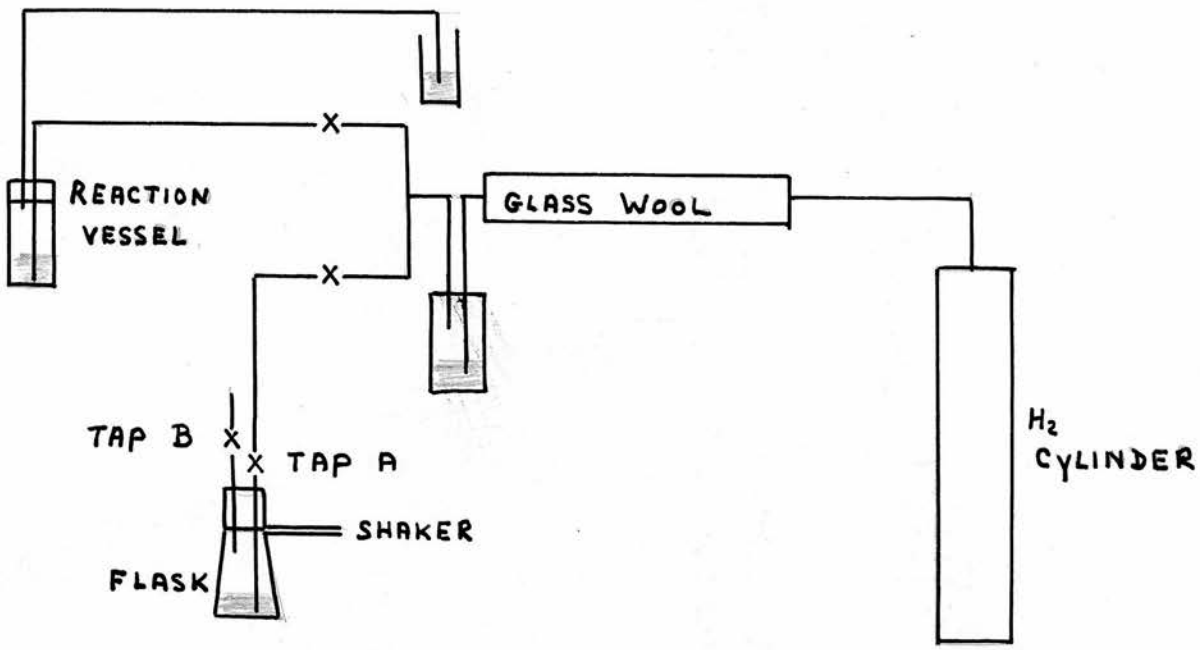
REACTION VESSEL
GLASS WOOL
TAP B
TAP A
SHAKER
FLASK
H_2 CYLINDER

Fig. 2. 8.

The hydrogen was bubbled through potassium hydroxide (0.2N) (fig. 2. 8.) before entering the reaction vessel or the flask containing the solution, and maintained at 2 or 3 cm. (water) above atmospheric pressure by passing the exit gas through a potassium hydroxide bubbler. The latter served as a check that the hydrogen flow through the reaction vessel was satisfactory.

Amylose solutions:-

Approximately 75 mg. of amylose were inserted in a weighing-stick, and dried in a vacuum drier (80°C) for 4 hours. The weighing-stick was then removed, stoppered and placed in a vacuum desiccater for 20 mins. for temperature equilibration. The sample was then weighed by difference, placed in a 50 ml. flask and 30 ml. of 0.2N potassium hydroxide added. The flask was immediately stoppered and flushed with hydrogen for 4 mins. The hydrogen stream was then discontinued by closing tap B (fig.2. 8.) and by leaving tap A open an hydrogen atmosphere (5lbs./sq.in above atmospheric) was maintained. The flask was then agitated on a "Microid" shaker for 4 hours. After filtration through a G.4 sintered glass filter, 20 ml. of the solution was placed in the reaction vessel and a stream of hydrogen passed through immediately. Passage of hydrogen was carried out for 30 mins. before irradiation started, during irradiation and for 10 mins. after irradiation ceased.

The irradiated solution was then divided into 5 parts: 5 ml. for β-amylolysis, 3 ml. for sedimentation, 5 ml. for viscosity and concentration, 5 ml. for diffusion, the remainder (1.5 ml. divided into 3 equal parts by an "Agla" syringe) for determination of concentration by the method of Lampitt, Fuller and Coton (86).

The "5 ml. for β amylolysis" was neutralised by a predetermined volume of hydrochloric acid (0.1N) and the estimation carried out as outlined under "β amylolysis".

The "5 ml. for sedimentation" was diluted with 0.2N potassium hydroxide (using an "Agla" syringe) to give 5 solutions the concentrations of which varied from 0.015 - 0.07% and the sedimentation coefficient determined as in "Sedimentation".

The sample for viscosity and concentration was placed in the Ubbelohde viscometer, 10 ml. of filtered potassium hydroxide added and the viscosity determined. Four 5 ml. successive additions of same solvent were then carried out, the viscosity being determined after each addition. The solution was then removed from the viscometer and 25 ml. (5x5 ml) of the solution used to determine the concentration.

The diffusion sample was diluted to give 4 samples with a concentration range 0.1 - 0.2% and the diffusion coefficient determined as in "Diffusion".

The above method gave 5 independent checks on the concentration of the solution. Volumes below 3 ml. were measured by "Agla" syringe.

Amylopectin solutions.

Amylopectin solutions were treated in the same manner as above with the exception that the solvent was 0.2N sodium chloride and the dilution range for sedimentation was 0.1 - 0.25%.

Glycogen solutions.

Glycogen solutions were treated in the same manner as above with the exception that the solvent was distilled water.

11. ESTIMATION OF HYDROGEN PEROXIDE.

Hydrogen peroxide was estimated by the method of Ovenston and Rees (98).

A volume of a neutral solution not exceeding 4 ml. and containing not more than 12 μg. of hydrogen peroxide is placed in a 10 ml. calibrated flask. 5 ml. of 0.2M potassium iodide solution and 0.1 ml. of 0.5 per cent W/V ammonium molybdate are added and the volume made up to the mark at 20°C. The solution is allowed to stand in the dark for 5 minutes and then the extinction coefficient of the solution at 353 m in a 1 cm. cell is measured. The reading is corrected for difference in cell thickness and the extiction reading of the reagent blank (prepared similarly but with 4 ml. of water in place of the hydrogen peroxide sample) is subtracted.

By use of known solutions of hydrogen peroxide, a calibration graph was determined for the concentration range 0 - 14 μg.

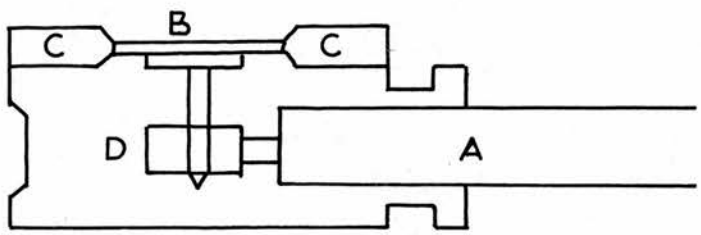

A coaxial cable
B quartz crystal
C face plate
D r.f. lead

Fig. 2.9.

12. ULTRASONIC GENERATOR.

The source of ultrasonic waves was a Mullard High Frequency Ultrasonic Generator type E.7562.

This is a piezo-electric type generator Radio-frequency voltages are generated by a silica triode which is capable of giving over a kilowatt output. The H.T. voltage for this is supplied by two grid-controlled mercury vapour rectifiers in a full-wave circuit. The output of the oscillator triode is controlled via the H.T. voltage, by varying the phasing on the rectifier grids; the actual control being a potentiometer giving continuous variation. The frequency of the oscillator can be altered by changing the oscillator coils.

The R.F. voltage is fed via a coaxial cable to the transducer-head (fig. 2. 9.) containing the crystal. The latter is an x-cut quartz disc, 4.5 cm. in diameter, silvered on both sides and mounted on the face plate of the transducer-head by "Araldite" thermosetting resin. The high potential side of the R.F. lead is applied to the back of the crystal, the return path to earth being from the front silvering to the outside of the transducer-head and the sheath of the coaxial cable. The whole of the transducer, including the cable entry, is water-tight and can therefore be mounted in a thermostated bath.

For all experiments, the frequency was 500 kilycycles and the transducer-head was mounted in a glass fronted thermostated bath at 25 ± 0.1°C.

The only modifications made on the generator were (1) the addition of accurate meter for measuring R.F. voltage (2) additional resistance inserted in series with the potentiometer to give the lower range of H.T. voltages required in the determination of the cavitation threshold.

13. REACTION VESSEL.

Due to the nature of ultrasonic waves the position with respect to transducer and the dimensions of an irradiation vessel are very critical. The percentage transmission of ultrasonic waves through a solid depends on the wavelength of the radiation and on the pathlength through the solid. It is a maximum when the pathlength equals an odd number of half-wavelengths. The percentage transmission from liquid to solid at a liquid/solid interface is dependent on the position of the solid. It is a maximum when the distance between solid and radiator is a whole number of wavelengths.

Various forms of glass reaction vessel were tried initially but found unsatisfactory. A stainless steel vessel, constructed as follows proved adequate and was used throughout the work.

The vessel consisted of a piece of stainless steel tube of 2 cm. internal diameter and 15 cm. long with one end welded onto a stainless steel plate 9.5 cms. in diameter and 0.25 cm. thick. To obtain maximum ultrasonic wave transmission into the reaction vessel the area of the plate corresponding to the actual base of the vessel was machined to 0.01 in. thick. The large flange was employed for anchoring the vessel.

The best position for the reaction vessel (relative to the

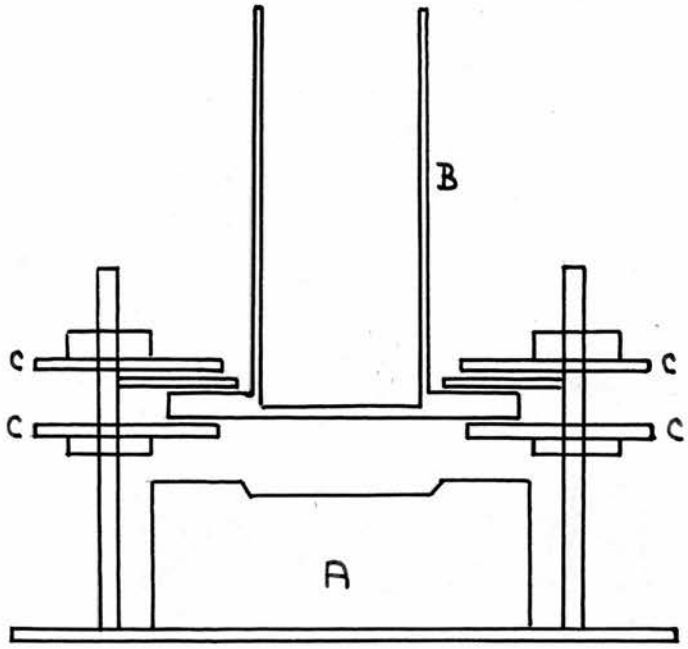

A TRANSDUCER

B REACTION VESSEL

C. BRASS CLAMPS.

Fig. 2.10.

crystal) was found by trial and error. It was then anchored as in fig. 2. 10. The position was not changed throughout the following work.

Cavitation occurred in the water between the crystal and the base of the reaction vessel with the result that bubbles collected in this area and acted as reflectors for the ultrasonic waves. To avoid this a circulating pump was arranged to drive a jet of water across this area and so carry the air bubbles away.

14. ULTRASONIC POWER.

The passage of ultrasonic waves through a liquid results in the dissipation of energy. This dissipation of energy appears in the form of heat. Therefore by measuring the heat produced it is possible to obtain a measure of the ultrasonic power.

20 ml. of distilled water were placed in the reaction vessel, hydrogen passed through and the generator switched on. After allowing the vessel to come to temperature equilibrium the rise in temperature was measured by means of a thermocouple (5 junctions). The cold junction was placed permanently in the thermostated bath and the other (preheated to 0.2° C above the temperature in the reaction vessel) was placed in the reaction vessel. The E.M.F. was measured by a Pye galvanometer. The minimum reading was taken as the value representing the difference in temperature. This method gave reproducible results and avoided any correction for heating of the thermocouple by ultrasonic waves.

A measure of the heat generated by the ultrasonic was obtained as follows. A small coil of "Nichrôme" wire (resistance 6 ohms) connected to a voltmeter, an ammeter and a variable scource of D.C. was used in the reaction vessel as a heater. 20 ml. of water were placed in the reaction vessel, hydrogen bubbled through and the resistance wire placed in the reaction

vessel. A current was passed through the resistance wire and adjusted until the temperature rise (measured as above and at a steady state) was the same as that caused by the ultrasonics. The current and voltage were then measured.

As the temperature of the thermostated bath was constant, it can be assumed that at any given temperature the heat loss from the water in the reaction vessel would be constant at the steady state and would be equal to the heat input either from the ultrasonics or from the resistance wire. Therefore, in the above experiment, the wattage dissipated by the wire would be equal to the heating effect of the ultrasonic waves and proportional to the ultrasonic power.

receiver could be either displayed on a cathode ray oscillograph or relayed onto headphones. By means of a two-way switch it was possible to replace the transducer connection by a connection from a signal generator.

The principle of operation is as follows;-
The transducer picks up all the frequencies generated in the reaction vessel. The signals are fed onto the aerial tuned circuits which accept all but on narrow wave band. If this narrow waveband contains a signal and the B.F.O. is switched on a tone is heard in the headphones. When the frequency of the B.F.O. is the same as the incoming signal then there is no tone. Hence as the tuning frequency is changed the position of a signal is signified by a tone either side of a minimum. If instead of employing the B.F.O. the magic-eye is used then the position of a signal is marked by a brightening of the light and a reduction in the dark area.

The frequency scale on the receiver was checked against a signal generator over the complete range by the method outlined above.

The cavitation threshold power was found by altering the ultrasonic power and noting the power at which there was a marked change in the sound spectrum.

PARTIAL SPECIFIC VOLUME.

In order to calculate the molecular weight of a polymer using the Svedberg equation $M = RTS/D(1 - \bar{v}\rho)$, it is necessary to know the partial specific volume $\bar{v}$ of the solute.

The partial specific volume of a component i may be defined as the increase in volume produced when 1 gm. of the component is added to very large volume of a system.

$$\bar{V}_i = \frac{\partial v_1}{\partial w_1} \qquad 2.\ 15.$$

Where V is the volume of solution, and W_i is the weight of the component i in the solution. The specific volume of the solution is given by

$$V = \frac{v}{\omega_1 + \omega_2 \cdots} \qquad 2.\ 16.$$

for a system of two components the weight fractions are given by

$$W_1 = \frac{\omega_1}{\omega_1 + \omega_2} \qquad W_2 = \frac{\omega_2}{\omega_1 + \omega_2} \qquad 2.\ 17.$$

from equation (2. 16.) if W_2 is a constant

$$dv = \frac{dv}{\omega_1 + \omega_2} - \frac{v\, d\omega_1}{\omega_1 + \omega_2} \qquad 2.\ 18.$$

and from equation (2. 17)

$$dW_1 = (\omega_1 + \omega_2)\, d\omega_1 - \frac{\omega_1\, d\omega_1}{\omega_1 + \omega_2}$$

$$= \frac{\omega_2\, d\omega_1}{\omega_1 + \omega_2} \qquad 2.\ 19.$$

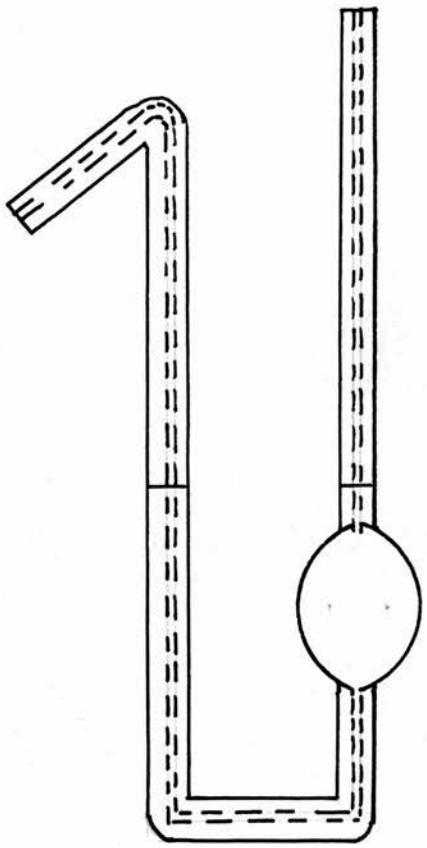

Fig. 2. 11.

and combining these equations (2. 18 and 2. 19.) the partial specific volume of component 1 can be expressed as

$$\bar{V} = v + w_2 \frac{dv_1}{dw_1} \qquad 2.\ 20.$$

Since partial specific volume determination are usually made by the pycnometer method, the equation (2. 20) for the partial specific volume may be expressed in terms of the mass (m) of liquid in pycnometer of volume .

that is $V = \frac{v}{m}$ $\qquad W_2 = 1 - W_1$

$$\frac{dV}{dw_1} = -\frac{v}{m^2} \frac{dm}{dw_1}$$

and $$\bar{V} = v\left\{1 - \frac{1-w_1}{m} \frac{dm}{dw_1}\right\}$$

or $$(1 - \bar{V}/\rho) = \frac{1-w_1}{m} \frac{dm}{dw_1} \qquad 2.\ 21.$$

If the densities of a series of solutions of known concentration are measured in a pycnometer, then by plotting the weight of each solution against the weight of the polymer present in it, the value od dm/dw, can be calculated.

Experimental:-

The pycnometer was of the same type as that described by Lipkin, Davidson, Harvey and Kurtz (100) and is shown in fig. 2. 11a. It consists of a precision bored capillary tube (0.6 - 1mm) with a 4 ml bulb blown on one arm and a bend on the other. The latter acts as a self filling device. Each

arm had reference marks etched on it.

The pycnometer was filled by dipping the bent arm into the liquid which was drawn into the apparatus first by capillary action and then by siphoning. Sufficient liquid was drawn into the pycnometer to ensure that the liquid levels were above the two etched marks. It was then placed in a thermostated bath (22.5 $\pm$ 0.001° C) and left to come to temperature equilibrium. The heights of the liquid levels above the marks were measured by cathetometer (reading 0.001cms). It was then removed dried carefully under standardised conditions and weighed. The empty pycnometer was subjected to the above treatment and then weighed. From the difference in the two weights the volume of liquid in the pycnometer was calculated.

The pycnometer was calibrated using "molecular weight purity" benzene. Different volumes of benzene were added to the pycnometer, the volume determined accurately and plotted against the sum of the liquid levels. In this way by measuring the heights of the liquid levels, it was possible to calculate the volume of liquid present in the pycnometer. The calibration curve is shown in fig. 5. 5A.

VISCOSITY.

High polymers possess the unique capacity to greatly increase the viscosity of the liquid in which they are dissolved, even when present in very low concentrations. The higher the molecular weight of a given polymer then the greater the increase in viscosity produced by a given weight concentration of polymer.

In "The molecular weights of polymers" it was stressed that a knowledge of the approximate shape of a molecule in solution is necessary in the calculation of molecular weights by sedimentation and diffusion.

The viscosity of a solution is dependent on the size and shape of the solute. Molecules which have an extended shape will offer a higher resistance to solvent flow than tightly curled molecules and hence their solutions will have a higher viscosity for the same molecular weight. The choice of solvent is important as the shape of a molecule in solution may change with solvent. When the interaction energies are unfavourable to the formation of polymer/solvent contacts, the polymer will seek to establish an increased number of polymer/polymer contacts by coiling back on itself more strongly. In the opposite case the tendency is to decrease the number of polymer/polymer contacts and increase the number of polymer/solvent contacts,

leading to extension of the molecular coil. Hence in a solvent with small polymer/solvent interaction there is a decrease in viscosity due to coiling of the molecules.

Einstein (101) showed that for a dilute solution of impervious spheres, large in comparison with the solvent

$$\eta_{sh} = \frac{5 \forall_2}{2} = \frac{5c}{2d_2} \qquad [\eta] = \frac{5}{2d_2} \qquad 2.22.$$

where d_2 is the density of the solute and $\forall$ and c are its concentration in volume fraction and in gm/ml. respectively. For solute and solvent particles of the same size with solvent-solvent and solvent-solute attractions equal, the viscosity of the solution should be identical with that of the pure solvent ie. $[\eta] = 0$. For spheres of intermediate size the viscosity behaviour should be intermediate between the above two extreme cases.

Solutions containing ellipsoidal particles have been dealt with theoretically by various authors. Simha (102) has deduced the following equation for prolate ellipsoids with a large axial ratio on the assumption that all orientations are equally probable

$$\eta_{sh} = \left\{ \frac{f^2}{15 \ln 2f - \frac{45}{2}} + \frac{f^2}{5 \ln 2f - \frac{5}{2}} + \frac{14}{15} \right\} \forall_2 \qquad 2.23.$$

Guth, Simha and Gold, extending Einstein's hydrodynamic treatment to allow for the mutual interference of the solute

have obtained

$$\eta_{sh} = 2.5V_2 + 14.1V_2 = \frac{2.5c}{d_2} + \frac{14.1c^2}{d_2} \qquad 2.24$$

This relationship may be extended and written in the general form

$$\eta_{sh} = A_0 + A_1C + A_2C^2 \qquad 2.25$$

where c is the concentration. Then since the specific viscosity of a pure solvent is zero by definition $\eta_{sh}/c = A_1 + A_2C$. Hence a plot of η_{sh}/c V.C. will have an intercept A_1 and slope A_2. The intercept A_1 is now defined as

Limiting viscosity number $= [\eta] = \lim_{c \to 0} (\eta_{sh}/c)$ = Intrinsic viscosity

Staudinger stated that the specific viscosity was directly proportional to the molecular weight of the solute and its concentration: $\eta_{sh.} = KMC$. However experimental and theoretical evidence led to the conclusion that the Staudinger equation was only an approximation. Mark (103) and Houwink (104) independently proposed

$$[\eta] = \lim_{c \to 0} (\eta_{sh}/c) = KM \qquad 2.27$$

where K is a constant independent of molecular weight but depends on polymer, solvent and temperature, is a constant dependent on the shape of the solute molecule and ranges in value from 0 for perfect spheres to 2 for rigid rods. The constants K and may be determined by employing narrow fractions of different

Fig. 2.12.

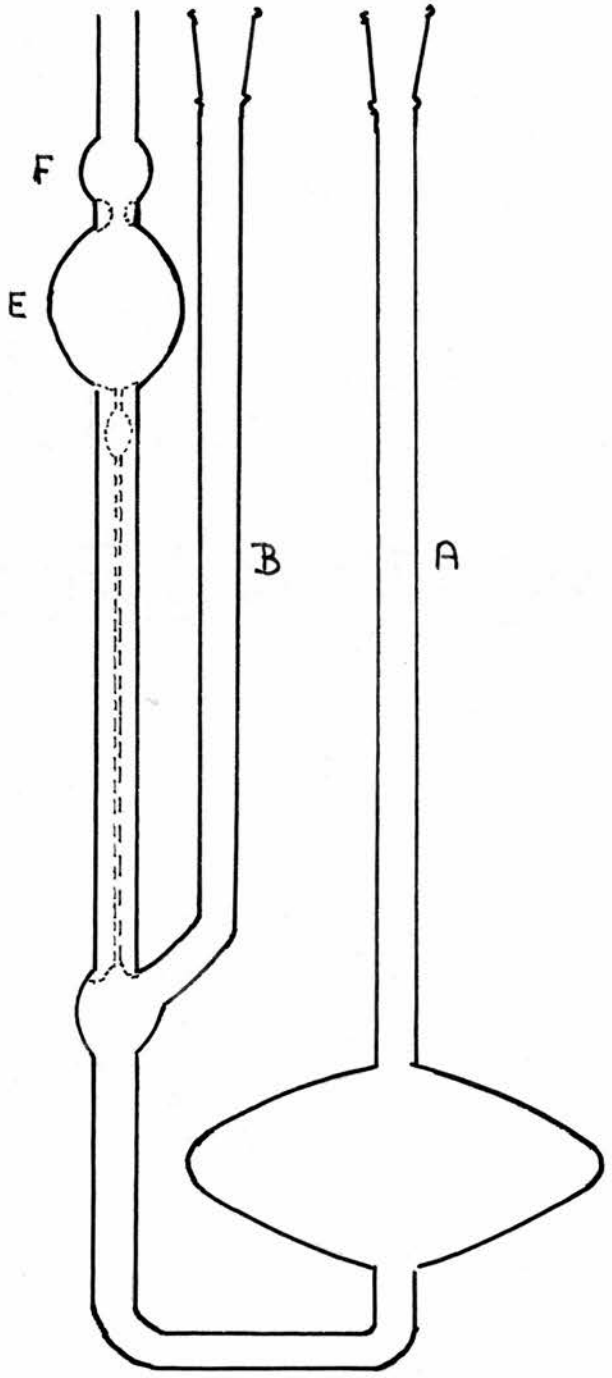

Modified Ubbelohde Viscometer

known molecular weight of the same polymer and measuring the viscosity of each fraction. Therefore, although the method is a very simple means of determining molecular weights, it suffers from the disadvantage that it is not absolute and requires samples of known molecular weight for calibration.

Various workers have attempted to arrive at a more quantitative theoretical basis for equation (2. 26). Flory and Fox (105) from theoretical consideration have deduced the relation

$$[\eta] = K'' M^{\frac{1}{2}} \alpha^3 \qquad 2.\ 27.$$

Where K is a constant dependent on the structure of the polymer and to some extent on the temperature T , and with α dependent on M and T according to the equation

$$\alpha^5 - \alpha^3 = 2C_m \psi (1 - \Theta/T) M^{\frac{1}{2}} \qquad 2.\ 28.$$

for a given system. ψ and Θ have values depending on the heat and entropy of dilution parameters characterising the given polymer solvent pair. Cm is a constant.

At the temperature $T = \Theta$ in a poor solvent $\alpha^5 - \alpha^3 = 0$ according to equation (2. 28) and α must equal unity irrespective of M, ie. at the theta temperature, the molecular dimensions are unperturbed by intramolecular interactions.

Experimental.

Viscosity measurements were carried out using a modified Ubbelohde viscometer (106) with a minimum working volume of 12 ml. (fig. 2. 12). The viscometer was clamped firmly in a

vertical position on a brass stand and determinations were carried out in a bath thermostated at 25 ± 0.01° C.

The solution was added by pipette down tube B (fig. 2. 12) and after allowing to come to temperature equilibrium tube B (fig. 2. 12) was closed with a ground glass stopper (B 10). Pressure was then applied via tube A until the liquid level was at mid-point of bulb F. The pressure was then released, the stopper removed and the time required for the liquid level to pass two marks (one above and one below bulb E) was measured. A stop watch reading to 0.05 sec. was used and the flow time of the solution taken as the mean of several readings.

Dilutions were made <u>in situ</u> by adding a given volume of solvent by a pipette down tube B, the solution mixed by blowing gently (filtered air) down tube B. To complete mixing, the liquid level was then raised in tube B to a level above that which the pipette touched, the pressure released and air gently blown down tube B to complete mixing.

The solutions were prepared as described in "Preparation of solutions" and the concentrations by the method of Lampitt, Fuller and Coton (86).

<u>Kinetic Energy Correction</u>.

The viscosity of a given volume of liquid flowing through a capillary is given by:

$$\eta = Kdt - B\,d/t \qquad 2.\ 29$$

where d is the density of the liquid, t is the time of flow and

K and B are the viscometer constant and kinetic energy correction factor respectively.

For a low kinetic energy correction factor the flow time of solvent should exceed 100 secs. In the viscometer employed the flow times were 200 secs. To determine whether the kinetic energy correction was significant, the flow time of several solvents of known viscosity were measured. The solvents employed were 3 x distilled water, "molecular weight purity" benzene, "Analar" acetone, and redistilled butan-1-ol. The absolute viscosities of the solvents were obtained from the International Critical Tables.

From these results the kinetic energy factor B was calculated using equation (2. 29). The value obtained was small enough to be neglected for this viscometer.

Shear Correction:-

According to Newton's law the velocity gradient in a liquid is directly proportional to the shearing force. However polymer solutions do not obey this law and apparent viscosity decreases with increase in velocity gradient due to increased orientation in the direction of flow.

The non-Newtonian behaviour of amylose in 0.2M potassium hydroxide was investigated using the modified Ubbelohde viscometer described by Immergut and Schurz (107).

The viscometer had four bulbs and the driving head in each could be calculated using Meissner's formula

$$h = \frac{m_1 - m_2}{\ln \frac{m_1}{m_2}} \qquad 2.30$$

where m_1 is the initial distance and m_2 is the final distance between top level of the liquid and the lower end of the capillary. The average rate of shear (γ) may be related to the relative viscosity assuming solvent and solution densities to be the same by

$$\gamma = \frac{r h g}{3 l v_0 \eta_{rel.}} = \frac{k}{\eta_{rel.}} \qquad 2.31.$$

where k is a constant for a given bulb and a given kinematic viscosity v_0 (ie. absolute solvent viscosity/solvent density).

The solution flow times for each bulb was plotted against γ calculated from equation (2.31.) for each concentration. Extrapolation to zero shear was made yielding $\eta_{rel.}$ at $\gamma = 0$ and η_{sp}/c could then be plotted against C from which $[\eta]_{\gamma=0}$ was obtained.

SECTION III

Sedimentation

SEDIMENTATION.

If the density of a particle, suspended or dissolved in a liquid differs from that of the liquid then if a force field is applied to the system, solute and solvent will separate. When the density of the solute is lower than that of the solvent, flotation occurs, when the densities are reversed, sedimentation takes place. For large particles (high density) the earth's gravitational field is of sufficient strength to cause sedimentation, but for colloidal particles and molecules it is not sufficient and artificial means of increasing the force field are required. Svedberg and his co-workers (108) accomplished the sedimentation of molecules by rotating the solution in an ultracentrifuge (force field 250,000g).

If a monomolecular polymer is dispersed in a solvent of different density (lower) and spun in a sufficiently high force field, the material will sediment and the rate of movement of the particles will be proportional to (1) the force field, (2) particle size and shape, (3) the density and viscosity of the media.

Svedberg showed that that the rate of movement of the molecules may be measured if certain conditions are fulfilled. One essential requirement is that no convection currents be set up, this he overcame by employing a sector shaped cell.

The movement of a sedimentation boundary in a centrifugal force field was defined by Svedberg as

$$S = \frac{\log x_2 - \log x_1}{\omega^2(t_2 - t_1)}$$

Where ω is the angular velocity in rads/sec., x_1 and x_2 are the mean distance in cms. of the boundary from the centre of rotation at times t_1 and t_2 respectively, and S is the sedimentation coefficient (usually quoted in Svedbergs

1 Svedberg = 1×10^{-13} c.g.s. units).

The S obtained from the above requires two corrections:
(1) S is usually dependent on the concentration and hence it is necessary to extrapolate the values to infinite dilution S^0.
(2) For comparison purposes it is essential that all quantities measured be reduced to the same origin. Sedimentation constants are usually quoted as corrected to water at 20 C by the following:

$$\frac{S_{w20}}{S} = \frac{\eta\,(1 - \bar{v}\rho_{w20})}{\eta_{w20}(1 - \bar{v}\rho_s}$$

The force on a molecule sedimenting in a centrifugal field is balanced by the frictional force,

$$M(1 - \bar{v}\rho)\omega^2 x = f\,(dx/dt)$$

where f is the frictional coefficient and t is time.
But for a dilute solution,

$$f = RT/D$$

Where R is the gas constant, T is absolute temperature and D is the diffusion coefficient.

If it is assumed that f for diffusion is equal to f for sedimentation then

$$M = \frac{RT}{D(1-\bar{V}\rho)} \frac{dx}{dt}$$

or $M = RTS/(1-\bar{V}\rho)D$.

Because a sectorial cell is imployed the concentration in the plateau region is not constant and decreases according to the following

$$C_t = C_0 (x_0/x_t)^2$$

where x_0 and x_t are the positions of the boundary with reference to the centre of rotation at $t = o$ and $t = t$ respectively.

Because of molecular entanglement, solvation and hydrodynamic interactions S is usually dependent on C. For small molecules and large molecules having a spherical shape the concentration dependence is small and linear. For large nonspherical molecules the concentration dependence may be large and curved. This leads to difficulties when an extrapolation to infinite dilution is attempted. Many attempts have been made to deduce mathematical expressions which would fit the concentration dependence data. Signer and Gross (109) found that 1/S V.C. was linear for polystyrene in chloroform, but this does not hold for many other systems. Gralen (90) proposed

$$S = S_0/(1 + K_sC)$$

which may be written $S = S_o \ (1 - K_s C + (K_s C)^2 \ldots\ldots)$ and is found to be true in the majority of cases but the significance of K has never been elucidated. One effect of the concentration dependence is to artificially sharpen the boundary.

Experimental.

The instrument employed was a "Spinco model E" ultracentrifuge which has a speed range of 12,000 - 60,000 r.p.m.

The solution to be analysed was contained in a 4° sector shaped cell which is a push fit into a hole in the rotor. The rotor was balanced by a counterpoise cell directly opposite the analytical cell. The counterpoise has two holes in it that act as reference marks.

The rotor containing analytical cell and counterpoise was connected to the drive, the temperature of the rotor noted (thermocouple), the vacuum chamber closed and the vacuum pumps started. When the pressure was 1 μ the drive was started and the rotor accelerated up to the desired speed. The maintenance of the correct speed is automatic. At the end of the run the temperature is again taken.

The position of the boundary is observed by means of a Philpot-Svenson schlieren optical system employing a high pressure mercury vapour lamp. Facilities are available for either photographing or viewing manually the schlieren diagram.

Calculation of sedimentation constant.

Photographs of the sedimenting boundary were taken at various times after the rotor had reached operational speed. The distance between the reference marks and the meniscus and the peak of the sedimenting boundary were measured employing a two dimensional travelling microscope. The distance of the reference marks from the centre of rotation had previously been determined (for all speeds). The measurements were corrected for optical magnification factors and $\ln x$ v. t plotted

now $$S = \frac{1}{\omega^2} \frac{d \ln x}{dt}$$

and S was obtained from the slope of the line, ω was measured during the run.

S was then corrected for temperature, density and viscosity.

The above S is that of the predominant species by weight. When however a weight or number average S is required the above method is not adequate and it is necessary to measure the entire boundary for dc/dx values as well as x values. The measurements required and the procedure in evaluating the required parameters is outlined in "Diffusion"

SECTION IV

Molecular Weight Distributions

MOLECULAR WEIGHT DISTRIBUTION.

Methods are available for converting the sedimentation velocity diagrams obtained on the ultracentrifugation of a polymer solution into molecular weight distributions (109 -119). Little work of this type has been carried out on the components of starch.

If the diffusion correction is negligible and the sedimentation coefficient (S) is independent of the concentration (C), the refractive index gradient curve can be converted directly into a distribution of sedimentation coefficients g(S) by the expression

$$g(S) = (dc/dx)\,\omega^2 x^3 / C_0 x_0^2$$

here, ω is the angular velocity (in rads/sec), t is time (in sec.) from the start of sedimentation; x is distance (in cms.) of a point in the boundary from the axis of rotation; x_0 is distance (in cms.) of the meniscus from the axis of rotation; C_0 is total concentration of the solution. However, the above conditions are obeyed by few polymers, and g(S) has normally to be corrected for three boundary effects, (1) the spreading with time due to diffusion, (2) the anomalous apparent concentration of any individual molecular species due to polymolecularity - the Johnston-Ogston effect (120) and (3) the narrowing due to the

concentration dependence of S. Diffusion can be corrected for by extrapolating an "apparent distribution" $g^*(S)$ V. $1/xt$ to infinite time (113-115). The other two effects can be corrected for either by extrapolating curves of $g^*(S)$ to infinite dilution (117, 118, 121), or correcting the curve of $g^*(S)$ at a single concentration for the dependence of S on C. The latter method of Baldwin was adopted here. In view of the complex series of manipulations involved, the method is given in outline below.

The apparent distribution of sedimentation coefficients $g^*(S)$.

This function can be derived from the relations

$$c = c_0 \left(\frac{x_0}{x}\right)^2 \qquad \text{and} \quad S = \frac{1}{\omega^2 t} \ln \frac{x}{x_0}$$

it follows that $dc = dc_0 (x_0/x)^2$ and $dS = (1/\omega^2 x t)\, dx$, and the combination of these equations gives

$$dc_0/dS = (dc/dx)(x/x_0)^2 \omega^2 x t$$

The curve of dc/ds versus S is not a conventional distribution since the area under it is not unity but C_0. Normalization of the function therefore gives the apparent distribution of sedimentation coefficients $g^*(S)$ as

$$g^*(S) = (dc/dS)\, C_0^{-1} = (dc/dx)\, (x/x_0)^2 \omega^2 x t\, C_0^{-1}$$

This function was calculated for each sedimentation diagram for about 20 incremental values of x (ie. $x_i \cdots$ etc) by taking the corresponding values of $(dn/dx)_{x_i}$ for $(dc/dx)_{x_1}$ and

$$\Delta x \sum_{x=0}^{x=\infty} \frac{dn}{dx} \quad \text{for } C_0$$

the proportionality factors disappear in the quotient $(dc/dx)/C_0$. Conversion of the values of x_i into the corresponding values of sedimentation constant S_i ($by\ S_i = (1/\omega^2 t) \ln(\frac{x_i}{x_0})$) then enabled the graph of $g^*(S)$ versus S to be plotted for the different times of sedimentation.

Elimination of the diffusion effect.

From the graphs of $g^*(S)$ versus S, values of $g^*(S)$ for discrete values of S (ie. 10, 20, 30 x 10^{-13}) were taken and plotted as $g^*(S)$ versus $1/x_i t$. A graphical extrapolation was then made to $1/x_i t = 0$ to yield values of the apparent distribution corrected for diffusion effects $g'(S)$.

Transformation of $g'(S)$ into dc/dx. Before corrections can be applied for the Johnston-Ogston effect (120), the function $g'(S)$ versus S has to be transformed into dc/dx versus x. The original distribution can be rewritten in this instance

$$dc/dx = g'(S)\, x_0^2 C_0 / x^3 \omega^2 t$$

where t is now the average time ie. the time in the middle of the run. Values of $(dc/dx)_{x_i}$ were therefore calculated from corresponding values of $g'(S)$. When values of S_i were converted to x_i by the expression $x_i = x_0 \exp(S_i \omega^2 t)$, the graph of dc/dx versus x was obtained.

Correction of polymolecularity.

In order to correct for polymolecularity, the distribution curve dc/dx versus x is divided into a number of equispaced lamellae, and these are regarded as different components. Every molecular species i present in a given plane x changes in concentration at that plane, if its sedimentation coefficient S_i varies with the total concentration C_i. Baldwin (116) has shown that the change in concentration of the species (ΔC_i) is related to the change in its sedimentation coefficient (ΔS_i) in terms of a parameter ($\tau / \omega^2 x$) where

$$\frac{\tau}{\omega^2 x} = \frac{\ln \frac{x_j}{x_o}}{\omega^2 t} = S_i + C_i \frac{\Delta S_i}{\Delta C_i}$$

whence

To carry out these calculations, about 20 values of dc/dx at a fixed increment, Δx were tabulated against x, and the parameter $\ln (x/x_o)/\omega^2 t$ was calculated. The change in concentration of each of the components in each successive plane was then calculated in a stepwise manner by Baldwins method (116).

For the first lamella (x_1), only component 1 is present and therefore its concentration

$$C_1 = \Delta x \left(\frac{dc}{dx}\right)_{x_1}$$

For the second lamella (x_2) the total concentration is $\Delta x \sum_{x=0}^{x=\infty} (dc/dx)$, which is an increase of $\Delta x(dc/dx)_{x_2}$ is S = So (1 - KC) the sedimentation coefficient of component 1 in this lamella $(S_i)_{x_2}$ therefore decreases by an amount $(\Delta S_1)_{x_2}$ given by $-KSo_1 \Delta x(dc/dx)_{x_2}$ where $So_1 = S_1 / 1 - KC_1$. From Baldwins work (104), the corresponding change in concentration $(\Delta C_1)_{x_2}$ is thus equal to

$$(\Delta C_1)_{x_2} = C_1(\Delta S_1)_{x_2} \Big/ \left\{ \ln \frac{x_2}{x} / \omega^2 t \; - Si_{x_2} \right\}$$

The true concentration of component 2 is thus greater than $\Delta x(dc/dx)_{x_2}$ by $-(\Delta C_1)_{x_2}$

This calculation was repeated for all the components (i) in each lamella until the corrected concentration (C_{oi}) of each are known. Then since $C_{oi} = \Delta x(dc/dx)_{x_i}$, it follows that $(dc/dx) = C_{oi} / \Delta x$ hence values of the corrected distribution function g(S) were calculated from

$$g(S) = (C_{oi}/\Delta x)(x/x_o)^2 (\omega^2 x t / C_o)$$

and the graph of g(S) versus S obtained.

Correction for the concentration dependence of S:

The extrapolation of g(S) to infinite dilution. The distribution of sedimentation coefficients at infinite dilution $g(S_o)$ is derived from g(S) (dS/dS_o), since

$g(S_o) = C_o^{-1} \; dc/dS_o = C_o^{-1} \; (dc/dS) \; (dS/dS_o)$. (dS/dS_o) was obtained from tabular differentiation of S_{oi} and S_i values; S_{oi} being calculated from $S_i = S_{oi} \; (1 - KC_i)$ where $C_i = \Delta x \sum_{x=x_o}^{x=x_i} (dc/dx)$ as above. Values of $g(S_o)$ when plotted against the corresponding values of S gave the true sedimentation coefficient distribution curve.

Calculation of the molecular weight distribution.

Since the distribution of molecular weight g(M) is given by

$$g(M) = C_o^{-1} (dc_o/dM) = C_o^{-1} \; (dc/dS) \; (dS/dM)$$

values were calculated from $g(S_o) \; dS_o/dM$.

SECTION V

Results

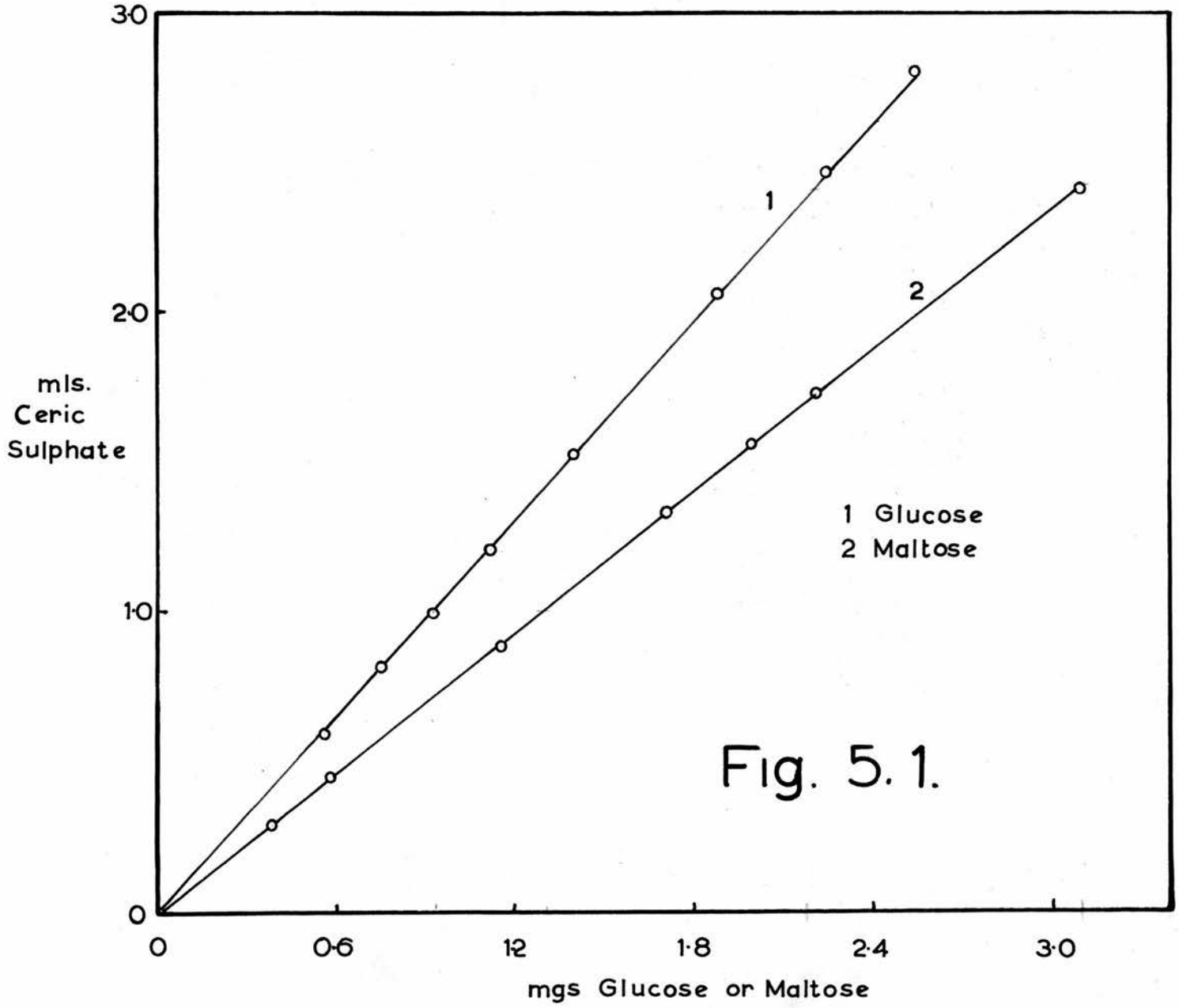
3·0
2·0
1·0
0
mls.
Ceric
Sulphate
1
2
1 Glucose
2 Maltose
0
0·6
1·2
1·8
2·4
3·0
mgs Glucose or Maltose

Fig. 5. 1.

Fig. 5. 2.

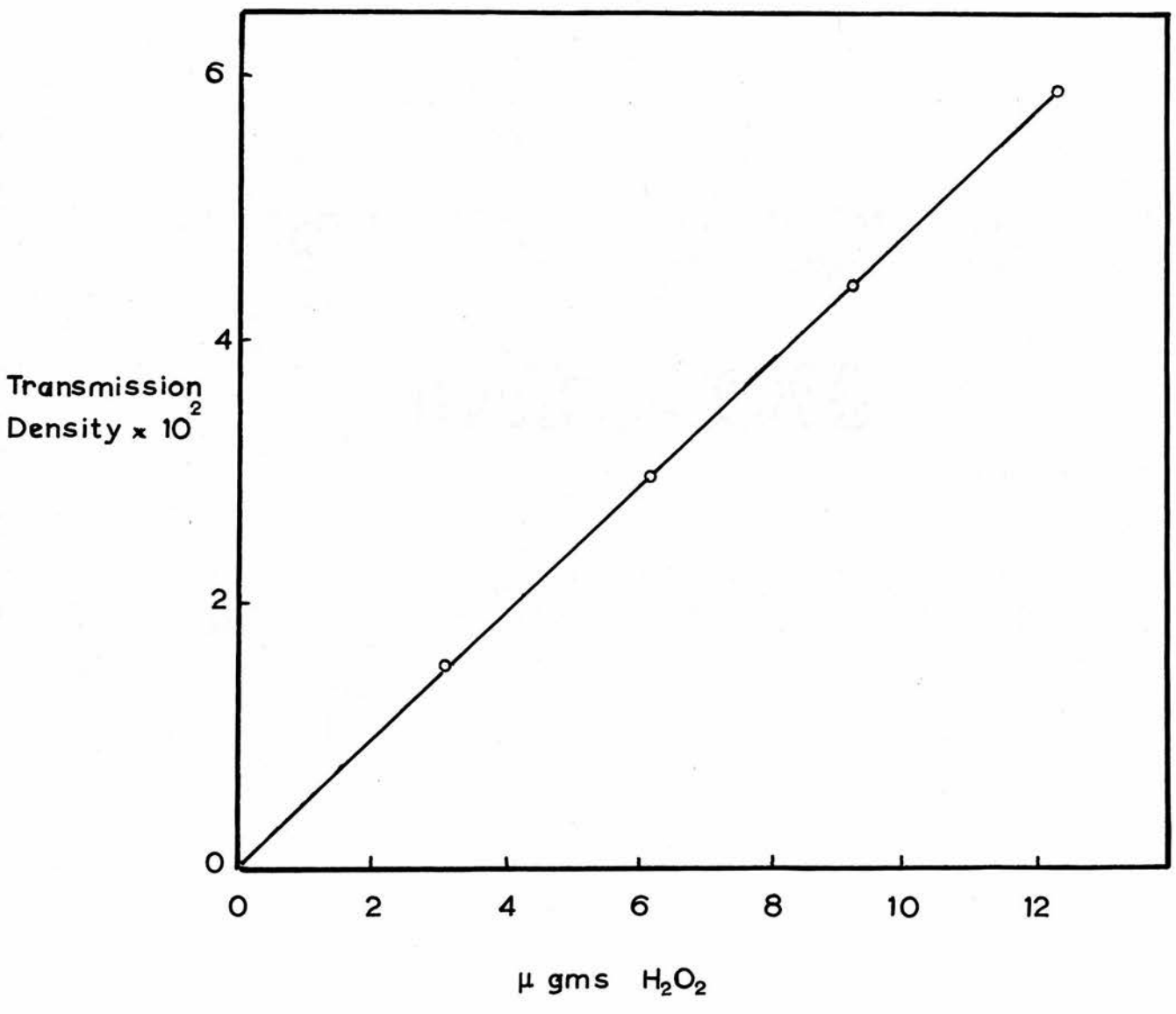

20. ESTIMATION OF MALTOSE AND GLUCOSE.

Fig.5. 1. shows the calibration graph employed in the estimation of glucose and maltose. The double set of points on the glucose curve represent "Analar" glucose and "Analar" starch.

21. ESTIMATION OF HYDROGEN PEROXIDE.

Fig.5. 2. shows the calibration graph employed in the estimation of hydrogen peroxide.

Table 5. 1.

Atmosphere	Radiation time mins.	T.D. x 10	ug.H_2O_2
Hydrogen	0.0	0.0	0.0
"	5.0	0.0	0.0
"	20.0	0.1	0.1
"	40.0	0.1	0.1
"	90.0	0.0	0.0
"	150.0	0.1	0.1
"	300.0	0.0	0.0
"	450.0	0.0	0.0
Air	5	3.85	8·0
"	10	5·50	11·5
"	15	6·50	13·1

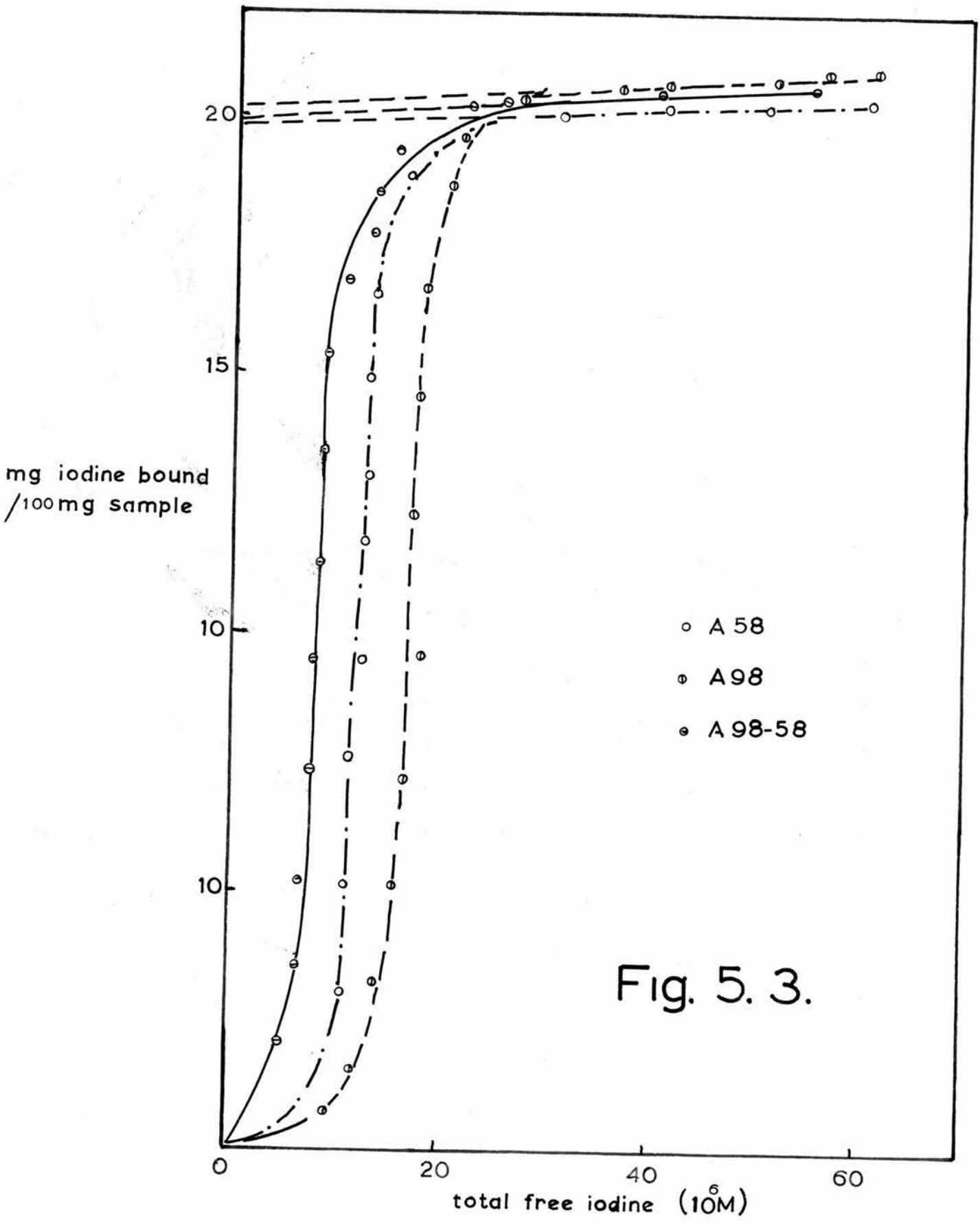
20
15
10
10
mg iodine bound
/100 mg sample
A 58
A 98
A 98-58
0
20
40
60
total free iodine (10⁶M)

Fig. 5. 3.

From the above it would appear that the formation of hydrogen peroxide had been greatly reduced and probably eliminated.

22. PURITY OF AMYLOSE, AMYLOPECTIN AND GLYCOGEN.

Table 5. 2.

	A98	A98-58	A58	Amylopectin	Glycogen
% Polysaccharide	98	101	98	99	99
β Limit	75	59	98	54	42
Optical rotation	-	-	-	-	191
Iodine affinity	203	199	198	-	-

Fig. 5. 3. shows plots of mg. iodine bound v. free iodine for A98, A98-58 and A58.

23. ULTRASONIC POWER AND CAVITATION THRESHOLD.

Table 5. 3.

Voltage (kv.)	0	1.66	2.5	2.9	2.29
	f.	f.	f.	f.	f.
	498-500	498-500	498-500	498-500	498-500
		472	472	472	472
		461	461	461	461
		458	458	458	458
			X 445-53	445-53	443-53
			X 429	429	429
		422	422	422	422
		412	412	412	412
		382	382	382	382
	380	380	X 379-80	379-80	379-80
	370	370	X 351-77	351-77	351-77
	350	350	X 303-30	303-30	303-30
	329	329			
		271	271	271	271
	269	269	269	269	269
		259-61	259-61	259-61	259-61
			X 250	250	250
		243	243	243	243
			X 205-19	205-19	205-19
			X 184-200	184-200	184-200
	170	170	170	170	170
			X 158-68	158-68	158-68
			X 135	135	135
		125	X 125-9	125-9	125-9
		115	115	115	115
		110	X 105-10	105-10	105-10
		100	X 84-100	84-100	84-100
		87			
		82	X 78-82	74-82	74-82
		80			
		79			
		70	70	70	70

where f. is frequency present in kilocycles.

Table 5. 1. gives the list of frequencies (kc.) present in the solution in the range 70-500 kc. at different powers. At 0 volts the generator was switched on but no ultrasonic waves irradiated. The results in this column are due to stray frequencies picked up by the barium titanate transducer. At 1.66 kv., the power is below the cavitation threshold power for water in the reaction vessel but is above that for the water between the quartz transducer and the base of the reaction vessel. The frequencies in column (table 5. 3.) are therefore due to cavitation outside the reaction vessel but they are strong enough to penetrate the reaction vessel base and hence are picked up on the barium titanate transducer. If the power is increased slowly then at 2.5 kv^2 there is a marked change in intensity of all the frequencies and also some new frequencies appear (marked X in table 5. 3). The latter although probably generated outside the reaction vessel have not the power to penetrate the base and hence are only received when cavitation occurs inside the reaction vessel. The increase in the intensities of the other frequencies was of the order of tenfold. Unfortunately, it was impossible to measure the change in intensity accurately as no pulse wave analyser was available. If the power is increased to 2.9 kv^2 then there is no change in the sound spectrum and only a slow increase in the intensities. If the power is now decreased then the cavitation threshold power is no longer at 2.5 kv^2 and the cavitation

Fig. 5. 4.

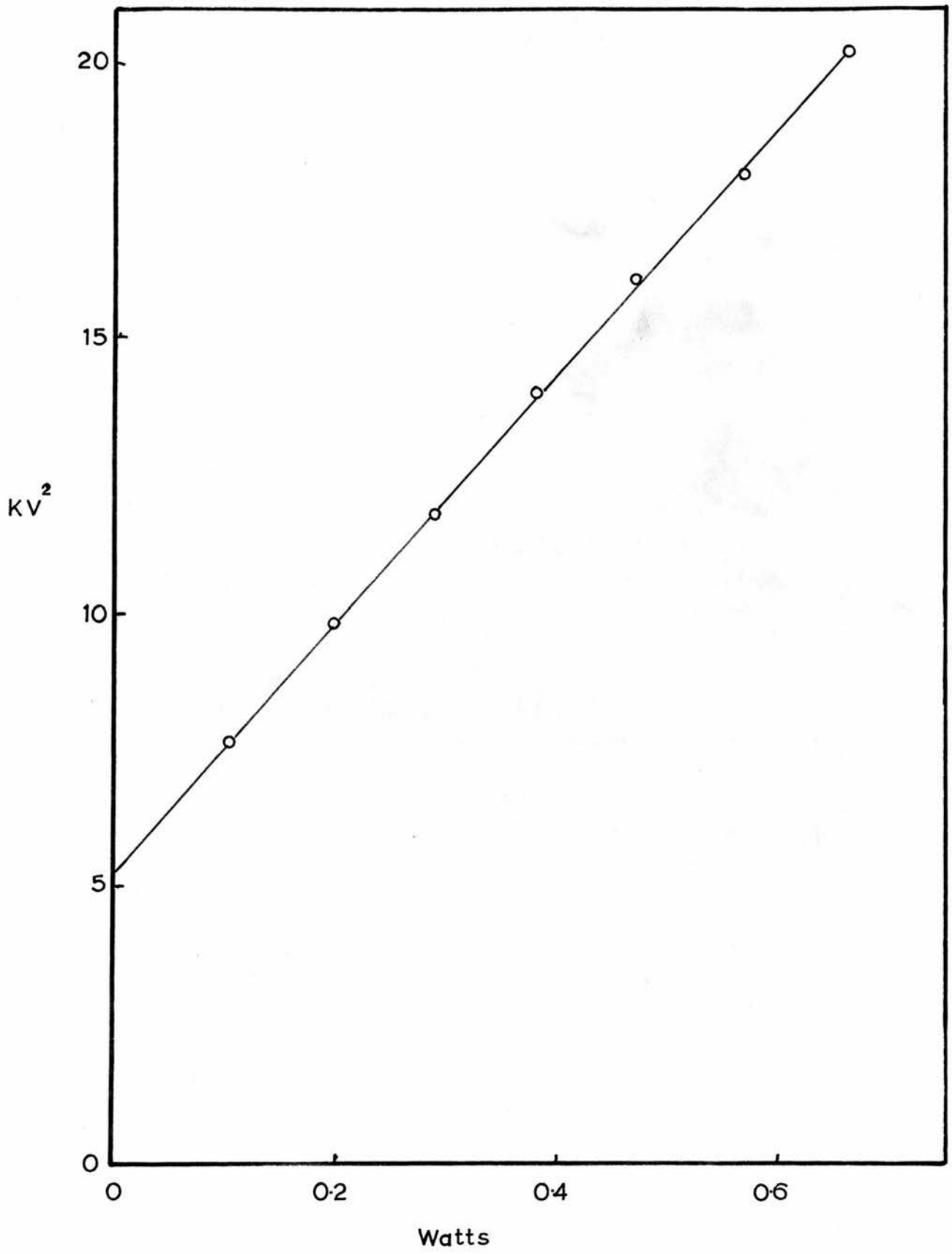

spectrum persists until 2.29 kv is reached and only then is there a marked decrease in the intensities. In column 4 (table 5. 3.) is shown the frequencies present at 2.29 kv (voltage decreasing). This apparent anomaly is not due to backlash on any of the instruments employed but is an actual phenomenon and has previously been reported (122).

From the above it appears that cavitation is occurring and that the cavitation threshold power is 2.5 kv^2 with increasing voltage but 2.29 kv^2 with decreasing voltage.

Fig. 5. 4. shows the plot of watts v. kv^2 obtained by the method described in section 2. The cavitation threshold power is beyond the limit for which it was possible to measure accurately the concurrent rise in temperature. Any extrapolation of the curve would be misleading, as there is a marked rise in absorption at the cavitation threshold. From the graph, the cavitation threshold power is less than 0.1 watt. As the reaction vessel was 2 cm. in diameter this is equivalent to approx. 0.03 watts/$cm.^2$. The value quoted in the literature is 0.03 watts/$cm.^2$.

Fig. 5.5.

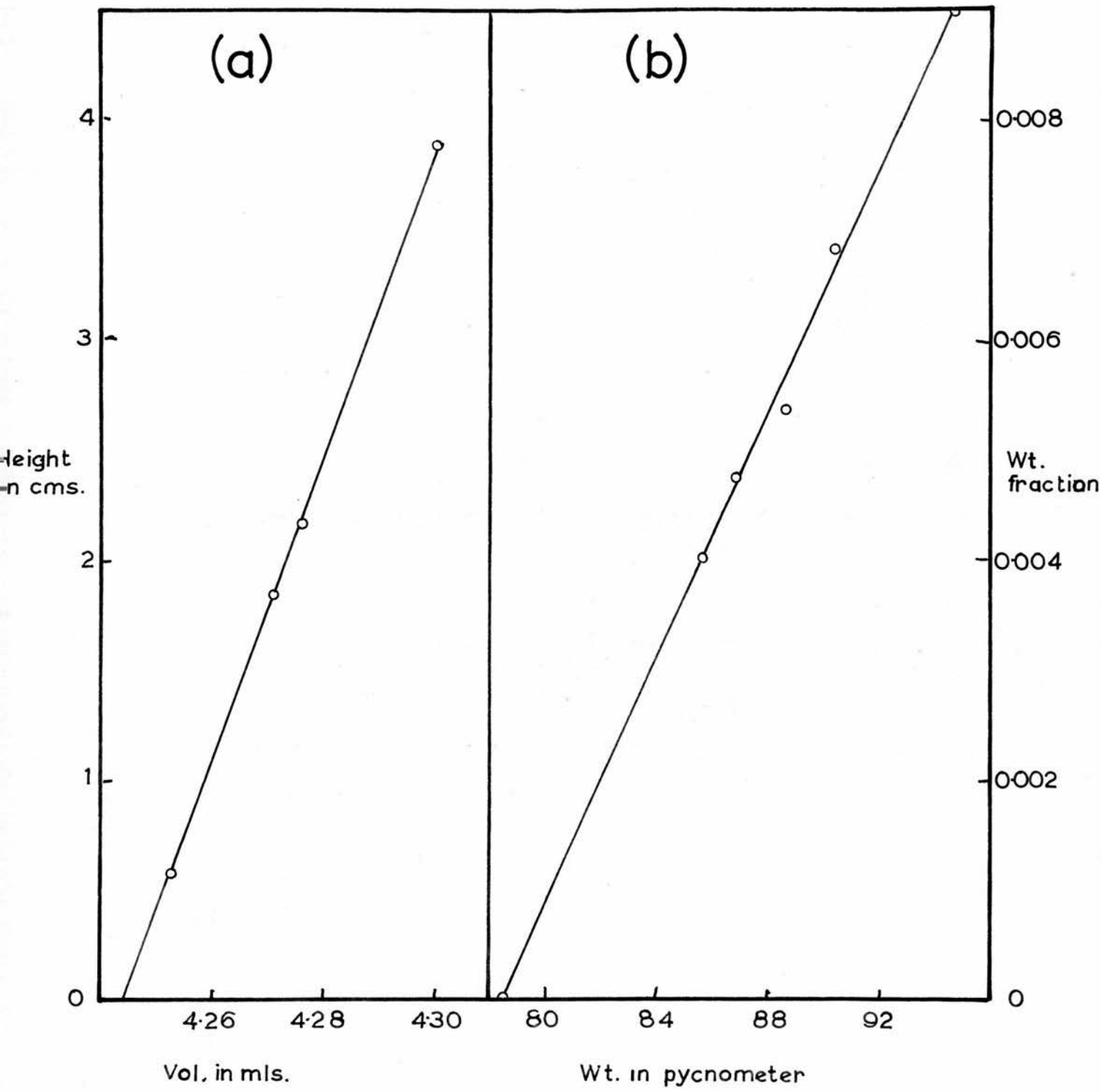
(a)
(b)
4
3
2
1
0
Height in cms.
4·26
4·28
4·30
Vol. in mls.
0·008
0·006
0·004
0·002
0
Wt. fraction
80
84
88
92
Wt. in pycnometer

24. PARTIAL SPECIFIC VOLUME.

Calibration of pycnometer.

Table 5. 4.

		1	2	3	4
Average height above marks.	cms.	3.875	1.825	0.575	2.150
Weight of water.	gms.	4.30521	4.27110	4.25299	4.27651
Density of water		0.9976846			

Fig. 5. 5a. shows a plot of weight of water versus average height of the liquid in the capillaries. The above results give the following relationship between volume of solution and average height by the method of least squares

$$\text{volume of solution} = 4.24651 + 0.00781\ h.$$

Partial specific volume of amylose.

Fig. 5. 5b. shows a plot of weight of solution in pycnometer versus weight fraction of solute. dm/dw_1 was obtained from the slope of the line and the partial specific volume calculated using

$$(1 - \bar{v}\rho) = \frac{(1 - w_1)}{m} dm/dw_1.$$

The partial specific volume of amylose in 0.2N potassium hydroxide is 0.617.

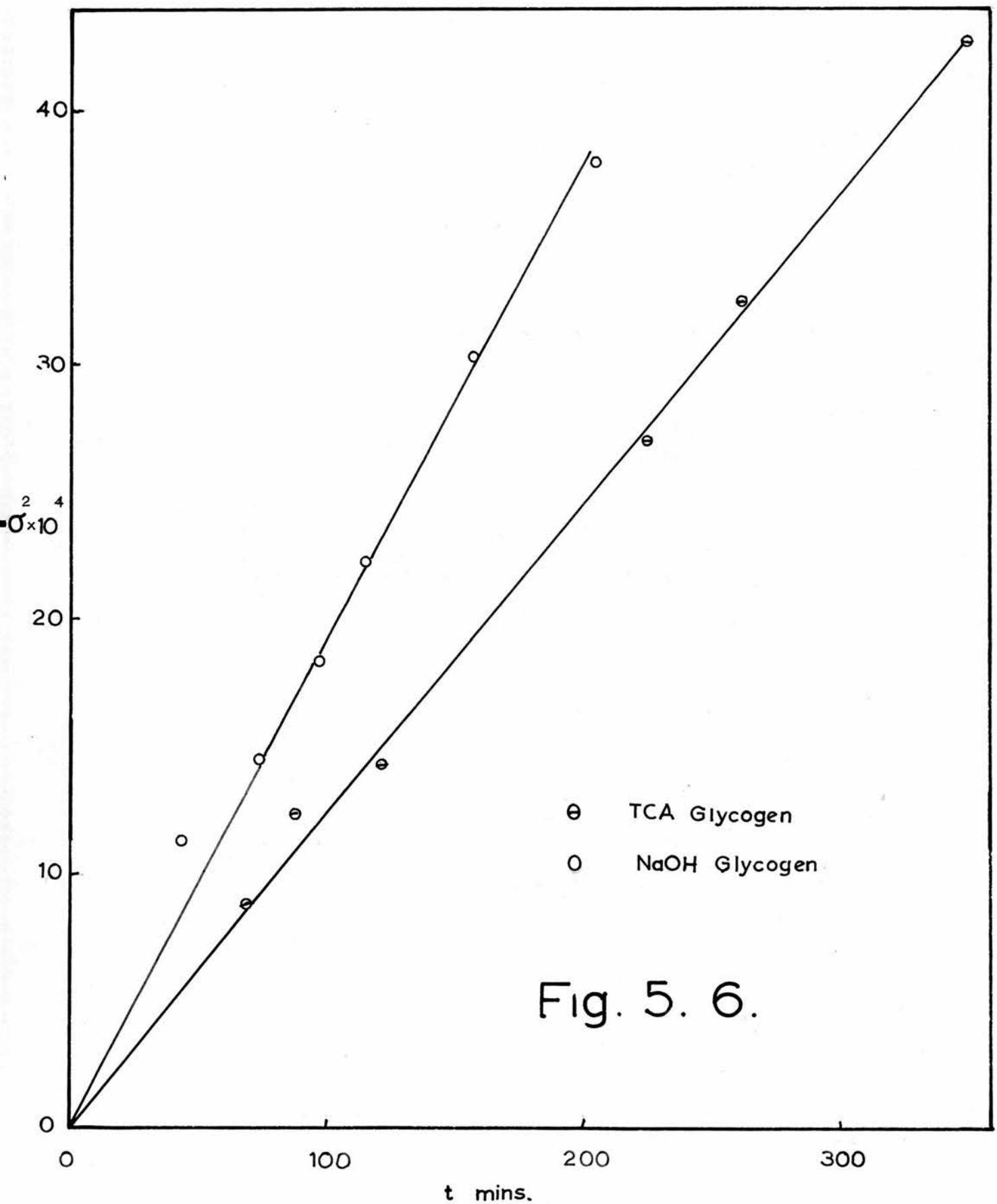
40
30
20
10
0
$\sigma \times 10^{2}$
$\sigma \times 10^{4}$
0
100
200
300
t mins.
θ TCA Glycogen
O NaOH Glycogen

Fig. 5. 6.

25. DIFFUSION.

That no time correction was necessary when using the new cell was pointed out in section 2. The results quoted were those for known substances with a high diffusion coefficient, where the time correction - if any - was likely to be largest. Fig. 5. 6. shows a plot of σ^2 v. t. for a TCA glycogen and a NaOH glycogen. As may be seen from the graph the time correction is small.

Table 5. 5.

Substance		$D_m \times 10^7$	Substance		$D_m \times 10^7$
A58	0	0.95	A98	0	0.80
	10	1.11		10	0.92
	20	1.21		20	1.01
	42	1.30		40	1.16
	90	1.37		90	1.35
	150	1.50		150	1.47
	240	1.66		240	1.82
	450	2.00		450	1.98
A98-58	0	0.74	A98-58	150	1.40
	10	0.90		240	1.55
	20	1.03		450	1.90
	40	1.10	TCA Glycogen		1.02
	90	1.30	NaOH	"	1.56

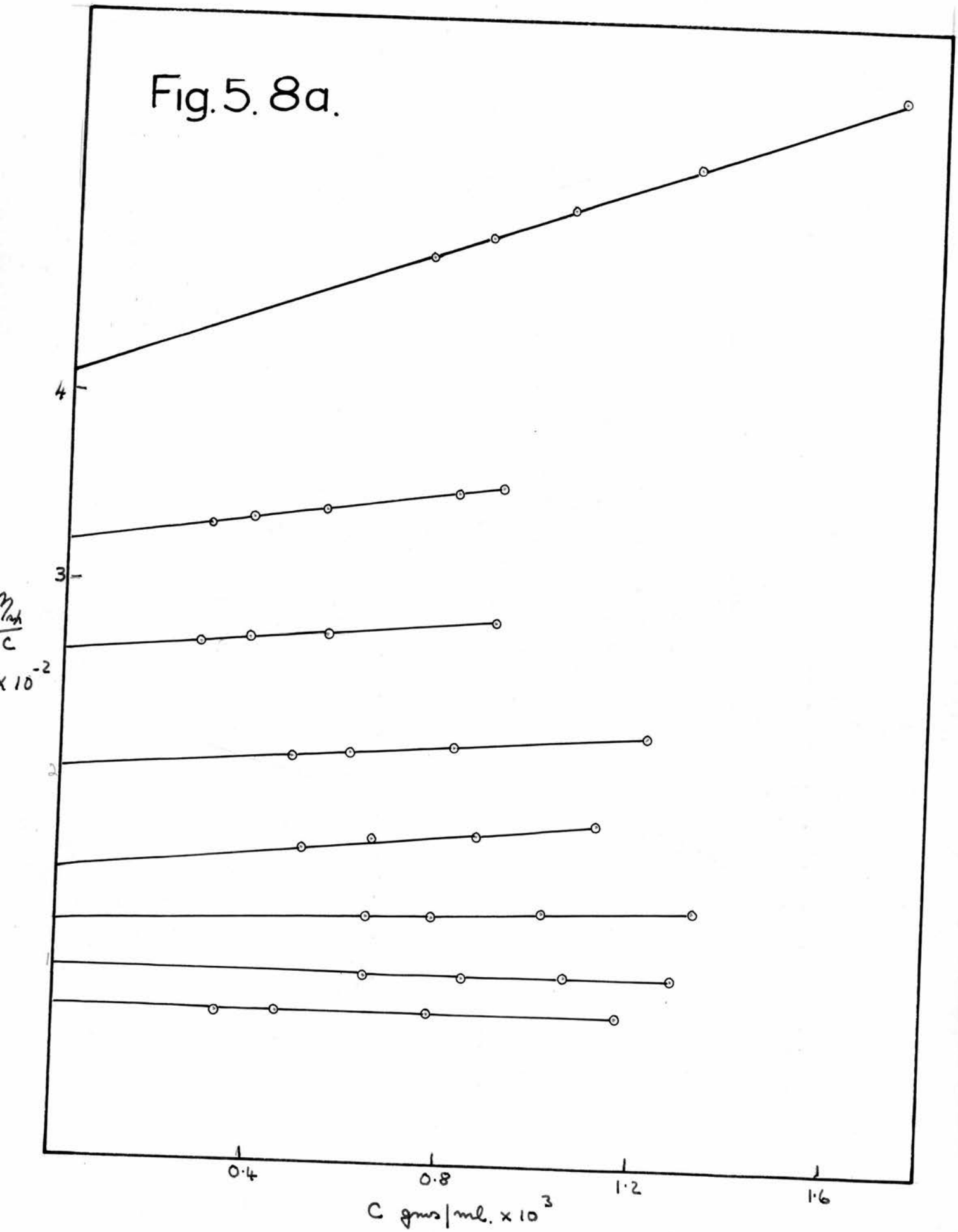
Fig. 5. 8a.
4
3
$\frac{\eta_{sp}}{c}$
$\times 10^{-2}$
0·4
0·8
1·2
1·6
C gms/ml. $\times 10^{3}$

The D_m-values for the various amylose samples listed in table 5. 5. were determined in the concentration range 0.1 - 0.25%. The narrow range was necessitated by the size of the cell (0.1%) and the low concentration required for the ultrasonic experiments. No measurable concentration dependence was detectable over and above the experimental error.

If the concentration dependence of S for amylose is any guide then the above results may be very far from accurate. As will be shown later, S in the concentration range 0.1 to 0.2% has a small concentration dependence whilst the extrapolated value (0.015 0) may be 3 times the value at 0.2%.

It was found impossible to measure the diffusion constant of amylopectin in either water, sodium hydroxide (0.2N), or sodium chloride (0.2M). In some cases the results were not reproducible and in others the schlieren diagram was still a straight line after 14 hr. (cf. glycogen and amylose a peak in 30 mins.).

Inaccuracies in determining the molecular weight of the above type substances are unfortunately entirely due to difficulties inherent in determining the respective diffusion coefficients accurately.

26. VISCOSITY.

Viscosities were measured as outlined in section 4. Fig 5. 8a shows the viscosity of 8 samples of A98 at different concentrations and the extrapolation of those to infinite dilution. All intrinsic viscosities quoted were determined in this manner.

Table 5. 7.

Substance		$[\eta]_{1230}$ *	$[\eta]_{y=o}$	$\overline{DP}_n \times 10^{-3}$
A58	0	300	390	2.22
	10	225	292	1.66
	20	190	246	1.40
	42	166	216	1.23
	90	145	188	1.07
	150	124	161	0.92
	240	110	143	0.82
	450	82	106	0.61
A98-58	0	480	429	3.55
	10	330	357	2.44
	20	275	286	2.03
	40	220	216	1.63
	90	166	184	1.23
	150	142	162	1.05
	240	125	110	0.93
	450	85	110	0.63
A98	0	410	533	3.03
	10	320	415	2.37
	20	264	343	1.95
	40	203	264	1.50
	90	150	195	1.11
	150	120	156	0.89
	240	100	130	0.74
	450	78	101	0.58

$[\eta]_{1230}$ is the intrinsic viscosity at $\gamma = 1230$ sec.$^{-1}$.

$[\eta]_{y=o}$ is the intrinsic viscosity at $\gamma = o$.

The final column in table 5. 7. has been calculated employing the following formula suggested by Cowie and Greenwood (123)

$$7.4[\eta]_{1230} = \overline{DP}.$$

The relationship between $[\eta]_{y=o}$ and $[\eta]_{1230}$ is

$$0.77[\eta]_{y=o} = [\eta]_{1230}$$

* I wish to thank Dr. J.McK.G. Cowie for determination of the shear correction.

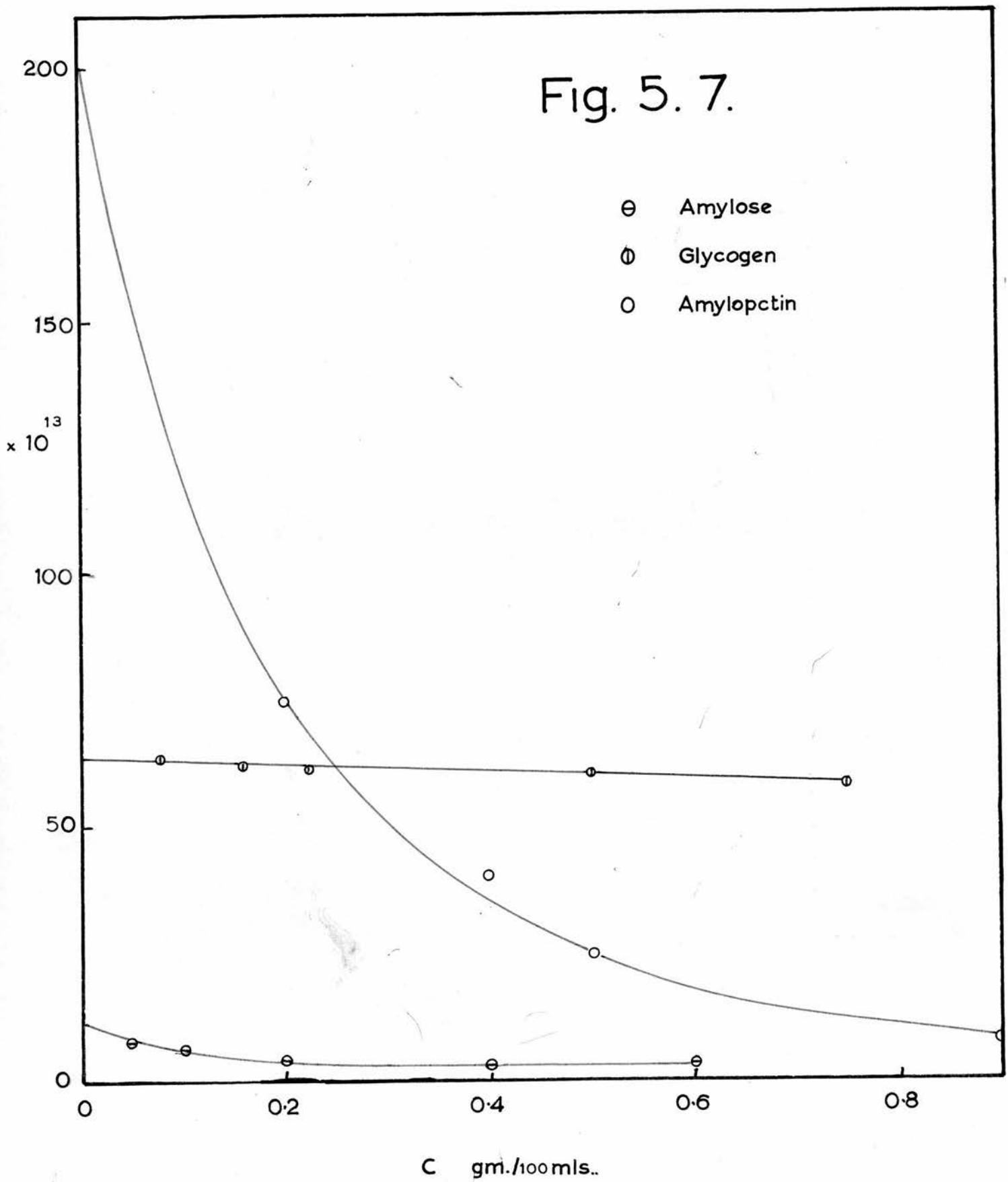
Fig. 5. 7.
Amylose
Glycogen
Amylopctin
200
150
100
50
0
x 10 13
0
0·2
0·4
0·6
0·8
C gm./100 mls.

26. SEDIMENTATION.

The relative concentration dependence of amylose, amylopectin and glycogen may be seen in fig. 5. 7. Glycogen has a small but measurable linear concentration dependence. Amylopectin has a large concentration dependence and this increases rather rapidly in the region 0.4 - 0% concentration, so much so that any determination above 0.4% is relatively inaccurate. This large concentration dependence is probably due to molecular entanglement and free sedimentation does not occur until in the very dilute range. Duc, however, to the polymolecularity and the large molecular weight, amylopectin is not amenable to study in the very dilute range.

Amylose has a moderate concentration dependence. The concentration range it is necessary to work in is 0 - 0.2%, as above this value all samples have approximately the same sedimentation coefficient.

In the determination of the sedimentation coefficient distribution it is impracticable to use a polynomial relation between S and C. It was therefore decided to try and utilise the linear portion of the curve near infinite dilution.

At this stage a 30 mm. Kel F cell was available and it was found that it was then possible to measure modal sedimentation coefficients down to 0.01% concentration. For a distribution, it is necessary that the entire peak has left the meniscus. With this cell, such measurements were practicable down to about 0.06%. This concentration range was still on the linear portion

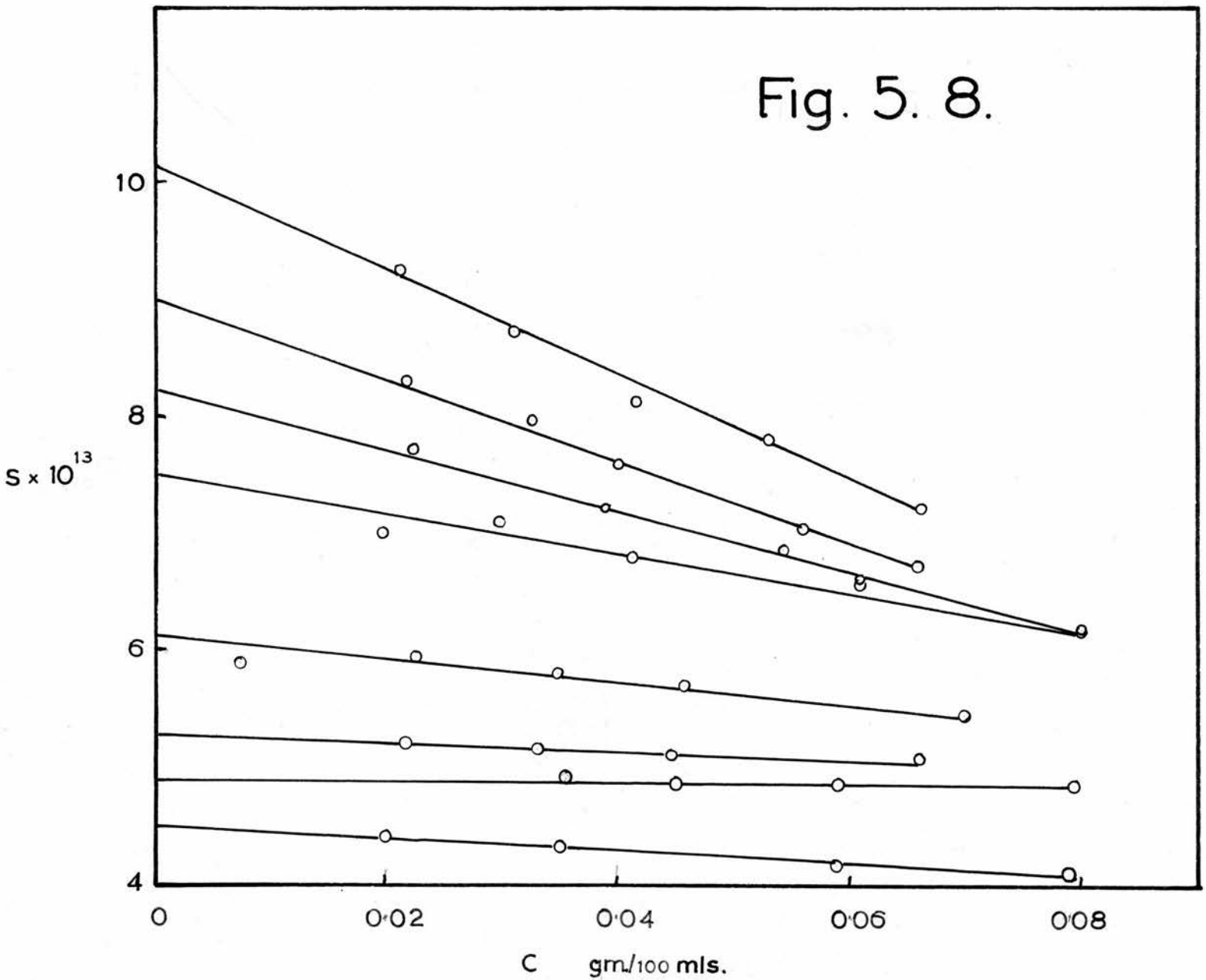
Fig. 5. 8.
10
8
6
4
S x 10^13
0
0·02
0·04
0·06
0·08
C gm./100 mls.

of the curve (see fig. 5. 8.). Fig. 5. 8. also shows the extrapolation to infinite dilution of 8 samples of A98. All S values quoted in the following were extrapolated similarly and the extrapolated value is quoted.

Table 5. 6.

Substance		$S_o \times 10^{13}$	$D_m \times 10^7$	$M_{sd} \times 10^{-5}$	$\overline{DP}_{sd} \times 10^{-3}$
A60	0	8.2	0.95	5.5	3.42
	10	7.35	1.11	4.25	2.59
	40	6.75	1.30	3.33	2.05
	90	5.80	1.37	2.71	1.68
	240	4.90	1.66	1.89	1.17
	450	4.10	2.00	1.31	0.81
A98	0	10.14	0.80	8.12	5.02
	10	9.0	0.92	6.27	3.87
	20	8.2	1.01	5.21	3.21
	40	7.5	1.16	4.14	2.55
	90	6.08	1.35	2.88	1.78
	150	5.30	1.47	2.31	1.42
	240	5.00	1.82	1.76	1.08
	450	4.50	2.00	1.44	0.88
A98-58	0	11.0	0.74	9.52	5.88
	10	9.1	0.90	6.47	3.99
	20	8.3	1.03	5.16	3.19
	40	7.5	1.10	4.36	2.69
	90	6.3	1.30	3.11	1.92
	150	5.9	1.40	2.70	1.66
	240	5.5	1.55	2.27	1.40
	420	4.0	1.90	1.35	0.83

From the family of curves in fig. 5. 8. a relationship between S, S_o and C was derived.

$$S = S_o (1 - 4.52 \times 10^{-24} S_o^2 C).$$

This equation was employed in the calculation of the sedimentation coefficient distribution.

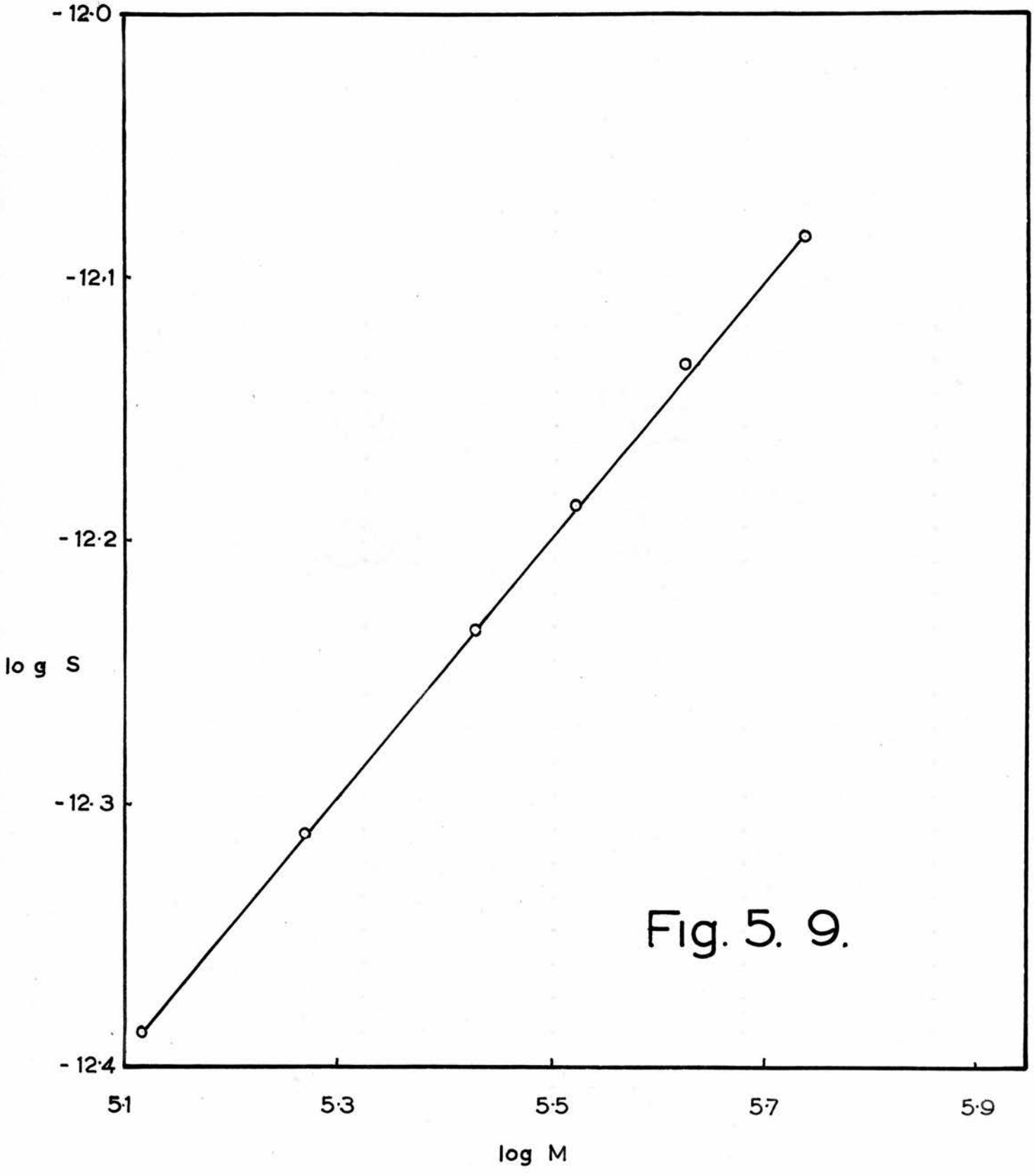

Fig. 5. 9.

27. DISTRIBUTION OF MOLECULAR WEIGHTS.

The sedimentation coefficient distributions were determined as in section 4.

Amylose:- The relationship between S and M was then obtained from a graph of log S v. log M for A58 (fig. 5. 9.) and the molecular weight distribution calculated employing

$f(m)dm = g(S_o)ds$ or $f(m) = g(S_o)ds/dm$

but from fig. 5. 9. $S_o = K'M^{0.492}$ or $S_o/M^{0.492} = K'$.

Table 5. 8. shows values of K' calculated from S_o and $M^{0.492}$ values for A98.

Table 5. 8.

$M \times 10^{-5}$	$S_o \times 10^{13}$	$K' \times 10^{15}$
8.12	10.14	1.248
6.27	9.00	1.272
5.21	8.20	1.264
4.14	7.50	1.288
2.88	6.08	1.240
2.31	5.30	1.214
1.76	5.00	1.316
1.44	4.50	1.298

It can be seen therefore that within experimental error the value of K' for this sample (= 1.27×10^{-15}) is constant.

Fig. 5.10.

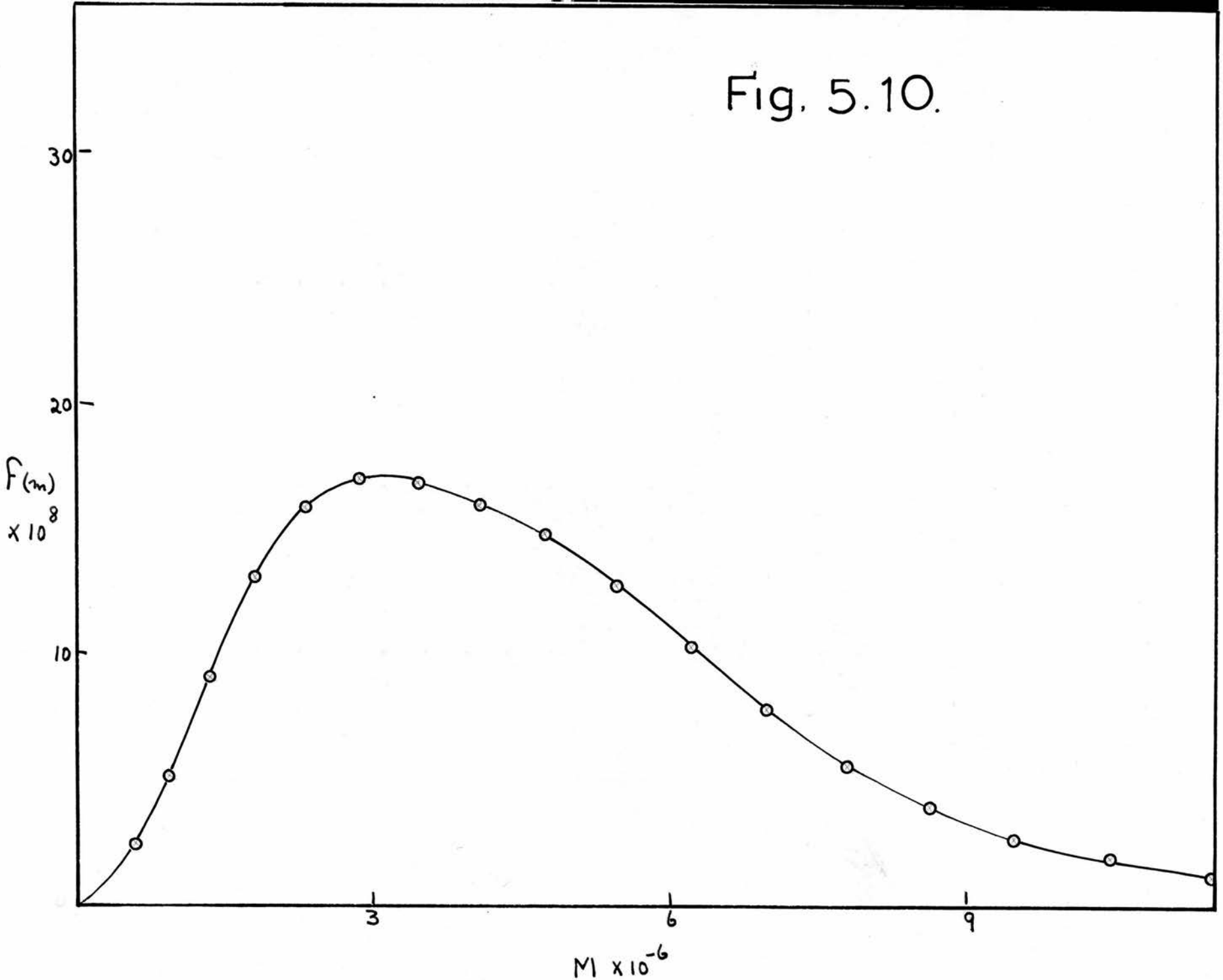

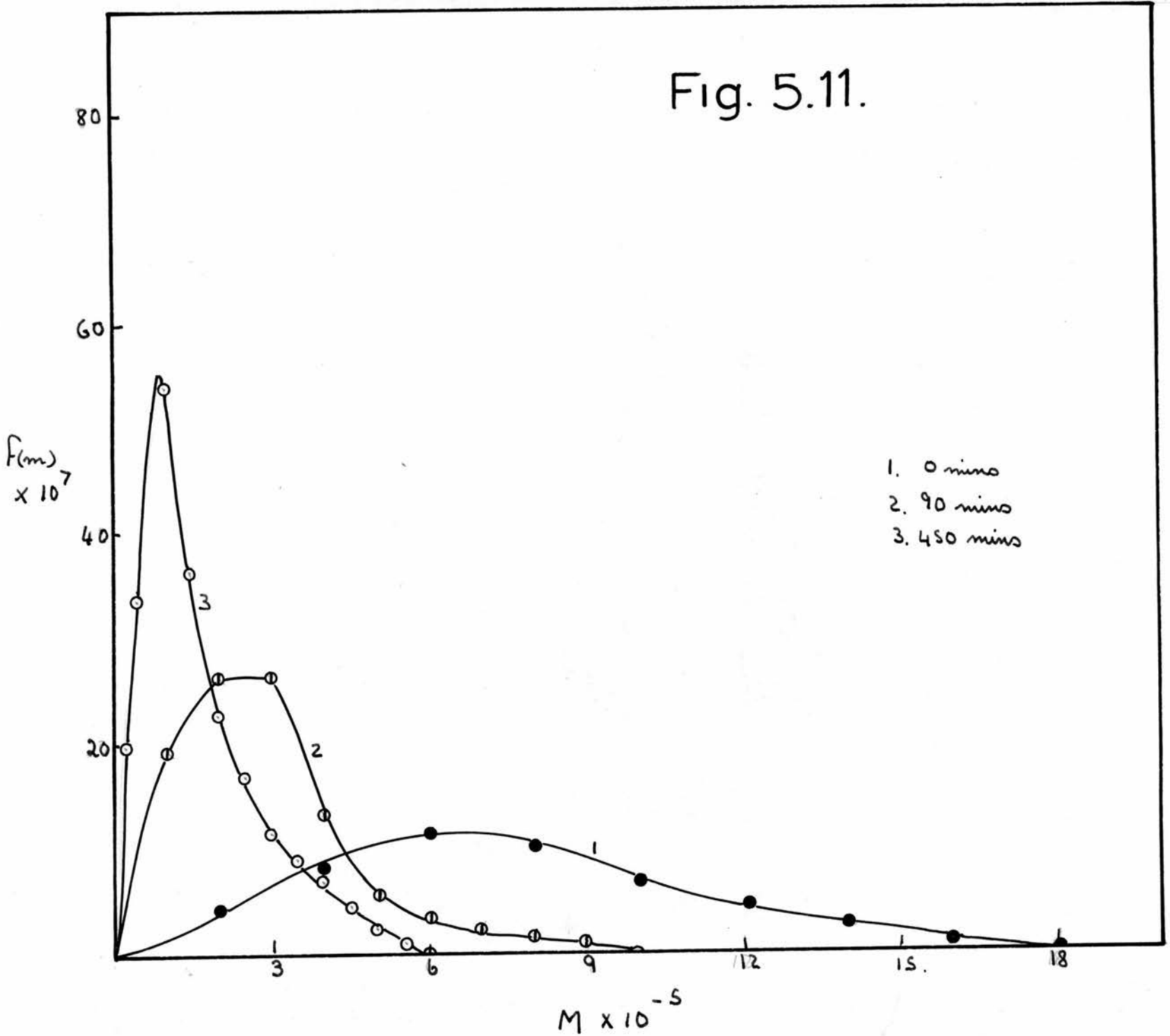
Fig. 5.11.
80
60
40
20
F(m) x 10^7
1. 0 mins
2. 90 mins
3. 450 mins
1
2
3
3
6
9
12
15.
18
M x 10^-5

Fig. 5.12.

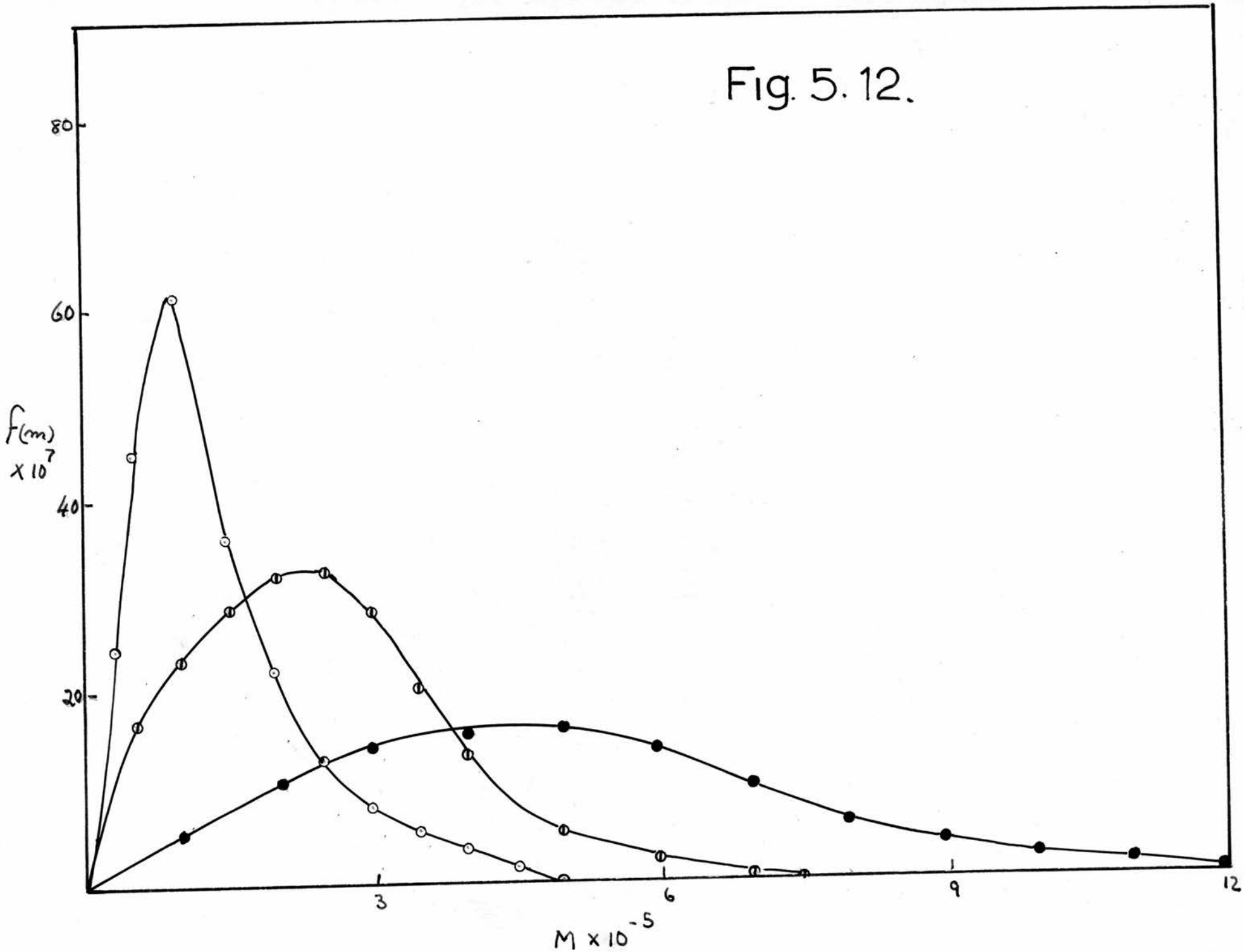

Fig.5.13.

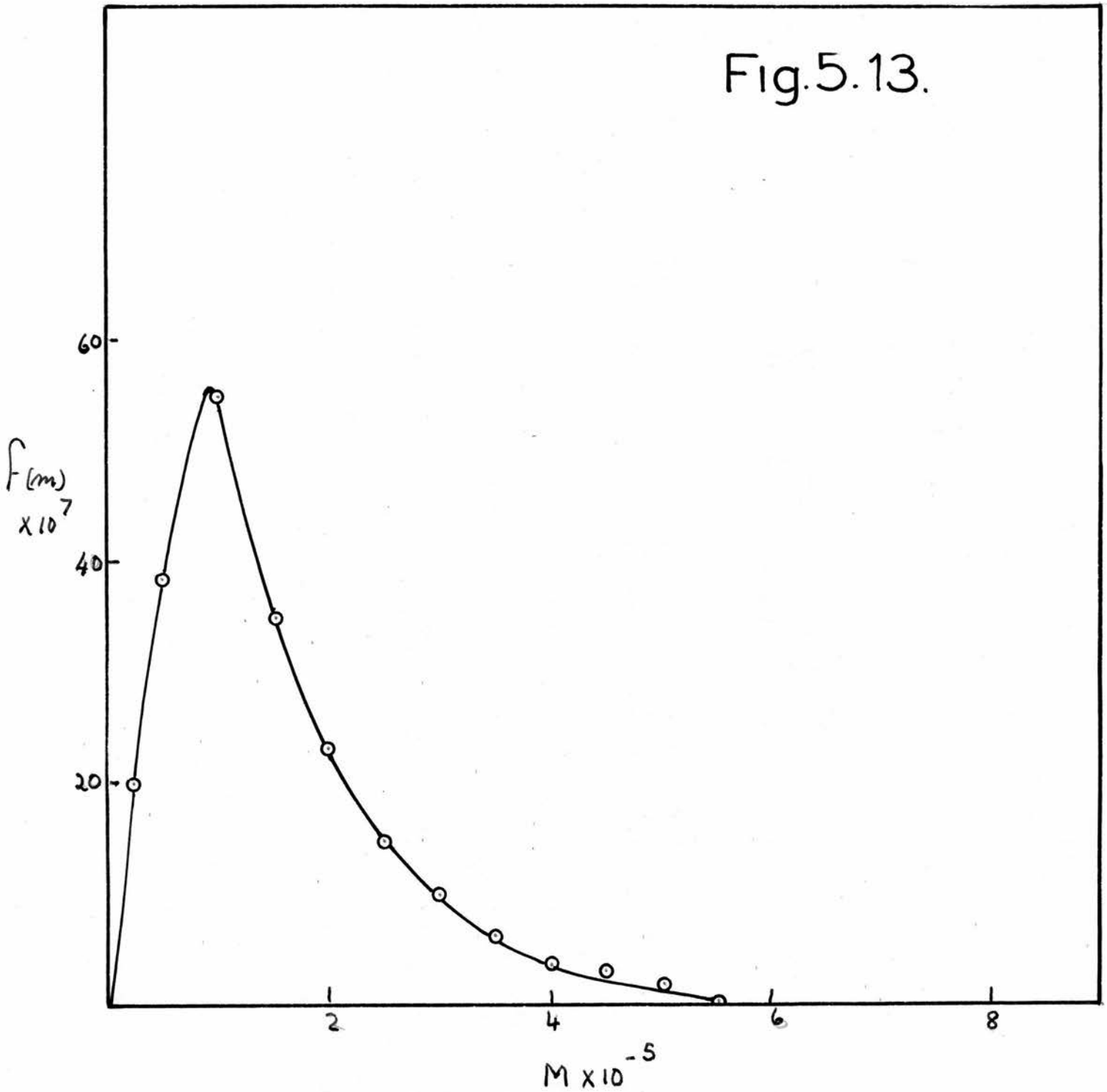

It can therefore be assumed that for amylose in 0.2N potassium hydroxide the relation $S = 1.27 \times 10^{-15} M^{0.492}$ holds

and $ds/DM = 6.25 \times 10^{-16} M^{-0.508}$

hence $f(M) = g(S_o)\ 6.25 \times 10^{-16} M^{-0.508}$

This equation was employed in evaluating the molecular weight distribution of amylose.

In figs. 5. 10, 11, 12 and 13 are shown the resultant distributions for glycogen, A98 after 0, 90 and 450 mins., degradation by ultrasonics, A58 after 0, 90 and 450 mins., degradation by ultrasonics and A98-58 at 450 mins., degradation by ultrasonics, respectively.

The sedimentation coefficient distributions have no pronounced skew at any time during the degradation. This fact is in agreement with the results obtained when the ratio of the weight average $\overline{DP}$ to number average $\overline{DP}$ is calculated.

Table 5. 9.

Substance		$\overline{DP}_{sd}/\overline{DP}_n$	Substance		$\overline{DP}_{sd}/\overline{DP}_n$
A98	0	1.66	A58	0	1.54
	10	1.63		10	1.56
	20	1.64		42	1.67
	40	1.70		90	1.57
	90	1.61		240	1.43
	150	1.60		450	1.33
	240	1.54			
	450	1.46			

28. HYDRODYNAMIC BEHAVIOUR

The sedimentation, diffusion and viscosity measurements on the different amylose samples were used to calculate various hydrodynamic quantities as shown in tables 5. 10. and 5. 11.

Table 5. 10.

Substance		$[\eta]_{y=o}$	J		$\eta/\bar{v}$	f / fo	$1/D_{sd}$
			Simha	Burger			
A98	0	533	94	188	860	4.56	127
	10	415	82	164	670	4.32	113
	20	343	74	148	554	4.19	105
	40	264	64	128	426	3.93	92
	90	195	53	110	315	3.80	85
	150	156	47	94	252	3.77	84
	240	130	42	84	210	3.33	63
	450	101	37	73	163	3.24	60
A60	0	390	80	152	630	4.36	114
	10	292	68	134	471	4.07	99
	20	246	61	122	397	-	-
	42	216	57	114	348	3.76	83
	90	188	52	105	303	3.84	87
	150	161	47	94	260	-	-
	240	143	45	90	231	3.57	74
	450	106	38	75	171	3.34	64

Table 5. 11.

Substance	Simha			Burger			S and D		
	d	l	$\bar{I}$	d	l	$\bar{I}$	d	l	$\bar{I}$
A98 0	25.7	2420	0.483	20.4	3840	0.76	23.2	2954	0.588
10	24.6	2020	0.522	19.5	3200	0.827	22.17	2505	0.647
20	24.0	1780	0.555	19.0	2810	0.875	21.36	2240	0.698
40	23.3	1492	0.585	18.5	2370	0.930	20.72	1900	0.745
90	27.0	1166	0.655	17.2	1890	1.062	18.81	1600	0.900
150	21.3	1000	0.705	16.9	1590	1.12	17.57	1466	1.03
240	20.2	848	0.785	16.0	1340	1.24	17.59	1155	1.03
450	19.7	730	0.830	15.7	1150	1.31	16.80	1007	1.14
A60 0	23.8	1904	0.557	19.22	2920	0.854	21.12	2425	0.709
10	23.08	1570	0.606	18.41	2467	0.953	20.39	2010	0.776
40	22.57	1286	0.628	17.90	2040	0.995	19.89	1654	0.807
90	21.68	1127	0.670	17.19	1820	1.075	18.28	1592	0.948
240	20.20	909	0.777	16.04	1444	1.234	17.12	1270	1.085
450	18.92	719	0.888	15.09	1132	1.400	15.9	1017	1.256

where f / fo was calculated from

$$f / fo_{sd} = \left(\frac{4}{3}\right)^{1/3} \frac{1}{6\eta}\left(\frac{RT}{\pi N}\right)^{2/3} \left\{\frac{1 - \bar{v}\rho}{D_M^2 S_o \bar{v}}\right\}^{1/3}$$

$$d \text{ from } d = \left[\frac{6M\bar{v}}{\pi N \, 1/d}\right]^{1/3}$$

$$\text{and } f / fo_{sd} = 0.506 \, (1/d)^{0.454} \qquad 5. \; 1.$$

$$\text{and } \bar{I} = 1 / \overline{DP}_{sd}$$

Fig. 5.14.

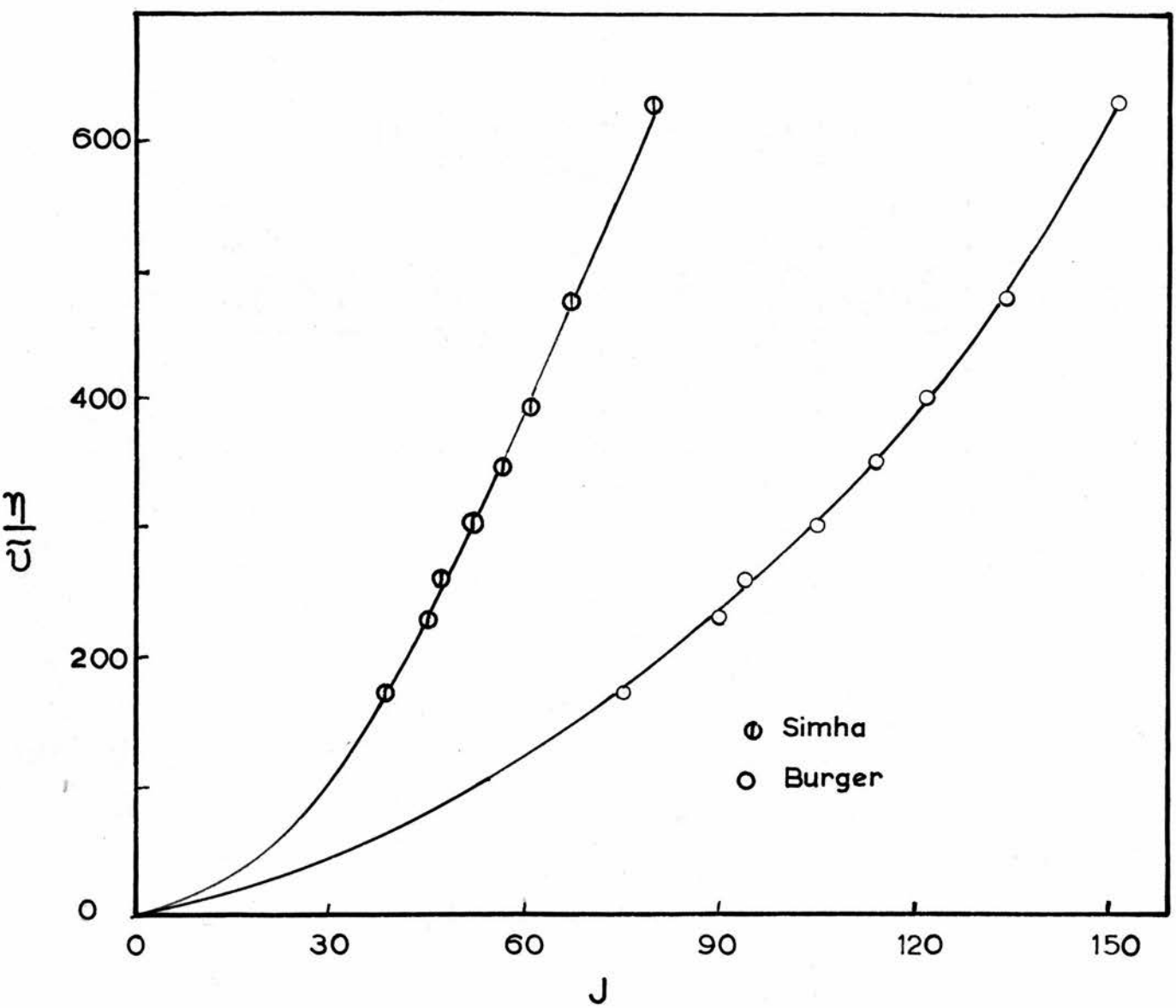

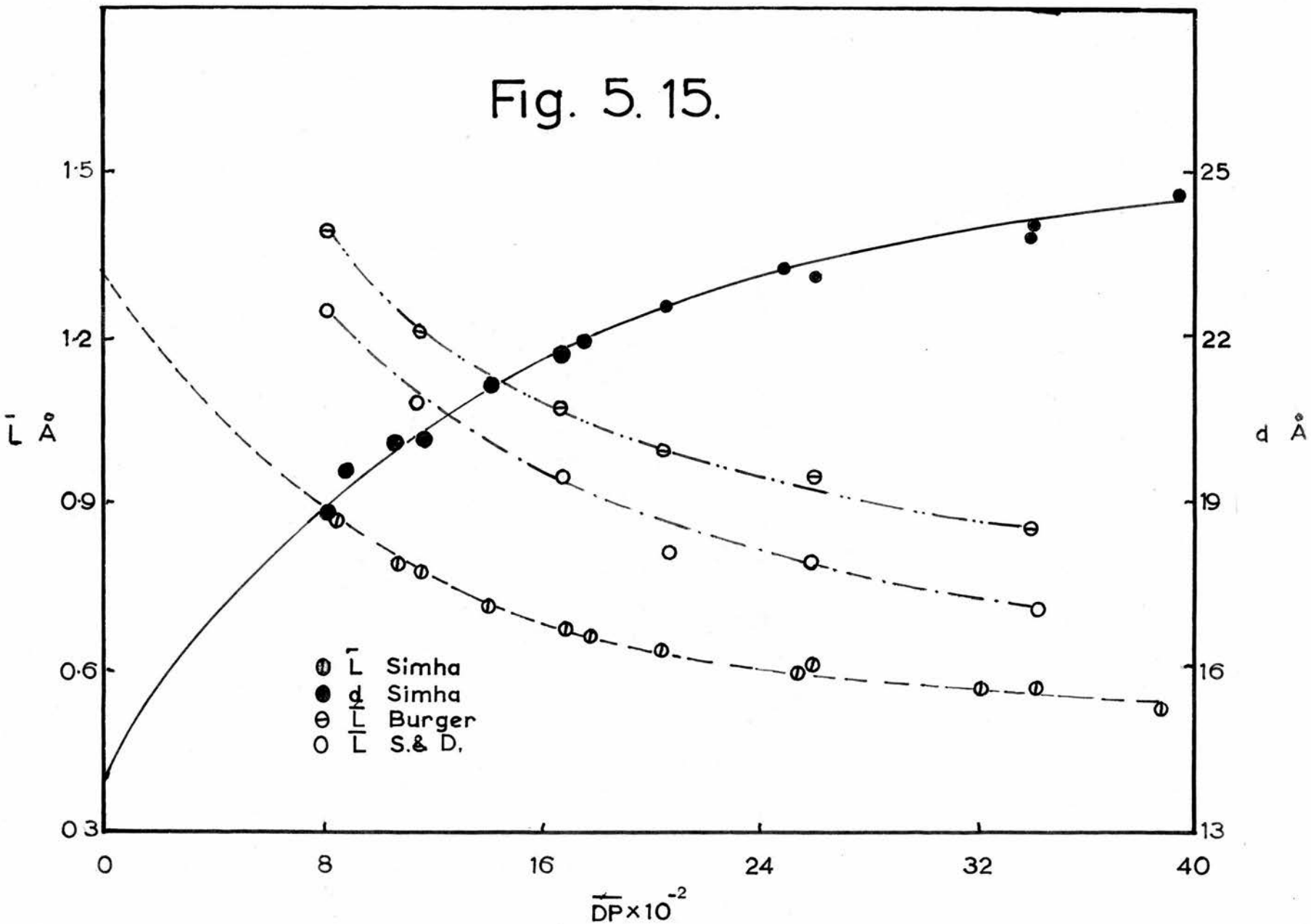
Fig. 5. 15.
1·5
1·2
0·9
0·6
0 3
$\bar{L}$ Å
25
22
19
16
13
d Å
0
8
16
24
32
40
$\overline{DP} \times 10^{-2}$
$\bar{L}$ Simha
d Simha
$\bar{L}$ Burger
$\bar{L}$ S.& D.

From table 5. 10, the axial ratio calculated by the Burger equation gives a value twice that obtained by the Simha method, whilst that calculated from S and D by equation 5. 1. gives a value midway between the two. Fig. 5. 14. shows a plot of $[\eta]_{\gamma=0} / \bar{v}$ v. J for both Simha's and Burger's functions. When, however, d and $\bar{l}$ are calculated, the Simha results extrapolate to $\bar{l} = 1.3\overset{\circ}{A}$ and $d = 14\overset{\circ}{A}$ (fig. 5. 15.). A similar extrapolation for Burger's results gives $d = 11\overset{\circ}{A}$ and $\bar{l} = 2.0\overset{\circ}{A}$. On the basis of X-ray measurements, the glucose unit will occupy $1.3\overset{\circ}{A}$ and the helix is $13.0\overset{\circ}{A}$ in diameter (62). From fig. 5. 15. it appears that in the limit for high molecular weights $\bar{l}$ equals half the glucose length and d is twice the diameter. This variation could indicate that the amylose helix has a tendency to double back on itself with increase in molecular weight.

According to Simha (124) $D = KM^{-(\frac{1}{3} + 0.454P)}$ and $S = K'M^{\frac{2}{3} - 0.454P}$ where D is the diffusion coefficient, S is the sedimentation coefficient and P is a parameter dependent on molecular shape.

For P = 0 and 1 the above equations reduce to

P = 1	$D = KM^{-0.79}$	$S = K'M^{0.21}$
P = 0	$D = KM^{-\frac{1}{2}}$	$S = K'M^{\frac{2}{3}}$

For A98 and A60, the graph of log S and log D v. log M shows that $D \propto M^{-0.526}$ and $M^{-0.54}$ respectively whilst $S \propto M^{0.5}$

for both samples. The corresponding values of P calculated from the above equations are 0.425, 0.455 and 0.383. Since the limits of P are - $0 < P < 1$ - the lower limit characterising the ideal coil, and the upper one a straight rigid chain, it would therefore appear that amylose is intermediate in behaviour between the above two extreme cases.

No conclusive evidence as to the shape of amylose was obtained from a study of the distributions when theoretical averages were calculated for different molecular shapes (cf. Singer (78)).

When, however, $\sum f(m)M / \sum f(m)$ ($\equiv$ to a weight average) and $\sum f(m) / \sum f(m) / M$ ($\equiv$ to a number average) were calculated for the three A58 distributions the calculated and observed values were in agreement within experimental error (table 5. 12.).

Table 5. 12.

A58	$\sum f(m)M / \sum f(m)$	$\overline{DP}_{sd}$	$\sum f(m) / \sum f(m) / M$	$\overline{DP}_{n}$
0	3.08	3.42	2.23	2.22
90	1.6	1.68	1.23	1.07
450	0.83	0.81	0.574	0.61

29. Ultrasonic Degradation

Jellinek and White (29) have studied the dependence of the rate constant of degradation by ultrasonic waves on the chain length for polystyrene in benzene and found that the rate constant varied with chain length and had a maxima in the curve at approximately 4350 $\overline{DP}$. Also all samples tended to the same limit. Mostafa (27) studied the effect of power on the rate constant and final chain length for polystyrene in benzene and found that the rate constant increased with increasing power, was independent of chain length above a limiting value and varied throughout the reaction. The above results were obtained by applying kinetic schemes derived by the individual authors.

If the ultrasonic power is increased (frequency constant) then the amount of cavitation will increase as the stronger of the weak nuclei take part. An increase in the power will not increase the amplitude of the resonating cavity to any marked extent, as it is the time of vibration (dependent on ultrasonic frequency) that is the controlling factor. An increase in power will, however, shorten the time between when a cavity starts vibrating and when it reaches resonance. As the shock wave will not increase in amplitude, the size of the micro-cavities will stay approximately the same. This will result in little or no increase in the flow of solvent and hence the

overall effect will be negligible. Therefore the change in the ultimate chain length with change in power should be negligible in contradiction to Mostafa's results.

An increase in power will increase the amount of cavitation, and will also increase the effects due to emission of light, electrical discharge and high temperatures. As was stated earlier, there is no conclusive evidence that sonoluminescence does occur in organic solvents. It is therefore a doubtful procedure to base an argument on the emission of light or electrical discharge. The high temperature effect does not fall into the same category, as it is a direct consequence of a collapsing cavity. It should be noted that neither of the above workers report any special drying of the benzene and "Analar" benzene contains up to 0.1% water.

When the power is increased there will be an enhanced probability that a polymer molecule is nearer to a collapsing cavity and therefore the interaction between the products from the collapsing cavity and polymer may be greater.

It is thought by the author that the dependence of ultimate chain length on power may be due to increased side-effects and the increased probability of interaction between those and polymer. This would mean that two different reactions are proceeding at the same time: (1) degradation due to frictional forces and (2) degradation due to side-effects.

Reaction (2) will continue until the irradiation ceases, whereas reaction (1) will be completed in a finite time dependent on the power employed. This may account in part for Mostafa's result that the rate constant changed with time of reaction.

Theoretical considerations also suggest that various types of side-reactions occur. The influence of ultrasonic radiation on a polymer molecule dissolved in an organic solvent results predominantly in mechanical degradation due to frictional forces. However, this degradation cannot occur without the simultaneous formation of free radicals, i.e.

$$P - P \xrightarrow{\text{ultrasonics}} P\cdot + P\cdot$$

This type of free radical can be destroyed in several ways, e.g.

(1) $P\cdot + P\cdot \longrightarrow P - P$

(2) $P - P\cdot \longrightarrow P = P$

(3) $P_1\cdot + P_2 \longrightarrow P_1 + P - \dot{P} - P \longrightarrow P - P = P$

$$\begin{array}{l} \downarrow P\cdot \\ P - \underset{\displaystyle P}{\underset{|}{P}} - P \cdots\cdots \text{Branching} \end{array} \qquad \downarrow P\cdot$$

and may result in the formation of high molecular weight branched products. Further, if the ultrasonics causes free

radical formation from the solvent, then these free radicals themselves may cause additional degradation. The overall picture may therefore be complicated.

Mostafa irradiated a polystyrene solution in presence of and absence of diphenylpicrylhydrazyl (D.P.P.H.) and found that the rate of degradation increased in the presence of D.P.P.H. This may indicate that polymerization was occurring and would explain the high degradation threshold (3.12 watts / cm^2) which he quoted.

This threshold value is too large for benzene by comparison with the results obtained here, but too small to be accounted for by complete degassing of the solvent. Although the solution may have been partially degassed, the possibility also exists that any degradative effects were counterbalanced by side-effects of either simple polymerization or changes in shape due to branching as outlined above. If the changes in the system are followed by viscosity, then such effects will be difficult to determine.

Such side-effects may have influenced the reactions studied in this work, but as irradiation conditions were kept constant and results are used for comparative purposes, conclusions should be valid.

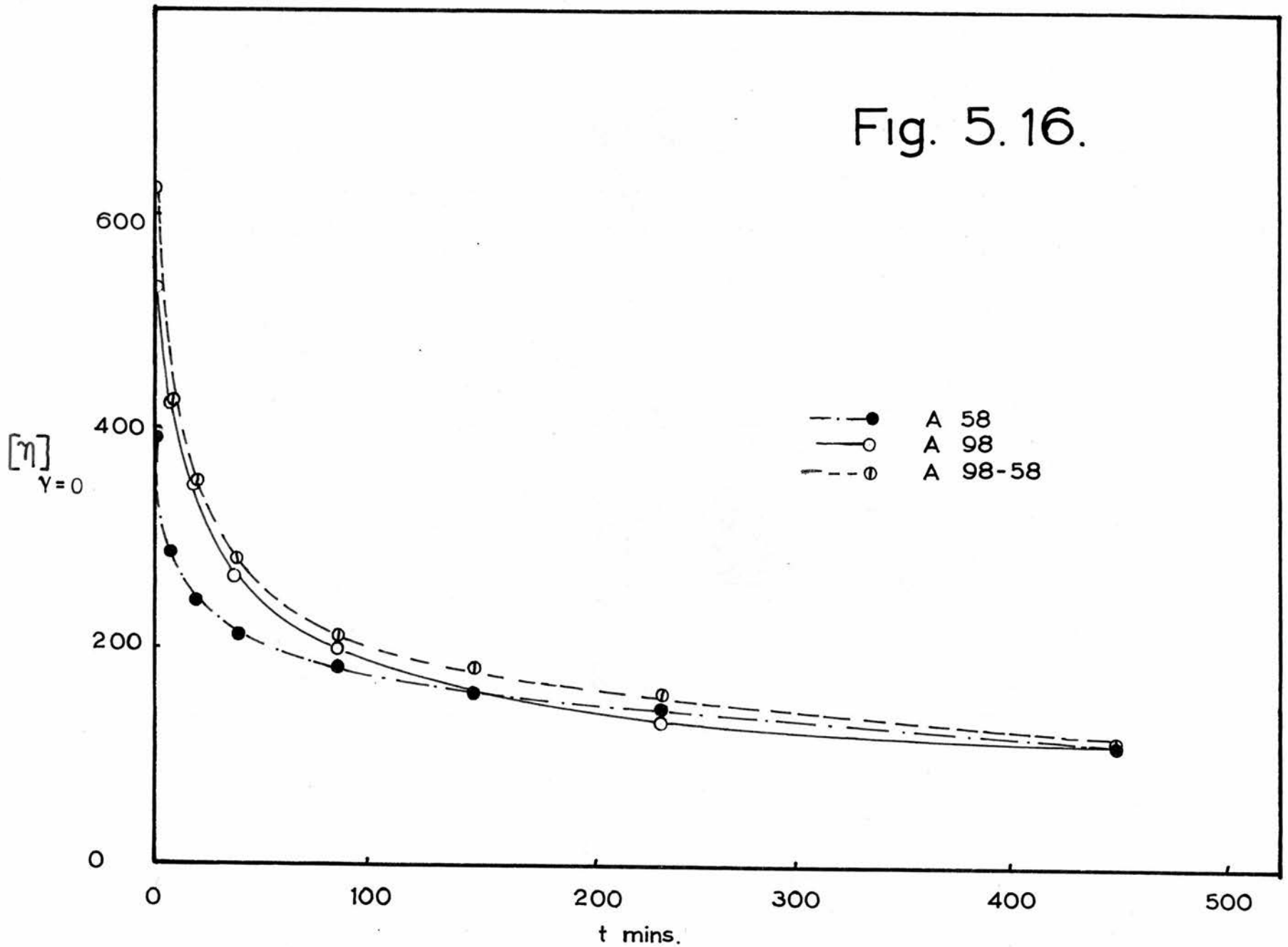
Fig. 5.16.
600
400
200
0
[η]
γ=0
A 58
A 98
A 98-58
0
100
200
300
400
500
t mins.

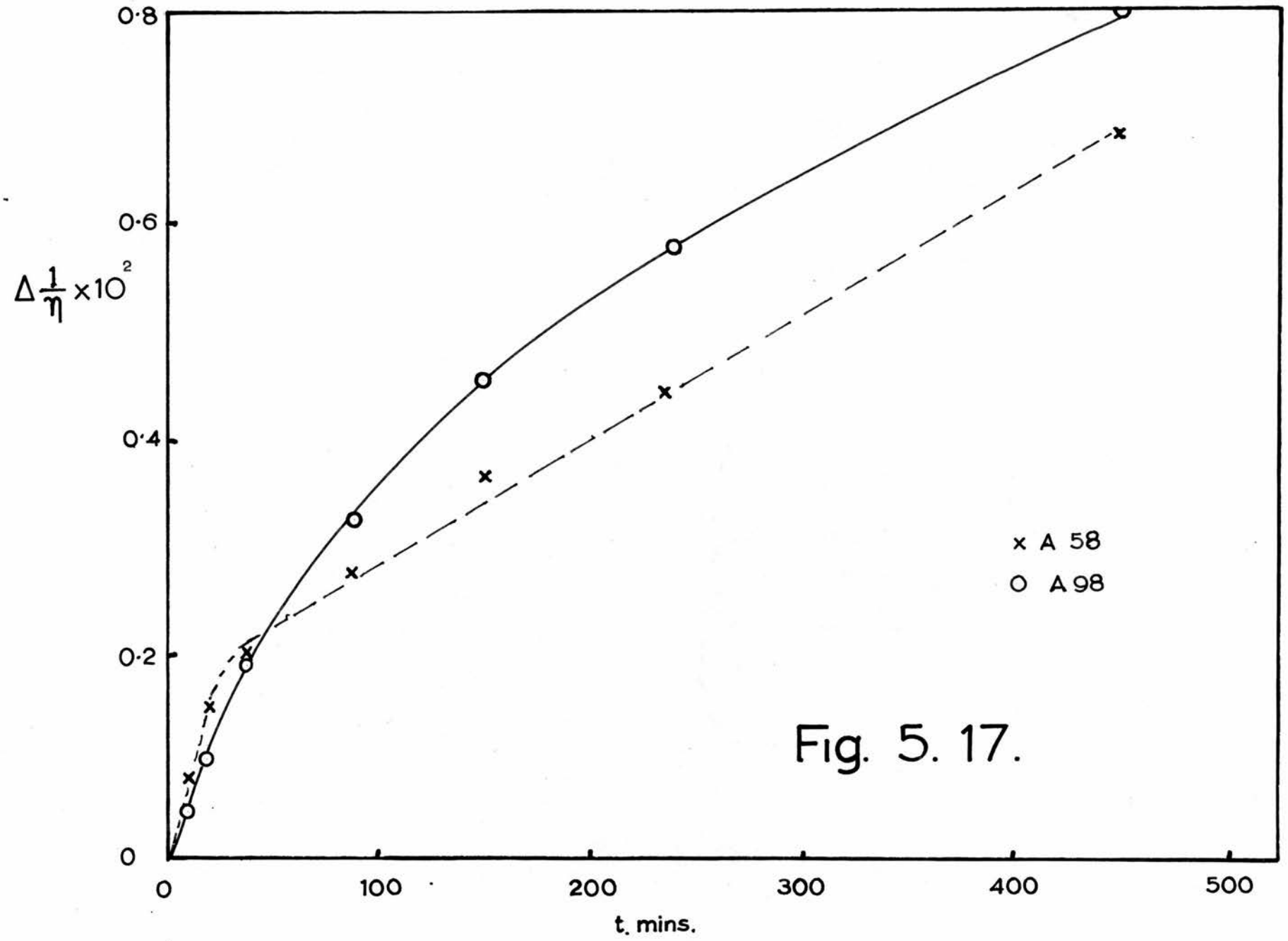
0·8
0·6
0·4
0·2
0
$\Delta \frac{1}{\eta} \times 10^2$
0
100
200
300
400
500
t. mins.
x A 58
O A 98

Fig. 5. 17.

Results on starch-type polysaccharides.

The decrease in molecular weight with time of three amylose samples, an amylopectin and a glycogen occurring at 0.24 watts / cm^2 was followed viscometrically and by sedimentation velocity.

To show that the observed degradations were due to cavitation, an amylose solution was irradiated with the power below the cavitation threshold (see p.104). No degradation was found under these conditions.

Amyloses: Fig. 5. 16. shows plots of $[\eta]$ v. time of degradation for A98, A98-58, and A58. The corresponding $\overline{DP}_{sd}$ and $\overline{DP}_n$ have already been tabulated (table 5. 6.).

According to equation 1. 10., $\Delta\ 1/[\eta]$ v. t. should be a straight line passing through the origin (o. o.) unless a weak bond is present. For A58, $\Delta\ 1/[\eta]$ v. t. (fig. 5. 17) gives a straight line portion, which has a positive intercept. This indicates the presence of a weak bond in the sample. For A98, $\Delta\ 1/[\eta]$ v. t. (fig. 5. 17) gives a straight line with slope parallel to that for A58 after 150 mins. In this case the initial curvature is extended over a longer period and indicates that there are more weak bonds in this sample. A98-58 would appear to be comparable with A98.

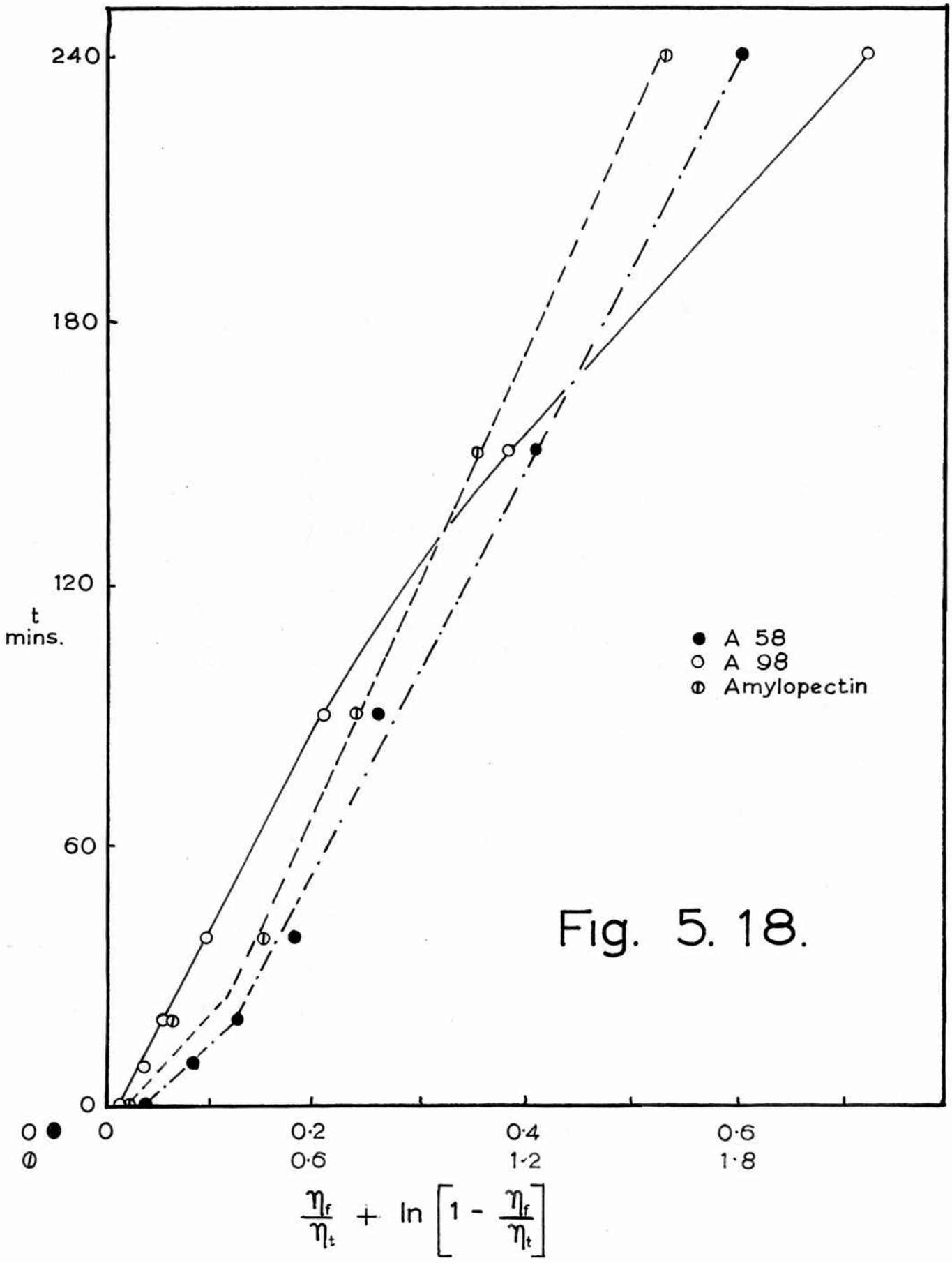
240
180
120
60
0
t
mins.
● A 58
○ A 98
⊕ Amylopectin
0
0·2
0·4
0·6
0
0·6
1·2
1·8
$\frac{\eta_f}{\eta_t} + \ln\left[1 - \frac{\eta_f}{\eta_t}\right]$

Fig. 5. 18.

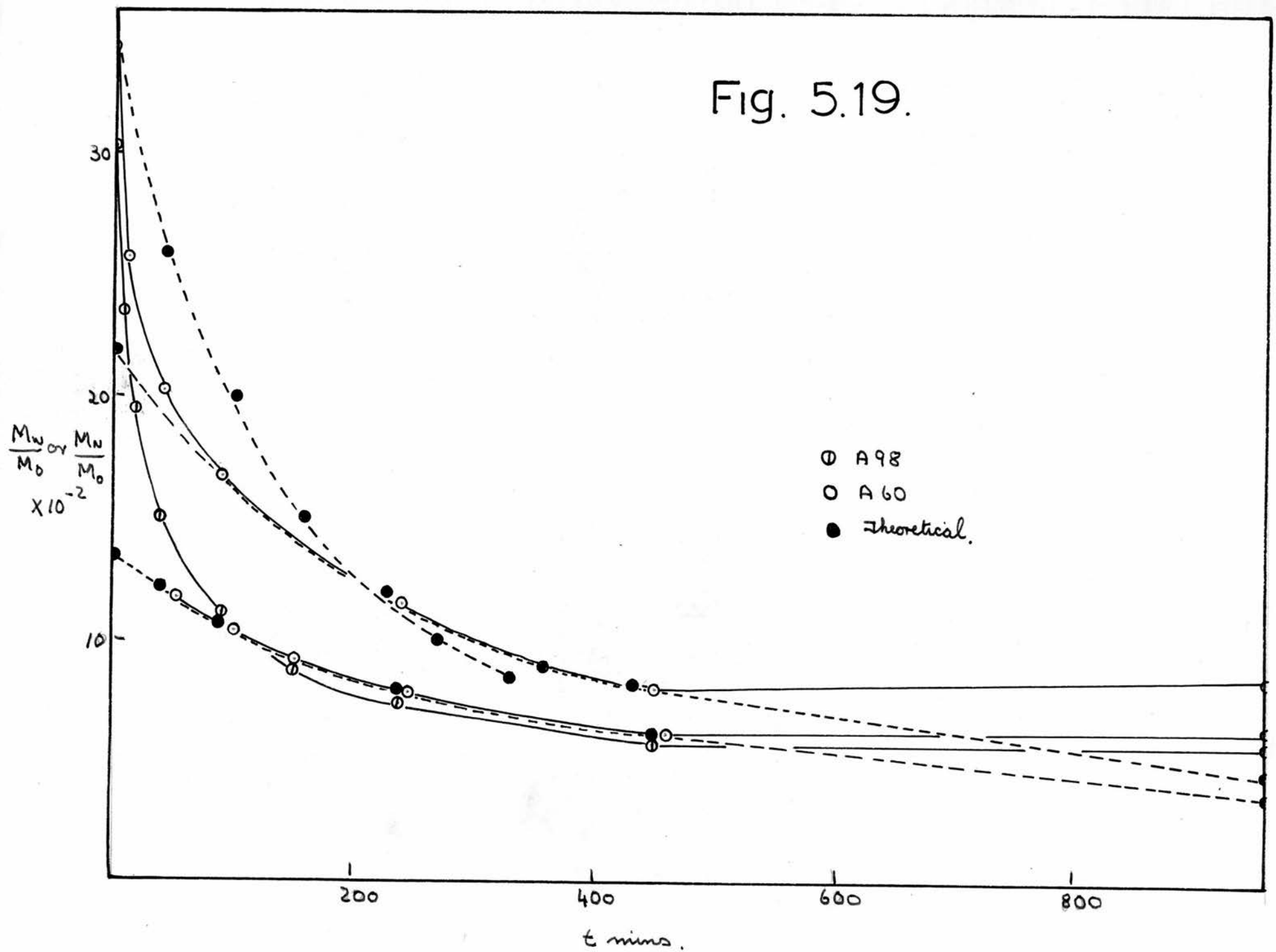
Fig. 5.19.
30
20
10
$\frac{M_N}{M_0}$ or $\frac{M_N}{M_0}$
$\times 10^{-2}$
A 98
A 60
Theoretical.
200
400
600
800
t mins.

The above results raise the question of whether the weak bonds in A58 are due to impurity. The β-amylolysis limit of 98 ± 2% gives a maximum impurity of 4% which could represent 8% of a substance with a 50% β-limit. This would be sufficient to cause the above results.

In fig. 5. 18, the results are plotted according to Jellinek's theory. It may be seen that whilst A58 gives a reasonably straight line, A98 however gives a curve. When A98 was degraded at various powers and concentrations the results indicated the same behaviour as at 0.24 watts / cm^2 and 0.2% concentration. A98-58 again behaves similarly to A98.

If Mostafa's theory is applied, then a comparison of the molecular weight distributions, theoretical and experimental, gives no better agreement.

Jellinek and Mostafa both report that on long irradiation the chain length weight distribution has a peak in the region of 700 - 1000 $\overline{DP}$ (for polystyrene). All chain length weight distributions for amylose have a peak in the same region (fig. 5. 11. 12. 13.). However, there is not the sharp fall at 800 that Mostafa suggests. This may be due to insufficient irradiation.

Application of random degradation kinetics (see p.27) to A58 and A98 gives no better agreement (fig. 5. 19.). If it is assumed that the intercept on the $\Delta\,{}^{1}/[\eta]$ v. t. curve

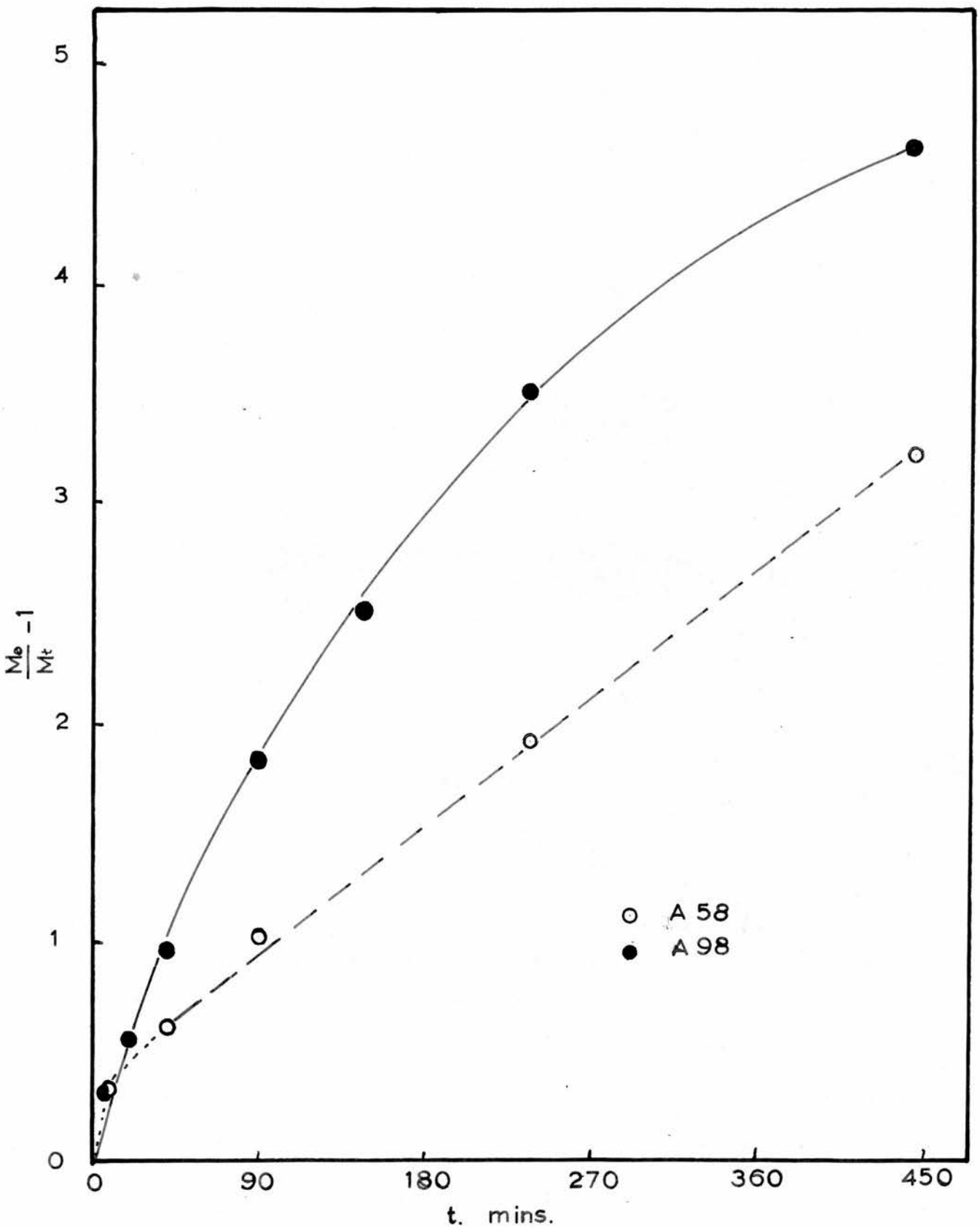

Fig. 5. 20.

is genuine, then the intercept value may be converted to a $\overline{DP}$, and this value taken as the initial $\overline{DP}$ for a random degradation kinetic scheme. When the results of such a calculation (using a velocity constant from the slope of the $\Delta\, 1/[\eta]$ v. t. curve) are compared with the experimental values then there is still no better agreement (fig. 5. 19). Therefore, although the initial phase of the breakdown may be random, the bulk of the reaction is not.

When the number of bonds broken per original molecule $[(m_o / m_t) - 1]$ is plotted against t., then A58 gives a straight line with a positive intercept, whilst A98 gives a curve (fig. 5. 20.).

All the above methods of representing the data suggest that weak bonds are present in all the samples; there being far more (i.e. 5x) in the A98 than in A58.

The major difference between A58 and A98 is their action with β-amylase. A58 has a limit of 98% whilst A98 has a 75% limit. To investigate whether the β-limit barrier and the weak link were the same, β-limits were measured. It was found that on irradiation the β-limit of A58 remained constant, whilst that of A98 gradually increases to 89% as shown below.

time mins.	0	20	40	150	240	450
β-limit	75	82	88	88	88.6	88.8

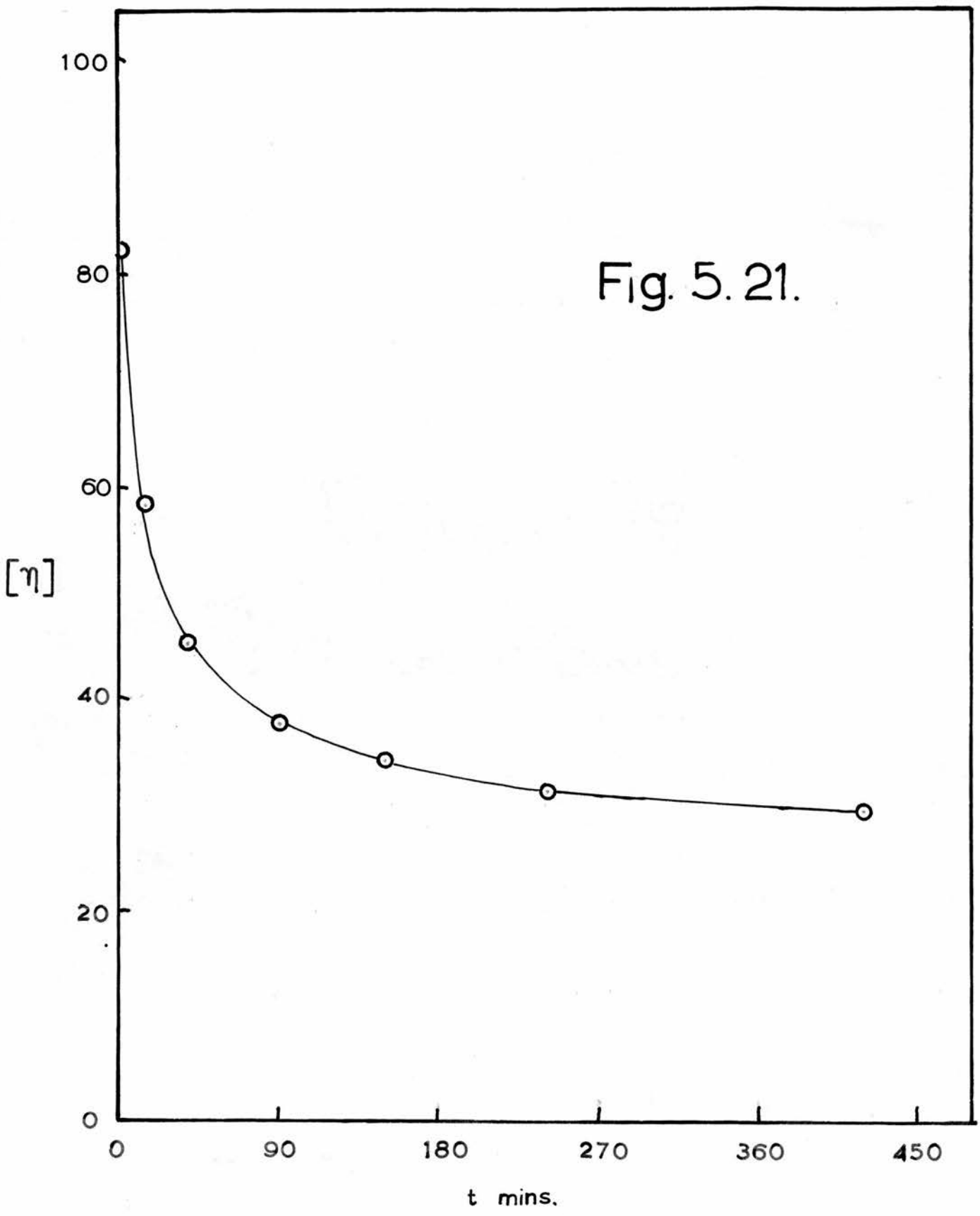

Fig. 5.21.

This suggests that the cause of the anomalous behaviour of A98 may be due to the fact that the weak bond and the β-limit barrier are not the same.

Amylopectin: Fig. 5. 21. shows the $[\eta]_{1230}$ v. t. curve for amylopectin. The $\Delta\ 1/[\eta]$ v. t. plot gives a slow but continuous curvature. When all the kinetic schemes considered above are applied to the amylopectin results, then only the Jellinek method results in a straight line (fig. 5. 18). This line is not parallel to that for A58. It would appear therefore that the reaction with amylopectin is totally different from that of amylose.

Glycogen: When glycogen was irradiated in both an air and a hydrogen atmosphere, little or no degradation occurred. It is thought that this is due to the molecule having a compact spherical SHAPE in solution. The extremely low limiting viscosity number of 7 (cf. amylopectin 70 amylose 500), the corresponding high molecular weight and near ideal sedimentation behaviour suggest that this is so.

SUMMARY

30. SUMMARY

The degradative effect of ultrasonic radiation on the components of starch - amylose, amylopectin - and glycogen has been critically examined by following changes occurring in the molecular weight and its distribution. As an essential preliminary to such investigations, methods had to be developed for measuring viscosity, sedimentation velocity and diffusion.

In particular, an apparatus has been described for carrying out diffusion on small quantities of polymer. The method of sedimentation velocity analysis has been critically examined, and the detailed methods of calculating the fundamental molecular weight distributions and its parameters are described. By these techniques, absolute molecular weight distributions are presented for some of these starch-type polysaccharides. Further, techniques have been evolved for irradiating polymer solutions with ultrasonics under controlled and reproducible conditions.

Theories of polymer degradation have been examined and applied to ultrasonic degradation.

The cavitation threshold power for distilled water saturated with hydrogen has been measured and the fact that

no degradation of amylose occurs in the absence of cavitation verified.

Amylose, amylopectin and glycogen have been subjected to ultrasonic waves of 0.24 watts / cm^2 and the physical properties of the degraded material studied. The relationships between diffusion coefficient, sedimentation coefficient, intrinsic viscosity and molecular weight have been determined. These physical constants were utilised to determine the hydrodynamic behaviour of amylose. It was concluded that, in solution, amylose behaves as a particle intermediate in shape between a free draining coil and a rigid rod.

Amylose and amylopectin are rapidly degraded by ultrasonics. The presence of weak bonds in amylose is postulated; these weak bonds are probably not identical to the barrier to β-amylolysis. The molecular weight distribution changes for amylose were determined.

At the powers employed in this work it was found that the effective degradation of glycogen by ultrasonics was small.

REFERENCES

References

1 Ono, S., Rev. Phys. Chem. Japan 14 (1940) 25

2 Thomas, R.M., et al., Ind. Eng. Chem. 32 (1940) 299
Sonntag, F., and Jenckel, E., Kolloid Z. 135 (1954) 1

3 Alexander, P., and Fox, M., J. Polymer Sci. 12 (1954) 533

4 Staudinger, H., and Dreker, E., Ber. 69B (1936) 1091

5 Bestul, A.B., and Belcher, H.V., J. Appl. Phys. 24 (1953) 1011
Morris, W.J., and Schnurmann, R., Nature 160 (1947) 674

6 Pat. Brit. 681548

7 Thomas, B.B., and Alexander, W.J., J. Polymer Sci. 25 (1957) 285

8 Flosdorf, E.W., Chambers, L.A., and Malisoff, W.M., J. Amer. Chem. Soc. 58 (1936) 1069

9 Virtanen, A.I., and Ellfolk, N., Acta Chem. Scan. 4 (1950) 93

10 Liu, S., and Wu, H., J. Amer. Chem. Soc. 56 (1934) 1005

11 Parke, A.V., and Taylor, D., J. Chem. Soc. (1956) 4442

12 Kling, A., and Kling, R., Compt. rend. 223 (1946) 1131

13 Weissler, A., Cooper, H.W., and Snyder, S., J. Amer. Chem. Soc. 72 (1950) 1769

14 Feuell, A.J., Research 2 (1949) 148

15 Mastagli, P., and Mahoux, A.P., Compt. rend. 228 (1949) 684

16 Flosdorf, E.W., and Chambers, L.A., J. Amer. Chem. Soc. 55 (1933) 3051

17 Kawahara, Ota and Karine, J. Electrochem. Soc. Japan 14 (1946) 172

18 Barrett, E.W., and Porter, C.W., J. Amer. Chem. Soc. 63 (1941) 3434

19 Porter, C.W., and Young L., ibid. 60 (1938) 1497

20 Lliboutry, L., J. Chim. Phys. 41 (1944) 173

21 Schumb, W.C., and Rittner, W.S., J. Amer. Chem. Soc. 62 (1940) 3416

22 Anderson, Boggs and Winters, Science 108 (1948) 18

23 Grabor, P., Prudhomme, R.O., J. Chim. Phys. 44 (1947) 145

24 Ostroski, A.S., Stambaugh, R.B., J. Appl. Phys. 21 (1950) 478

25 Grassie, N., The Chemistry of High Polymer Degradation Processes, Butterworths Scientific Publication, London 1956 p.102

26 Weissler, A., J. Appl. Phys. 21 (1950) 171

27 Mustafa, M.A.K., J. Polymer Sci. 28 (1958) 519

28 Grabor, P., and Prudhomme, R.O., J. Chim. Phys. 46 (1949) 667

29 Jellinek, H.H.G., and White, G., J. Polymer Sci. 6 (1951) 745
idem. ibid. 6 (1951) 757
Jellinek, H.H.G., and Brett, H.W.W., ibid. 7 (1951) 21 33;
ibid. 13 (1954) 441; ibid. 21 (1956) 535;
ibid. 22 (1956) 149

30 Schmid, G., and Rommel, C., Z. Electrochem. 45 (1939) 659

31 Idem., Z. phys. Chem. Leipzig 185A (1939) 97

32 Szalay, A., ibid. 164A (1933) 234

33 Schmid, G., Physik Z. 41 (1940) 326

34 Zhukov, I.I., and Khenokn, M.A., Doklady Akad. Nauk S.S.S.R. 68 (1949) 333

35 Fisher, J.C., J. Appl. Phys. 19 (1948) 1062

36 Briggs, Johnson, and Mason, J. Acoust. Soc. Amer. 19 (1947) 664

37 Komfeld, M., and Suvorov, L., J. Appl. Phys. 15 (1944) 495

38 Plesset, M.S., J. Appl. Mech. 16 (1949) 277

39 Willard, G.W., J. Acoust. Soc. Amer. 25 (1953) 669

40 Harvey, Barnes, McElroy, and Whitely, J. Amer. Chem. Soc. 67 (1945) 156

41 Pease, D.C., and Blinks, L.R., J. Phys. and Colloid Chem. 51 (1947) 556

42 Fox, F.E., and Herzfeld, K.F., J. Acoust. Soc. Amer. 26 (1954) 984

43 Briggs, L.J., J. Appl. Phys. 5 (1937) 290

44 Vincent, R.S., Proc. Phys. Soc. (London) 53 (1941) 126; idem. ibid. 55 (1945) 41

45 Lord Rayleigh, Phil. Mag. 34 (1917) 94

46 Harvey, E.N., J. Amer. Chem. Soc. 61 (1939) 2392

47 Kling, R., Rev. Sci. 85 (1947) 364

48 Ya. Frenkel, Acta Physicochim. U.R.S.S. 12 (1940) 317

49 Dognon, A., and Simonot, Y., Compt. rend. 228 (1949) 999 330

50 Griffing, V., J. Chem. Phys. 18 (1950) 997

51 Weissler, A., ibid. 18 (1950) 1513

52 Marboe, E.C., Chem. Eng. News 27 (1949) 2198

53 Weyl, W.A., and Marboe, E.C., Research 2 (1949) 19

54 Miller, N., Trans. Faraday Soc. 46 (1950) 546

55 Chambers, L.A., J. Chem. Phys. 5 (1937) 290

56 Schmid, G., and Rommel, O., Z. phys. Chem. (Leipzig) A185 (1939) 97

57 Schmid, G., Parret, G., and Pfleiderer, H., Kolloid Z. 124 (1951) 150

58 Schmid, G., Beuttenmueller, E., Z. Electrochem. 50 (1944) 209

59 Prudhomme, R.O., J. Chim. Phys. 47 (1950) 745

60 Schoch, T.J.,"The fractionation of starch", Advances in Carbohydrate Chemistry Vol.I p.274, Academic Press, New York 1946

61 Hassid, W.Z., and McCready, R.M., J. Amer. Chem. Soc. 63 (1941) 1632

62 Bates, F.L., French, D., and Rundle, R.E., ibid.65 (1943) 142

63 Haworth, W.N., and Machemer, H., J. Chem. Soc. (1932) 2270

64 Jackson, E.L., and Hudson, C.S., J. Amer. Chem. Soc. 59 (1937) 2049

65 Wolfrom, M.L., Tyree, J.T., Galkowski, T.T., and O'Neill, A.N., ibid. 73 (1951) 4927

66 Haworth, W.N., Hirst E.L., and Isherwood, F.A., J. Chem. Soc. (1937) 577

67 Staudinger, H., and Huseman, E., Annalen 527 (1937) 195

68 Meyer, K.H., and Bernfield, P., Helv. Chim. Acta 23 (1940) 875

Meyer, K.H., Wertheim, M., and Bernfield, P., ibid. 23 (1940) 865; ibid. 24 (1941) 378

69 Larner, J., Illingworth B., Cori, G.T., and Cori, C.F., J. Biol. Chem. 199 (1952) 641

70 Cowie, J.M.G., and Greenwood, C.T., J. Chem. Soc. (1957) 4640

71 Freudenberg, K., et al. Naturwiss 27 (1939) 850

72 Rundle, R.E., and French, D., J. Amer. Chem. Soc. 65 (1943) 1707

73 Karrer, P., and Nägeli, C., Helv. Chim. Acta 4 (1921) 263

Karrer, P., ibid. 4 (1921) 994

74 Carter, S.R., and Record, B.R., J. Soc. Chem. Ind. (London) 55 (1936) 218

75 Meyer, K.H., and Field, M., Helv. Chim. Acta 24 (1941) 375

76 Manners, D.J., Advances in Carbohydrate Chemistry 12 (1957) 262

77 Flory, P., Principles of Polymer Chemistry, Cornell University Press, New York (1953) p.313

78 Singer, S., Polymer Bulletin 1 (1945) 79

79 Ekenstam, A., Ber. 69 (1936) 549

80 Schulz, G.V., and Huseman, E., Z. Naturforsch 1 (1946) 268

81 McBurney, L.F., Cellulose and Cellulose Derivatives, 2nd ed., Ott, O., and Spurlin, H.M., eds. Vol.1. Interscience New York - London. 1954 p.99

82 Montroll, E.W., and Simha, R., J. Chem. Phys. 8 (1940) 721

83 Simha, R., J. Appl. Phys. 12 (1941) 569

84 Stetten, Katzen and Stetten, J. Biol. Chem. 222 (1956) 587

85 Peat, S., Pirt, S.J., and Whelan, W.J., J. Chem. Soc. (1952) 714

86 Lampitt, Fuller and Coton, J. Sci. Food Agric. 6 (1956) 656

87 Anderson, D.M.W., and Greenwood, C.T., J. Chem. Soc. (1955) 3016

88 Idem. Chem. and Ind. (1953) 476

89 Fick, Pogg. Ann. 94 (1855) 59

90 Gralen, N., Dissertation Uppsala 1944

91 Faxen, H., Arkiv. Mat. Astron. Fysik 21B (1929) No.3

92 Fujita, H., J. Chem. Phys. 24 (1956) 1084

93 Baldwin, R.L., Biochem. J. 65 (1957) 503

94 Idem. ibid. 65 (1957) 490

95 Greenwood, C.T., and Das Gupta, P.C., J.Chem.Soc. (1958) 703

96 Greenwood, C.T., ibid. at present in press

97 Lindström, O., J. Acoust. Soc. Amer. 27 (1955) 654

98 Ovenston and Rees, Analyst 75 (1950) 204

99 Mellen, R.H., J. Acoust. Soc. Amer. 26 (1954) 356

100 Lipkin, M.R., Davidson, J.A., Harvey, W.T., and Kurtz, S.S., Ind. Eng. Chem. (An) 16 (1944) 55

101 Einstein, A., Ann. Phys. 19 (1906) 289

102 Simha, R., J. Phys. Chem. 44 (1940) 25

103 Mark, H., "Der feste Korper" Leipzig (1938) 103

104 Houwink, R., J. prakt. Chem. 155 (1940) 15

105 Flory, P., and Fox, T.G., J. Amer. Chem. Soc. 73 (1951) 1904 1909 1915; idem. J. Polymer Sci. 5 (1950) 745

106 Ubbelohde, L., Anal. Chem. 9 (1937) 85;
Davies, W.E., and Elliot, J.H., J. Colloid Sci. 4 (1949) 313

107 Immergut, E.M., and Schurz, J., J. Polymer Sci. 9 (1952) 279

108 Svedberg, T., and Pedersen, K.O., The Ultracentrifuge, Oxford University Press 1940

109 Signer and Gross, Helv. Chim. Acta 17 (1934) 726

110 Bridgeman, J. Amer. Chem. Soc. 64 (1942) 2349

111 See Refs. in article by Kinell and Ranby in "Advances in Colloid Science" Vol.III Interscience Publ. Inc. New York 1950

112 Baldwin, Gosting, Williams and Alberty, Disc. Faraday Soc. 20 (1955) 13

113 Baldwin and Williams, J. Amer. Chem. Soc. 72 (1950) 4325

114 Gosting, L.J., ibid. 74 (1952) 1548

115 Williams, Baldwin, Saunders, and Squire, ibid. 74 (1952) 1542

116 Baldwin, R.L., ibid. 76 (1954) 402

117 Williams and Saunders, J. Phys. Chem. 58 (1954) 854

118 Williams, Saunders and Cercirelli, ibid. 58 (1954) 774

119 Baldwin, R.L., ibid. 58 (1954) 1081

120 Johnston, J.P., and Ogston, A.G., Trans. Faraday Soc. 42 (1946) 789

121 Gralen and Lagermalm, J. Phys. Chem. 56 (1952) 514

122 Connolly, W., and Fox., F.E., J. Acoust. Soc. Amer. 26 (1954) 843

123 Cowie, J.M.G., and Greenwood, C.T., J. Chem. Soc. (1957) 2658

124 Simha, R., J. Chem. Phys. 13 (1945) 188

Reprinted from

VOLUME XXV, ISSUE NO. 109 JULY, 1957

Journal of POLYMER SCIENCE

CONTENTS

continued inside

Published by INTERSCIENCE PUBLISHERS, INC.

Journal of **POLYMER SCIENCE**

Contents (continued) Volume XXV, Issue No. 109

Published monthly by Interscience Publishers, Inc., covering four volumes annually. Publication Office, 20th and Northampton Sts., Easton, Pa. Executive, Editorial and Circulation Offices at 250 Fifth Ave., New York 1, N. Y. Entered as Second-Class Matter February 17, 1950, at the Post Office at Easton, Pennsylvania, under the Act of March 3, 1879. Subscription price, $15.00 per volume. Foreign postage, $0.50 per volume.

Manuscripts should be submitted to one of the members of the Editorial Board or to the Editorial office, c/o H. Mark, Polytechnic Institute of Brooklyn, Brooklyn 2, New York. *Those in Europe should be submitted to* **Professor J. J. Hermans, University of Leiden,** *and those in England to* **Professor W. T. Astbury, The University, Leeds.**

*The Sedimentation Behavior of the Components of Potato Starch in Dilute Alkali**

Very few sedimentation measurements have been carried out on adequately purified and characterized starch components, notwithstanding the valuable information that this method can give regarding molecular weight and its distribution.[1] Studies on the unsubstituted components in aqueous solution are complicated by the tendency for both the linear amylose- and the branched amylopectin-components to aggregate. Previous experiments[2] have been carried out on derivatives dissolved in organic solvents, but we have found that sedimentation measurements may conveniently be made on the components dissolved in dilute alkali. Such solutions are stable for the length of time required for measurement, and the results are reproducible. This method therefore avoids complications due to degradative effects during the formation of derivatives.[1]

Samples of amylose and amylopectin isolated from potato starch have been investigated. Fractionation was carried out under conditions involving an oxygen-free atmosphere.[3] The amylose was precipitated first as the thymol complex, and then purified by repeated crystallization using butanol. The resultant complex was dehydrated with butanol and dried.[3] Amylopectin was obtained by freeze-drying directly the supernatant from the thymol-amylose complex. The two components were characterized by potentiometric measurements of iodine binding power under standard conditions.[4] The amylose bound 19.5% of iodine, and the amylopectin 0.9% (corresponding to less than 0.5% of linear material). Both components were dissolved directly before use in 0.2 *M* potassium hydroxide on shaking at room temperature.

Sedimentation rates were determined using a Spinco ultracentrifuge and a cell incorporating a Kel-F centerpiece. Preliminary experiments showed the optimum speed for solutions of amylose of concentrations greater than about 0.1 g./100 ml. was 60,000 r.p.m., while for more dilute solutions, 30,000 r.p.m. was more suitable. Amylopectin solutions were spun at either 30,000 or 15,000 r.p.m., depending on the concentration. Careful observation of the Schlieren patterns during the acceleration period showed that there was no rapidly sedimenting material. Analysis of the Schlieren diagrams showed that over 90% of each polysaccharide was present in solution. The results for typical runs are shown in Figures 1 and 2, where an acid-degraded amylose and amylopectin[5] and a glycogen[6] are also included for comparison.

Both components show a concentration dependence of the sedimentation constant; in the case of the undegraded amylopectin it is extremely large. This result is consistent with the concept of a linear amylose molecule, but it is unexpected for the branched component which is usually thought to be more spherical.[1] These results may indicate, however, that amylopectin is an elongated molecule. With increase in concentration, the outer

* This is Part IV in the series "Physicochemical Studies on Starches."

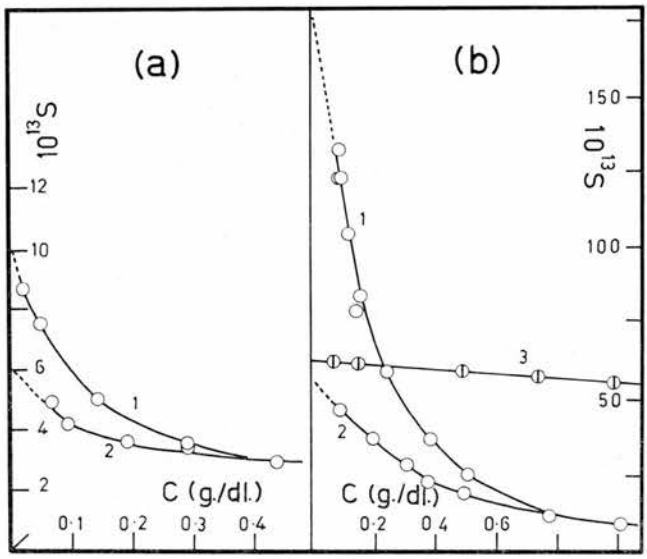

Fig. 1. The variation of sedimentation constant (S) with concentration (C) for the starch components in 0.2M-KOH. (*a*) Amylose (curve 1) and acid-degraded amylose (curve 2). (*b*) Amylopectin (curve 1) and acid-degraded amylopectin (curve 2). Curve 3 is yeast glycogen.

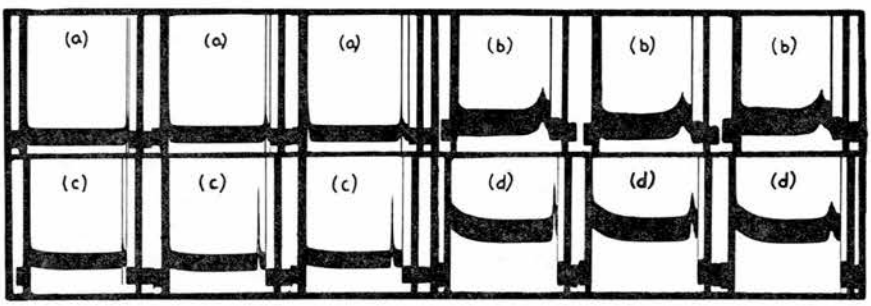

Fig. 2. Typical sedimentation diagrams for: (*a*) amylopectin: C = 0.79 g./dl.; speed = 30,000 r.p.m.; 5, 12, and 19 min., respectively, after reaching full speed; angle of Schlieren bar = 80°. (*b*) Amylopectin: C = 0.18 g./dl.; speed = 15,000 r.p.m.; 10, 12, and 14 min., respectively; angle of Schlieren bar = 40°. (*c*) Amylose: C = 0.30 g./dl.; speed = 60,000 r.p.m.; 10, 18, and 25 min., respectively; angle of Schlieren bar = 70°. (*d*) Amylose: C = 0.08 g./dl.; speed = 60,000 r.p.m.; 3, 7, and 12 min., respectively; angle of Schlieren bar = 45°.

chains of the highly branched amylopectin might well entangle, and strong secondary valency forces must occur even in the alkaline media. It is of interest that the sedimentation constant for glycogen is relatively independent of the concentration. This is further evidence of a fundamental difference in structure between the two branched glucans.[1]

For the starch components, free sedimentation only occurs at low concentrations (<0.2 g./100 ml. for amylose, and <0.4 g./100 ml. for amylopectin), and it is therefore necessary to carry out experiments at extremely

low dilutions. Unfortunately, lower limits of 0.02 g./100 ml. and 0.1 g./100 ml. for amylose and amylopectin, respectively, were fixed in these experiments by the sensitivity of the optical system. It is suggested that lower dilutions may be examined by the use of an alkali-resistant synthetic boundary cell. This is being investigated.

These experiments are being extended to include measurements of the appropriate diffusion constants so that estimates of molecular weight and shape can be obtained. Preliminary results indicate a value of the order of 5,000 for the DP of the amylose obtained by the above fractionation method.

The authors wish to thank the Rockefeller Foundation for financial assistance.

References

1. For review, see C. T. Greenwood, *Adv. Carbohydrate Chem.*, **11**, 335 (1956).
2. B. A. Dombrow and C. O. Beckmann, *J. Phys. & Colloid Chem.*, **51**, 107 (1947).
3. C. T. Greenwood and J. S. M. Robertson, *J. Chem. Soc.*, 3769 (1954).
4. D. M. W. Anderson and C. T. Greenwood, *J. Chem. Soc.*, 3016 (1955).
5. J. M. G. Cowie and C. T. Greenwood, unpublished experiments.
6. Supplied by Dr. D. J. Manners.

W. A. J. Bryce
J. M. G. Cowie
C. T. Greenwood

Department of Chemistry
The University
Edinburgh, 9
Scotland

Received February 26, 1957

*The Dose Rate Dependence of Kel-F Degradation by Ionizing Radiation**

In this study films of Kel-F 300 (polymonochlorotrifluoroethylene) were subjected to beta irradiation from strontium-90 sources of various intensities and the time for dielectric breakdown to occur was noted. The experimental arrangement is shown diagrammatically in Figure 1, and was used basically to measure the conductivities of three-mil thick Kel-F films while they were being irradiated in air.

Dielectric breakdown occurred when the films degraded physically into yellow powder. Table I shows the time T_D in days for degradation and short circuiting to occur as a function of beta source current density I_B in micromicroamp/cm.^{2}

* Based on a paper presented at the Winter General Meeting of the American Institute of Electrical Engineers, New York, N. Y., January 23, 1957.

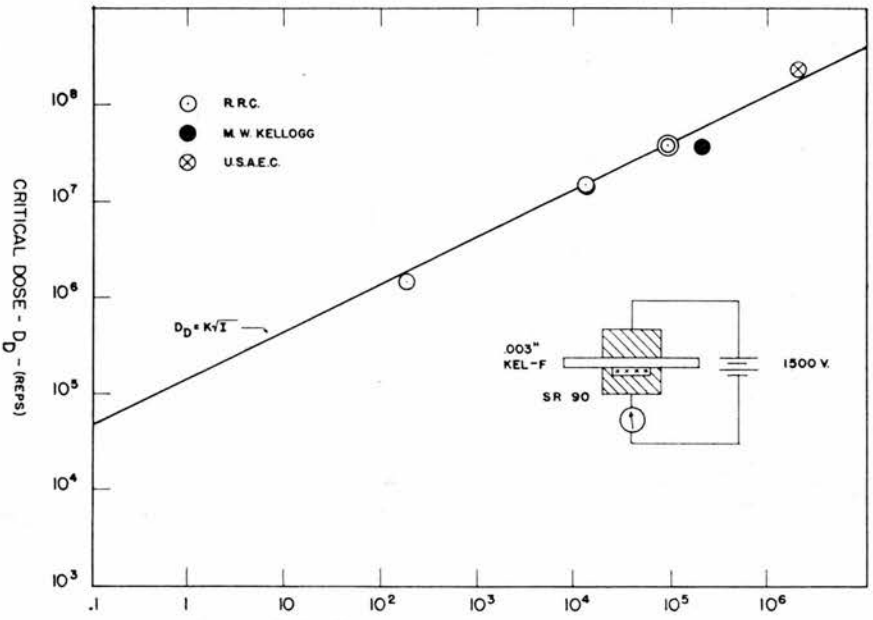

Fig. 1. Critical dose *vs.* radiation rate for Kel-F.

The current density I_B measured for each source is converted to reps/hr. by the relationship $^1/_4$ rep/sec. = 1 micromicroamp. The dose for degradation D_D was calculated by $D_D = IT_D$. These results are plotted in Figure 1 and closely fit the solid line representing the equation:

$$D_D = KI^{1/2}$$

where K is a constant. This result indicates the dose for degradation is not constant but depends on radiation intensity.

According to F. Honn[1] of the Minnesota Mining and Mfg. Corp., manufacturers of Kel-F, the degradation dose for gamma irradiation of Kel-F 500 is 4×10^7 reps at an intensity of 2×10^5 reps/hr. Sisman and Bopp[2] report that the tensile strength of Fluorothene, made by the Union Carbide Corp., drops to zero at a reactor dose of 2.5×10^{17} NVT of neutrons and gammas at a pile intensity of two megareps/hr.; using their conversion factor of 10^9 NVT/rep for the CH_2 group, one obtains $D_D = 250$ megareps.

TABLE I

	I_B, μμamp./cm.^{2}	I, reps/hr.	Temp., °C.	T_D, days	D_D, megareps
(1)	100	90,000	80	20	40
(2)			30	20	40
(3)	13	12,000	80	59	15
(4)			30	54	14
(5)	0.2	180	30	340	1.5

Journal of POLYMER SCIENCE

SPECIAL NOTICE

The Editorial Board of Journal of Polymer Science requests the cooperation of all contributors in order to aid the publisher in keeping costs of publication at a minimum. Your special attention is directed to items 3, 4, and 6–11, which should be rigorously followed.

Manuscripts and illustrations not conforming to the style of the Journal will be returned to the author for reworking, thus delaying their appearance.

INFORMATION FOR CONTRIBUTORS

1. Manuscripts for publication that have not been published elsewhere, books for review, and all correspondence regarding papers should be submitted to the Editorial Office. The editors desire to receive manuscripts based on original research in any phase of the chemistry, biochemistry, and physics of large molecules.
2. It is the preference of the editors that papers be published in the English language. However, if the author desires that his paper be published in French or German, it is necessary that a particularly complete and comprehensive synopsis be furnished.
3. Manuscripts should be submitted in duplicate (one *original*, one carbon copy), typed *double space*, on a *heavy* grade of paper, with margins of one inch on both sides. *It is most important to observe this request.*
4. A synopsis of the main contributions contained in the paper is required in *triplicate.* This synopsis should be carefully prepared, for it will appear in English, in French and in German, and is automatically the source of most abstracts. A complete summary of the whole paper, not the conclusions alone, should form the synopsis. If it is desired to summarize the conclusions separately, this should be done in the final section of the paper.
5. The paper should be reasonably subdivided into sections and, if necessary, subsections. Please refer to any issue of this Journal for examples.
6. The references should be numbered consecutively in the order of their appearance, and should be complete, including authors' initials and—for unpublished lectures or symposia—the title of the paper, the date, and the name of the sponsoring society. Please compile references on a separate sheet at the end of the manuscript.
7. Please do not use footnotes to the text. It is suggested that material intended for footnotes be inserted at the appropriate point in the manuscript proper, and marked for "small type" (or inserted in the text as parenthetical material).
8. Please supply numbers and titles for all tables. All table columns should have an explanatory heading.
9. It is particularly important that all figures be submitted in a form *suitable for reproduction.*
   Good positive *photographs* are required for *halftone* reproductions.
   For *line drawings* (graphs, etc.), the figures must be drawn clearly with India ink on heavy white paper, Bristol board, drawing linen, or coordinate paper with *very light blue* background (no other colors will be accepted). Lettering of graphs must be large, clear, and "open" so that the numbers and letters do not fill in with ink. Drawings should be so made that, on reduction, the final size does not exceed 4 × 7 inches. It is the usual practice to submit drawings that are twice the size of the final engravings. *If in doubt about the preparation of illustrations suitable for reproduction please consult the publishers* (250 Fifth Avenue, New York 1, N. Y.) and ask for a sample drawing.
10. Please supply legends for all figures and compile these on a separate sheet.
11. Authors are cautioned to *type—wherever possible—all mathematical and chemical symbols, equations, and formulas.* If these must be handwritten, please leave ample space above and below for printer's marks; please use only *ink. Your special attention to this point is requested.* The printer cannot work from pencilled-in or cramped technical material.
    All Greek or unusual symbols should be identified in the margin for the printer the first time used. Please distinguish in the margins of the manuscript between capital and small letters of the alphabet wherever confusion may arise (*e.g.*, k, K, κ). Please underline with a wavy line all vector quantities. Use fractional exponents to avoid root signs.
    The nomenclature sponsored by the International Union of Chemistry is requested for chemical compounds. Chemical bonds should be correctly placed, and double bonds clearly indicated. Valence is to be indicated by superscript plus and minus signs.
12. Authors will receive 50 reprints of their articles without charge. Additional reprints can be ordered and purchased by filling out the form attached to galley proof.
13. Unless requested otherwise by the author at the time the manuscript is submitted, no manuscripts will be returned.

Manuscripts should be submitted to one of the members of the Editorial Board or to the Editorial Office, c/o **H. Mark, Polytechnic Institute of Brooklyn, Brooklyn 2, New York.** *Those in Europe should be submitted to* **Professor J. J. Hermans, University of Leiden,** *and those in England to* **Professor W. T. Astbury, The University, Leeds.** *Address all other correspondence to* **Interscience Publishers, Inc., 250 Fifth Avenue, New York 1, N. Y.**

Reprinted from

VOLUME XXV, ISSUE NO. 111 SEPTEMBER, 1957

Journal of

POLYMER SCIENCE

CONTENTS

continued inside

Published by INTERSCIENCE PUBLISHERS, INC.

Journal of POLYMER SCIENCE

Contents (continued) Volume XXV, Issue No. 111

Published monthly by Interscience Publishers, Inc., covering four volumes annually. Publication Office, 20th and Northampton Sts., Easton, Pa. Executive, Editorial and Circulation Offices at 250 Fifth Ave., New York 1, N. Y. Entered as Second-Class Matter February 17, 1950, at the Post Office at Easton, Pennsylvania, under the Act of March 3, 1879. Subscription price, $15.00 per volume. Foreign postage, $0.50 per volume.

Manuscripts should be submitted to one of the members of the Editorial Board or to the Editorial office, c/o H. Mark, Polytechnic Institute of Brooklyn, Brooklyn 2, New York. *Those in Europe should be submitted to* **Professor J. J. Hermans, University of Leiden,** *and those in England to* **Professor W. T. Astbury, The University, Leeds.**

LETTERS TO THE EDITORS

Electrophoresis of Polyphenylene

Solutions of polyphenylene in pyridine-water mixtures show electrical conduction far in excess of that of corresponding pyridine-water mixtures.[1] This observation obviously invites an electrophoretic investigation of the polymer.

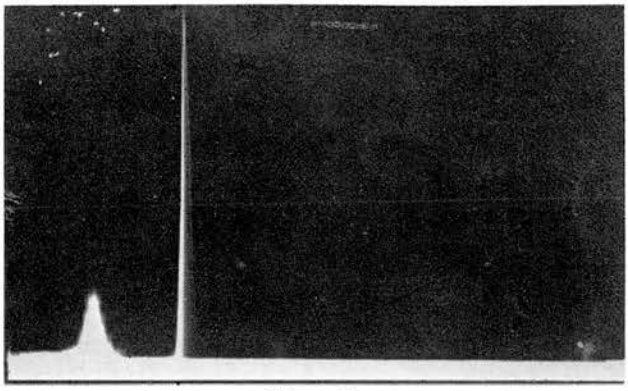

Figure 1.

Consequently, a solution containing 0.08 g./100 ml. of polyphenylene of a degree of polymerization of approximately 34 in a solvent of 1:20 pyridine-water (pH 8.8) was observed in a Spinco electrophoresis instrument at electric field strengths of 190 or 380 v./cm. In either case, one very sharp peak was observed (Fig. 1) whose rate of migration gives a mobility of 0.3 $\times 10^{-5}$ cm.^{2} volt^{-1} sec.$^{-1}$. Excluding most unlikely coincidences, the results indicate an amazing uniformity of degree of polymerization. This can be explained by assuming a continuous decrease in the reactivity of the terminal chlorine with increasing chain length.

Reference

1. *J. Polymer Sci.*, **16**, 589 (1955).

GEORGE GOLDFINGER

Armour Research Foundation
Department of Chemistry and Chemical Engineering
Chicago, Illinois

SIDNEY SHULMAN

University of Buffalo
School of Medicine
Buffalo, New York

Received April 9, 1957

The Degradation of High Polymers

During recent investigations of the degradation of the starch components, we have re-assessed methods of expressing the rate of polymer degradation.

Degradation studies are of great importance as they can indicate the presence of anomalous or "weak" linkages. In many instances throughout the literature, viscosity measurements ($[\eta]$ or η_{sp}/c) have been used to characterize the polymer degradation products, the rate of degradation then being expressed simply as the change of viscosity with time. The resultant curve (see, *e.g.*, Fig. 1a) has been interpreted as indicating the preferential scission of weaker bonds followed by a decreased rate of degradation to some limiting value. We wish to emphasize here that (*1*) changes in viscosity are *not* themselves directly a true measure of the degradation rate, and (*2*) the apparent limit in $[\eta]$ (or η_{sp}/c) is fallacious.

Considering first *qualitative* aspects of degradation, this process should be followed by number-average methods. Such methods are obviously insensitive to small initial changes, while weight-average methods (*e.g.*, viscometry) provide a sensitive measure of these. However, at high degree of degradation, when only relatively low molecular weight material is present, weight-average methods become insensitive to further changes and the measured quantity (say, viscosity) will then approach an apparent limit.

The correct formulation for measuring degradation can be obtained following the method of Ekenstam[1] and Schulz and Husemann:[2]

Consider a polymer system containing n gram moles of equally strong and accessible cleavable bonds/liter, then for a zero-order degradation reaction

$$dn/dt = -k_0$$

and for a first-order degradation reaction

$$dn/dt = -k_1 n$$

If there are w grams of polymer composed of repeating units of molecular weight (M_0), and having a number-average degree of polymerization (P), then the over-all condition must hold that

$$dP/dt = (dP/dn)(dn/dt)$$

But $$n = w(P - 1)/PM_0$$

Hence: $$dP/dn = M_0P^2/w$$

and for a *zero-order reaction:*

$$k_0 = w[P_t^{-1} - P_0^{-1}]/M_0t$$

where P_t and P_0 are the values for the number-average degree of polymerization at times t and 0, respectively.

Similarly, for a *first-order reaction*

$$k_1 = (1/t) \ln [(1 - P_0^{-1})/(1 - P_t^{-1})]$$

or

$$k_1 = (1/t)[P_t^{-1} - P_0^{-1}]$$

on expansion of the logarithm and ignoring terms higher than the first.

Hence for either a zero- or first-order reaction, the degradation rate constant in the initial stages is proportional *not to P but to* P^{-1}, and P^{-1} versus t will be linear. For large amounts of degradation, this relationship will still hold for a zero-order reaction, but ln $(1 - P^{-1})$ versus t is necessary for a first-order reaction as higher terms in the expansion are then required.

Thus if degradation is followed viscometrically and $[\eta] = KP$, the degradation rate constant is obtained *from the graph of* $[\eta]^{-1}$ *versus* t, and not $[\eta]$ versus t, in agreement with McBurney.[3] The presence of some rapidly degraded weak linkages will then be shown by $\lim_{t \to 0} [\eta]^{-1} \neq$ that for the original polymer. (If $[\eta] = KP^{\alpha}$, then degradation should be expressed as $[\eta]^{-1/\alpha}$ versus t.)

We have applied this concept to some results described in the literature for polystyrene and cellulose degraded by different methods. Results have been re-plotted as $\Delta[P^{-1}]$ versus t, rather than P^{-1} versus t to reduce the graphs to a common origin.

(a) Polystyrene. Figure 1(a) shows the $[\eta]$ versus t curves for the pyrolysis studies of Wall and co-workers[4] (curve 1) and Jellinek[5] (curve 2), and the ultrasonic studies of Melville and Murray[6] (curve 3). The corre-

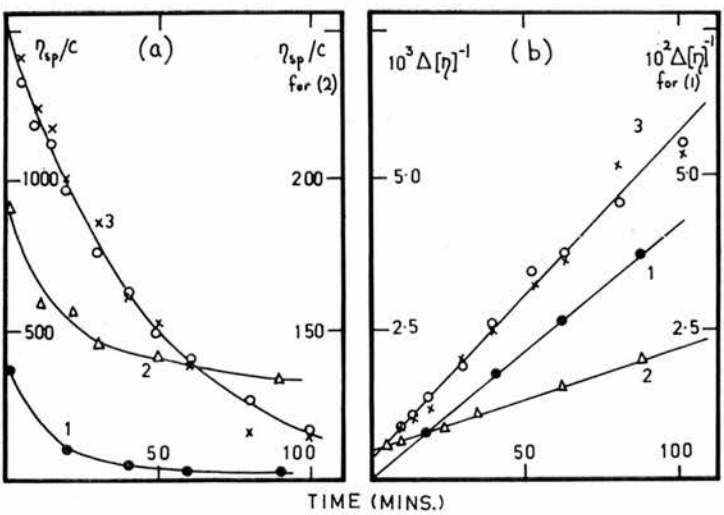

Fig. 1. (a) η_{sp}/c *vs* t for the degradation of polystyrene. Curve *1*. Pyrolysis of low molecular weight polymer.[4] Curve *2*. Pyrolysis of high molecular weight polymer.[5] Curve *3*. Ultrasonic degradation.[6] (b) $\Delta[\eta]^{-1}$ *vs.* t for the degradation of polystyrene. Curves *1–3* as for (a).

sponding plots of $\Delta[\eta]^{-1}$ versus t are shown in Figure 1(b). In all cases, there is *no evidence for a decrease in the degradation rate constant* with time. The results of Wall and co-workers[4] (who have already plotted their data as $[P_t^{-1} - P_0^{-1}]$ versus t) are included as an example of a system in which there is no evidence for either weak linkages or a decrease in degradation rate constant. However, for the higher molecular weight products studied by thermal methods,[5] and the lower molecular weight products studied by ultrasonic methods,[6] weak bonds are indicated (curves *2* and *3*, Fig. 1 (b)). This is in agreement with Jellinek's conclusions.[5] Such effects were not considered by Melville and Murray.[6] The results show further that a limiting value for molecular weight in ultrasonic degradation processes[6] is unlikely.

(b) Cellulose. Schulz and Husemann[2] have interpreted their results for the oxidative degradation of cotton cellulose as indicating the presence of weak links in the molecule. In Figure 2 some of these authors' data have been re-plotted (curves *1–4*). Degradation would appear to follow a zero-order reaction, as the rate constant varies approximately inversely to the concentration. Again, the rate constant does not alter with time. On the basis of the above, there is no evidence for weak bonds for the low concentrations (curves *1* and *2*), but indications of them for the higher concentrations (curves *3* and *4*). (It is of interest that Sharples[7] has suggested, from results plotted in a similar manner, that weak links are only introduced by the pretreatment of the cellulose.)

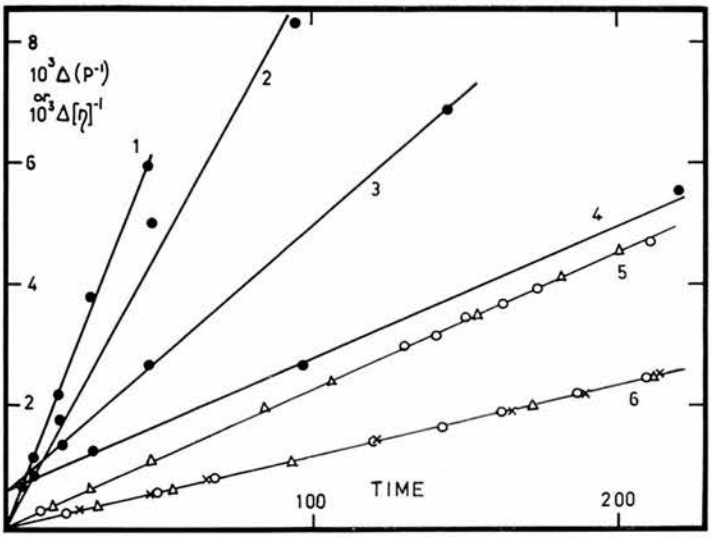

Fig. 2. Degradation rate constants for cellulose. Curves *1–4*. Oxidative degradation of cotton cellulose.[2] Time in minutes. Concentration of cellulose: 1, 2, 3, and 4 g./l., respectively. Curves *5* and *6*. Acid hydrolysis of methylated celluloses.[8] Time in hours. (Time-axis for curve 5 is doubled, *i.e.* curves *5* and *6* are actually coincident.) (○) Unfractionated commercial cellulose: curve *5*, concentration = 1.878 g./l.; curve *6*, concentration = 2.383 g./l. (×) Commercial cellulose fraction: concentration = 4.181 g./l. (△) Viscose rayon fraction: concentration = 2.488 g./l.

The results of Gibbons[8] for the homogeneous acid hydrolysis of various methylated celluloses are shown in curves *5* and *6* (Fig. 2). There is no concentration dependence for the rate constant. However, in contradiction to this author's conclusions, there appears to be conclusive evidence from the graphs that there are no weak bonds present in the methylated samples.

The authors wish to thank Dr. D. Taylor for helpful discussion.

References

1. A. af Ekenstam, *Ber.*, **69**, 549 (1936).
2. G. V. Schulz and E. Husemann, *Z. Naturforsch.*, **1**, 268 (1946).
3. L. F. McBurney in *Cellulose and Cellulose Derivatives*, 2nd ed., E. Ott and H. M. Spurlin, eds., Vol. I, Interscience, New York-London, 1954, p. 99.
4. L. H. Wall, D. W. Brown, and V. E. Hart, *J. Polymer Sci.*, **15**, 157 (1955).
5. H. H. G. Jellinek, *J. Polymer Sci.*, **4**, 1 (1949).
6. H. W. Melville and A. J. R. Murray, *Trans. Faraday Soc.*, **46**, 996 (1950).
7. A. Sharples, *J. Polymer Sci.*, **14**, 95 (1950).
8. G. C. Gibbons, *Shirley Inst. Mem.*, **25**, 233, 246 (1951).

W. A. J. Bryce
C. T. Greenwood

Department of Chemistry
The University
Edinburgh 9, Scotland

Received April 9, 1957

Applicability of the Stokes' Equation to Macromolecules

The Stokes' equation is

$$f = n\pi r\eta_0 v \tag{1}$$

where f is the frictional force on a sphere of radius r moving with a velocity v in a fluid continuum having a viscosity η_0, and where the numerical factor $n = 6$ has been verified experimentally for spheres of radius down to about 1300 A.[1] However, for molecules having radii of 3–6 A. (based on their van der Waals volumes V_w[2]) the numerical factor must be reduced to 5.[3, 4] It has been speculated previously[4] that for macromolecules such as proteins, which have radii of about 17 A. or more, equation (1) should be used with $n = 5$. However, it is shown below, using essentially the arguments of Polson[5] in another connection, that more probably the unmodified Stokes' equation is valid for these particles.

The effective hydrodynamic volume of a molecule is given by V_wH, where H is a "hydration factor" which equals unity when the molecule is unhydrated. It has been shown[6] that this volume may be used in applying the Einstein viscosity equation to solutions of small molecules, in the form

$$[\eta] = \frac{\nu N V_w H}{100M} \tag{2}$$

where $[\eta]$ is the intrinsic viscosity of the solution, ν the "viscosity increment" of the solute particle, N Avogadro's number, and M the molecular weight of the solute. On the other hand, the diffusion coefficient D of the solute is given by

$$D = \frac{kT}{n\pi\eta_0}\left(\frac{f_0}{f}\right)\left(\frac{4\pi}{3V_w H}\right)^{1/3} \tag{3}$$

where k is Boltzmann's constant, T the temperature, and (f/f_0) the "frictional ratio"[7] to correct, where necessary, for the nonspherical shape of the molecule. Then

$$V_w H = \frac{100[\eta]M}{\nu N} = \frac{4\pi}{3}\left(\frac{kT}{n\pi\eta_0 D}\right)^3\left(\frac{f_0}{f}\right)^3$$

or

$$D^3[\eta]M = \frac{4\pi\nu N}{300}\left(\frac{kT}{n\pi\eta_0}\right)^3\left(\frac{f_0}{f}\right)^3 \tag{4}$$

For a given molecule both ν and (f/f_0) are determined by its asymmetry, and for the special case of an ellipsoidal molecule they may be calculated from its axial ratio.[7, 8] Hence $\nu(f_0/f)^3$, which we shall designate as the "shape factor" s, may be calculated from axial ratios. Some values are given below.

Axial ratio	s (prolate ellipsoid)	s (oblate ellipsoid)
1.0	2.50	2.50
2.0	2.53	2.52
4.0	2.81	2.55
6.0	3.11	2.58
10.0	3.68	2.59

For solutions in water at 20°, equation (4) becomes

$$D^3[\eta]M = 5.33 \times 10^{-14} s/n^3 \tag{4a}$$

and so for $n = 5$

$$D^3[\eta]M \geqslant 10.6 \times 10^{-16} \tag{4b}$$

and for $n = 6$

$$D^3[\eta]M \geqslant 6.16 \times 10^{-16} \tag{4c}$$

Polson[5] found for aqueous solutions of the small molecules, pentaerythritol, DL-valine, α-alanine, and β-alanine, values of $D^3[\eta]M$ between 10.55–12.0×10^{-16}, in agreement with (4b). However, for aqueous solutions of glycine, sucrose, and glucose, $D^3[\eta]M$ was between 7.5–8.2×10^{-16},

Journal of **POLYMER SCIENCE**

SPECIAL NOTICE

The Editorial Board of Journal of Polymer Science requests the cooperation of all contributors in order to aid the publisher in keeping costs of publication at a minimum. Your special attention is directed to items 3, 4, and 6–11, which should be rigorously followed.

Manuscripts and illustrations not conforming to the style of the Journal will be returned to the author for reworking, thus delaying their appearance.

INFORMATION FOR CONTRIBUTORS

1. Manuscripts for publication that have not been published elsewhere, books for review, and all correspondence regarding papers should be submitted to the Editorial Office. The editors desire to receive manuscripts based on original research in any phase of the chemistry, biochemistry, and physics of large molecules.
2. It is the preference of the editors that papers be published in the English language. However, if the author desires that his paper be published in French or German, it is necessary that a particularly complete and comprehensive synopsis be furnished.
3. Manuscripts should be submitted in duplicate (one *original*, one carbon copy), typed *double space*, on a *heavy* grade of paper, with margins of one inch on both sides. *It is most important to observe this request.*
4. A synopsis of the main contributions contained in the paper is required in *triplicate*. This synopsis should be carefully prepared, for it will appear in English, in French and in German, and is automatically the source of most abstracts. A complete summary of the whole paper, not the conclusions alone, should form the synopsis. If it is desired to summarize the conclusions separately, this should be done in the final section of the paper.
5. The paper should be reasonably subdivided into sections and, if necessary, subsections. Please refer to any issue of this Journal for examples.
6. The references should be numbered consecutively in the order of their appearance, and should be complete, including authors' initials and—for unpublished lectures or symposia—the title of the paper, the date, and the name of the sponsoring society. Please compile references on a separate sheet at the end of the manuscript.
7. Please do not use footnotes to the text. It is suggested that material intended for footnotes be inserted at the appropriate point in the manuscript proper, and marked for "small type" (or inserted in the text as parenthetical material).
8. Please supply numbers and titles for all tables. All table columns should have an explanatory heading.
9. It is particularly important that all figures be submitted in a form *suitable for reproduction.*
   Good positive *photographs* are required for *halftone* reproductions.
   For *line drawings* (graphs, etc.), the figures must be drawn clearly with India ink on heavy white paper, Bristol board, drawing linen, or coordinate paper with *very light blue* background (no other colors will be accepted). Lettering of graphs must be large, clear, and "open" so that the numbers and letters do not fill in with ink. Drawings should be so made that, on reduction, the final size does not exceed 4 × 7 inches. It is the usual practice to submit drawings that are twice the size of the final engravings. *If in doubt about the preparation of illustrations suitable for reproduction please consult the publishers* (250 Fifth Avenue, New York 1, N. Y.) and ask for a sample drawing.
10. Please supply legends for all figures and compile these on a separate sheet.
11. Authors are cautioned to *type—wherever possible—all mathematical and chemical symbols, equations, and formulas.* If these must be handwritten, please leave ample space above and below for printer's marks; please use only *ink. Your special attention to this point is requested.* The printer cannot work from pencilled-in or cramped technical material.
    All Greek or unusual symbols should be identified in the margin for the printer the first time used. Please distinguish in the margins of the manuscript between capital and small letters of the alphabet wherever confusion may arise (*e.g.*, k, K, κ). Please underline with a wavy line all vector quantities. Use fractional exponents to avoid root signs.
    The nomenclature sponsored by the International Union of Chemistry is requested for chemical compounds. Chemical bonds should be correctly placed, and double bonds clearly indicated. Valence is to be indicated by superscript plus and minus signs.
12. Authors will receive 50 reprints of their articles without charge. Additional reprints can be ordered and purchased by filling out the form attached to galley proof.
13. Unless requested otherwise by the author at the time the manuscript is submitted, no manuscripts will be returned.

Manuscripts should be submitted to one of the members of the Editorial Board or to the Editorial Office, c/o **H. Mark, Polytechnic Institute of Brooklyn, Brooklyn 2, New York.** *Those in Europe should be submitted to* **Professor J. J. Hermans, University of Leiden,** *and those in England to* **Professor W. T. Astbury, The University, Leeds.** *Address all other correspondence to* **Interscience Publishers, Inc., 250 Fifth Avenue, New York 1, N. Y.**

Reprinted from the Journal of the Chemical Society,
February, 1958, (138), pages 711—715.

138. *Physicochemical Studies on Starches. Part XII.* The Molecular Weight of Glycogens in Aqueous Solution.*

By W. A. J. Bryce, C. T. Greenwood, I. G. Jones, and D. J. Manners.

Molecular weights are presented for 23 samples of glycogens isolated from various biological sources. Ultracentrifugal analysis showed that most of the samples were polydisperse. The molecular weights of the main components lie in the range (3—9) $\times 10^6$. The polydisperse nature of the glycogens has been confirmed by light-scattering measurements. The effects of varying the isolation procedure, and of alkali, on the molecular weight have also been studied.

Glycogen and amylopectin are both highly branched, essentially α-1 : 4-linked glucosans. However, their hydrodynamic properties are completely different. This must be related to fundamental differences in fine structure and molecular shape.[1,2] In this paper, we describe the solution properties and hydrodynamic behaviour of glycogens isolated from a variety of biological sources. Estimations of molecular weight and its distribution have been obtained, and the effects of variations in the method of isolation, and of alkali, on the molecular weight have been studied. A preliminary account of some of this work has already appeared.[3]

Experimental

Sedimentation Measurements.—The methods described in Part XI [4] were employed. M- and 0·1M-sodium chloride and 0·2M-potassium hydroxide were used as solvents.

The sedimentation constant (S_{20}) was virtually independent of the solvent, and the majority of the measurements were carried out in either M- or 0·1M-sodium chloride. Results were corrected to water at 20°.

The apparent amount of each component in a resolvable polydisperse system was estimated by direct measurement of the areas under the refractive-index gradient curves. An enlarged image (3×) of the photographic plates was projected on smooth paper and the upper outline traced. An image of the base line (from a comparative run with solvent alone in the cell) was then superimposed by alignment of the reference lines, and traced on. The refractive-index gradient curves were carefully divided, in the usual manner, on the assumption that each component had a symmetrical distribution, and the appropriate areas between the peaks and the base-line were measured with a planimeter. Values were expressed to the nearest 5%.

Estimations of the polymolecularity of the major component of some of the glycogen samples were obtained by using Gralen's function,[5] dB/dX, where B is an estimate of the "width" of the sedimentation gradient curve and is equal to H/A (A = area of the Schlieren diagram; H = the height of the maximum ordinate), and X = the distance of the peak from the axis of rotation. In all instances, B varied linearly with X. Although this function should be extrapolated to infinite dilution, the value at $c = 1$ g. per 100 ml. was taken as a standard for comparison of the polymolecularity of different samples.

Diffusion Measurements.—The method is outlined in Part X.[6] The solvent was 0·1M-sodium chloride, and values of the diffusion constant (D_{20}) were calculated by the moment method.

Partial Specific Volume.—The partial specific volume ($\bar{V}$) of glycogen was taken as 0·62, the value calculated from density measurements on aqueous solutions of one sample.

Light-scattering Measurements.—The apparatus and the methods used to clarify and dilute the glycogen solutions were similar to those previously described for the *Zea mays* polysaccharides,[6] 0·1M-sodium chloride being the solvent. Although 15% aqueous magnesium chloride has been recommended,[7,8] we found this solvent to have no advantages. The value of the molecular weight of a given sample was the same in both the above solvents. Glycogen

* Part XI, preceding paper.

solutions were clarified by careful filtration (cf. ref. 8) through sintered glass (G4). Repeated filtration caused some small loss in turbidity, whilst little improvement occurred in the apparent dissymmetry. (For example, a sample after one filtration had $M = 8{\cdot}4 \times 10^6$, dissymmetry = 1·41; after five filtrations, $M = 7{\cdot}7 \times 10^6$, dissymmetry = 1·34, the concentration being assumed to be unchanged by filtration.) Solutions were therefore filtered once, before dilution. This procedure gave reproducible results. Hc/τ was independent of c for all samples. The particle scattering factor ($P_{90°}$) was calculated from the dissymmetry, the molecules being assumed to be spherical.[6] The refractive-index increment (dn/dc) for glycogen was found to be 0·146 (c = g./ml.) in 0·1M-sodium chloride at 546 mμ.

Isolation of Glycogens.—Unless otherwise stated, samples of glycogen had been isolated from the tissue by the classical Pflüger method involving digestion with 30% aqueous potassium hydroxide at 100°, followed by precipitation of the glycogen with ethanol and with acetic acid.[9] Commercial samples of glycogen from British Drug Houses Ltd. (I), and Nutritional Biochemicals Corporation, Ohio, U.S.A. (II), were also examined. Methylated horse-muscle glycogen was kindly provided by Dr. D. J. Bell.

Results and Discussion

Sedimentation Coefficients.—Typical sedimentation data are shown in Table 1. It was apparent that for all the glycogens studied in detail, the sedimentation constant (S_{20}) was dependent on the concentration (c), and varied by about 10% for a 1% change in concentration. This is in general agreement with Larner, Ray, and Crandall's results,[10] but, whilst these authors suggested that S_{20} was a function of c^2, our values were best

Table 1. *Typical sedimentation results.*

		$10^{13}S_{20}$ at c (g./100 ml.)							
Glycogen sample	Solvent	1·0	0·75	0·50	0·25	0·16	0·125	0·08	0 (extrapol.)
Ascaris lumbricoides ...	0·1M-NaCl	47	47	47	48	—	—	—	48
Brewer's yeast	0·1M-NaCl	56	—	60	61	—	62	—	64
,, ...	1M-NaCl	54	—	—	—	—	—	—	—
,, ...	0·2M-NaOH	56	58	60	61	62	—	63	64
Commercial, II	0·1M-NaCl	65	67	69	71	—	—	—	73

represented by a linear function. The relations was expressed by $S_{20} = (S_{20})_0(1 - kc)$, where $(S_{20})_0$ is the value of S_{20} at infinite dilution, and c was expressed in g./100 ml. With the exception of the *Ascaris lumbricoides* glycogen (which was relatively concentration-independent; see Table 1), the average value of k was 0·10 ± 0·02. Values of $(S_{20})_0$ for glycogens examined at only one concentration were therefore calculated from this value, and are shown in parentheses in the second and third columns of Table 2.

Molecular Weight and its Distribution.—Table 2 shows the results of the sedimentation measurements for the 23 samples examined. Typical sedimentation diagrams are shown in the Figure. Most samples proved to be polydisperse on ultracentrifugation. Diagrams *a* and *b* (for oyster and *Helix pomatia* glycogen) illustrate the type of Schlieren diagram observed for the most obviously polydisperse samples. This feature is unusual, although Polglase, Brown, and Smith [11] reported similar results for samples of human-liver glycogen. The amounts of main components quoted in the Table are only approximate as no attempt was made to correct for boundary anomaly effects.[12] For many samples, an extremely wide molecular-weight distribution was indicated; the leading sedimentation boundary was extremely asymmetric and reached nearly to the bottom of the cell after a short time of centrifugation. It was difficult to prove whether or not this leading boundary was a second component, and hence no attempt was made to estimate either its amount or its approximate sedimentation constant. Samples which showed this probable fast component are indicated by the symbol S_{20}(F) in the Table. In some other samples, a corresponding asymmetric lower molecular weight distribution was apparent. Again, no analysis of this was attempted and this is indicated by the symbol S_{20}(S) in Table 2.

Diffusion measurements showed that for methylated horse muscle the diffusion coefficient (D_m) = $1{\cdot}0 \times 10^{-7}$; for brewer's yeast glycogen, $D_m = 1{\cdot}1 \times 10^{-7}$; for com-

mercial glycogen I, $D_m = 2{\cdot}0 \times 10^{-7}$; and for commercial glycogen II, $D_m = 1{\cdot}1 \times 10^{-7}$ The molecular weights shown in Table 2 for the main components in the other samples are calculated by assuming a value of $1{\cdot}1 \times 10^{-7}$ for D_m in agreement with other workers.[2] All the molecular weights are in the range (3—9) $\times 10^6$, and, together with the values of the frictional ratio (f/f_0), are of the same order as those previously reported from sedimentation and diffusion measurements.[2,13] It should be noted, however, that the values for

Typical sedimentation diagrams. For all samples, c = 1 g./100 ml.; solvent, 1·0M-sodium chloride; speed = 20,000 r.p.m. Movement of the peaks is from right to left. The figures in parentheses after the times indicate the angle of the Schlieren bar.

Oyster glycogen: 8 (55°), 15 (45°), 18 (35°), 30 (30°), *and* 47 (25°) *min. after reaching full speed.*

Helix pomatia *glycogen*: 6 (65°), 14 (45°), 25 (45°) 37 (45°), *and* 50 (35°) *min. after reaching full speed.*

Brewer's yeast glycogen: 9 (65°), 17 (50°), 26 (45°), 37 (40°), *and* 52 (40°) *min. after reaching full speed.*

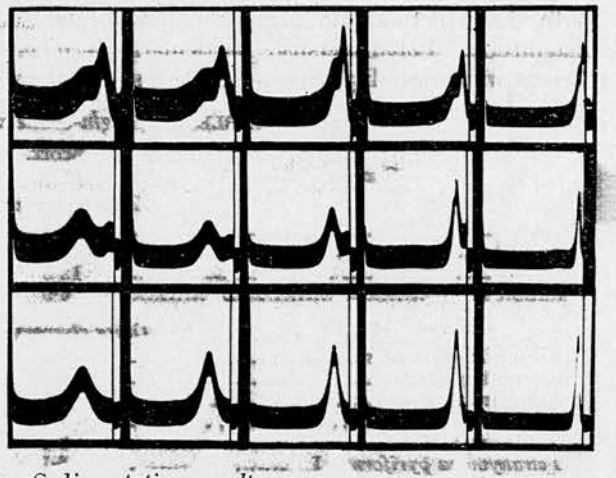

TABLE 2. *Sedimentation results.*

Glycogen sample	$10^{13}S_{20}$ of components [a] major	minor	Major component (%)	dB/dx [b]	$10^{-6}M$ [c]	f/f_0 [d]
	(a) *Mammalian livers*					
Cat I	75	F, S	—	0·8	4·4	—
,, IV	84	F, S	—	—	4·9	—
,, VI	(102)	F, S	—	1·0	5·9	—
Human (glycogen-storage disease)	(53)	(220)	70	1·8	3·1	—
Fœtal sheep	110	F	—	1·1	6·4	—
Fœtal pig	(49)	(11)	70	0·8	2·9	—
Rabbit II	94	—	95+	—	5·5	1·7
,, (fructose-infused *)	(80)	F	—	1·1	4·7	—
,, (galactose-infused *)	(153)	S	—	—	9·0	—
,, (normal *)	(145)	F	—	1·8	8·4	—
	(b) *Mammalian muscles*					
Horse (methylated)	23	—	95+	—	2·8	1·4
Human	(85)	(20)	85	0·8	4·9	—
Rabbit I	79	—	95+	0·7	4·6	1·9
	(c) *Other glycogens*					
Ascaris lumbricoides	48	F	—	—	2·8	—
Brewer's yeast	64	—	95+	—	3·7	2·0
Commercial, I	24	—	95+	—	0·7	1·9
,, II	73	—	95+	—	4·0	1·7
Helix pomatia II	(63)	(300, 7)	80	0·9	3·6	—
Mytilus edulis I	(93)	F	—	0·9	5·4	—
Oyster *	(45)	(90, F)	—	—	2·6	—
Tetrahymena pyriformis I	(69)	S	—	—	4·0	—
Trichomonas foetus I	(70)	S	—	—	4·0	—
Trichomonas gallinae I	(84)	S	—	—	4·9	—

[a] For values in parentheses and meaning of F and S, see text. [b] Value for main component at *c* (total) = 1·00 g./100 ml. [c] Molecular weight calculated from $M = \boldsymbol{R}T(S_{20})_0/(1 - \bar{V}\rho)D_m$. [d] Frictional ratio calculated from $f/f_0 = 10^{-8}[(1 - \bar{V}\rho)/D_m{}^2(S_{20})_0\bar{V}]^{1/3}$.

* Samples kindly supplied by Dr. M. Schlamowitz.

rabbit liver and muscle are considerably lower than those recently reported by Stetten, Katzen, and Stetten [8] (see below).

The values of (dB/dx) confirm qualitatively the extremely polymolecular nature of glycogen (cf. ref. 5) in agreement with the distributions evaluated by Larner and his co-workers.[10] Further, in agreement with these authors, mammalian-muscle glycogens appear to be less polymolecular than liver glycogens.

The polydisperse nature of most of the samples studied was confirmed by turbidimetric measurements. Although the molecular weight from these measurements is a true weight-average whilst that from sedimentation and diffusion is less well-defined,[14] the results from both these methods on a given polymolecular sample should be of the same order of magnitude. Polydispersity, particularly if it involves components of high molecular weight will cause disparities. Table 3 shows the results of light-scattering measurements

TABLE 3. *Light-scattering results.*

Sample	Uncorr. 10^{-6}M	Dissymmetry	$1/P_{90°}$	Corr. 10^{-6}M
Liver glycogens				
Cat I	10·5	1·48	1·30	13·6
,, IV	8·8	1·85	1·52	13·4
,, VI	12·8	1·67	1·40	17·9
Rabbit II *	6·9	1·20	1·13	7·8
Other glycogens				
Ascaris lumbricoides	7·1	1·40	1·26	8·9
Brewer's yeast *	4·0	1·15	1·10	4·4
Commercial, I	1·7	1·19	1·12	1·9
,, II *	4·9	1·15	1·10	5·4
Rabbit muscle I *	3·7	1·17	1·11	4·1
Tetrahymena pyriformis I	6·1	2·50	1·85	11·3

* Samples exhibiting no polydispersity.

on the ten samples which appeared to be the least obviously polydisperse on ultracentrifugation. For four of these, the agreement is reasonably good, indicating that they were only polymolecular, whilst the presence of S_{20}(F) in the other samples is convincingly illustrated by the higher turbidimetric molecular weight. It is therefore suggested that a given glycogen sample should be examined by both the sedimentation and the light-scattering method in order to prove unambiguously whether or not it is polydisperse. Without further investigations, it is not possible to decide whether polydispersity occurs in native glycogen in the tissue or is an artefact resulting from degradation during isolation. Polglase and his co-workers [11] consider that such variations occur naturally.

Effect of Isolation Procedure on Molecular Weight.—The classical Pflüger method involving digestion of tissue with 30% potassium hydroxide has often been criticised [15] on the assumption that alkaline degradation occurs. Table 4 shows the results for the determination of S_{20} for glycogen samples isolated from the halves of two rabbit livers severally with boiling water and 30% aqueous potassium hydroxide. Within experimental error, S_{20} is the same for all samples. It is concluded that, in the presence of air, the extent of degradation of glycogen by 30% potassium hydroxide solution at 100° is no greater than that which might be caused by boiling water. Similar results have been obtained by Staudinger,[16] and Bridgman [17] reported that glycogen extracted with cold trichloroacetic acid and hot alkali from two halves of a rabbit liver had a similar molecular weight. However, recent light-scattering work by Stetten, Katzen, and Stetten [8] has shown that if extraction with trichloroacetic acid is for a limited time at 0° the glycogen from rabbit liver has an average molecular weight of $(11—80) \times 10^6$ rather than the $(2—6) \times 10^6$ as in hot potassium hydroxide extractions. This suggests that it is difficult to avoid degradation during extraction, and that the molecular weights reported here and previously [2] may not be representative of " native " glycogen.

Effect of Dilute Alkali and Acetic Acid.—In contrast to the behaviour of hot 30% alkali,

hot *dilute* alkali appears to degrade glycogen rapidly. Digestion of rabbit-liver glycogen in 8% aqueous sodium hydroxide at 100° for 1·5 hr. reduced S_{20} from 86 to 57 $\times$ 10^{-13} c.g.s. units (see Table 4), and increased the polymolecularity (as shown by a broadening of the peak of the Schlieren pattern).

It has been suggested [18] that purification of glycogen by precipitation with glacial acetic acid may render it unsuitable for ultracentrifugal analysis. However, when rabbit-liver and brewer's yeast glycogens were reprecipitated with 80% acetic acid there was no change in the value of S_{20} (see Table 4). Precipitation of glycogen by acetic acid does not, therefore, alter the hydrodynamic properties or cause degradation of glucosidic linkages to any appreciable extent.

TABLE 4. *Effect of isolation procedure on the sedimentation constant.*

Sample	Method of isolation	$10^{13}S_{20}$ at c = 1 g./100 ml.
Rabbit liver XII	Hot water	85
	30% KOH at 100°	86
Rabbit liver XIII	Hot water	76
	30% KOH	83
	30% KOH + repptn. with AcOH	83
Rabbit liver IV	30% KOH	86
	30% KOH + 8% NaOH at 100° for 1½ hr.	57
Brewer's yeast	30% KOH	64
	30% KOH + repptn. with AcOH	63

The authors thank Professor E. L. Hirst, F.R.S., for his interest in this work, and the Rockefeller Foundation for financial support, also the D.S.I.R. for a maintenance grant (to W. A. J. B.).

DEPARTMENT OF CHEMISTRY,
THE UNIVERSITY, EDINBURGH, 9. [*Received, August 12th*, 1957.]

[1] Part IV, Bryce, Cowie, and Greenwood, *J. Polymer Sci.*, 1957, **25**, 251.
[2] Greenwood, *Adv. Carbohydrate Chem.*, 1956, **11**, 335; Manners, *ibid.*, 1957, **12**, 261.
[3] Greenwood and Manners, *Proc. Chem. Soc.*, 1957, 26.
[4] Preceding paper.
[5] Gralén, Inaugural Diss., Uppsala, 1944.
[6] Part X, Greenwood and Das Gupta, *J.*, 1958,
[7] Putzeys and Verhoeven, *Rec. Trav. chim.*, 1949, **68**, 817.
[8] Stetten, Katzen, and Stetten, *J. Biol. Chem.*, 1956, **222**, 587.
[9] Bell and Manners, *J.*, 1952, 3641; Manners and Archibald, *J.*, 1957, 2205.
[10] Larner, Ray, and Crandall, *J. Amer. Chem. Soc.*, 1956, **78**, 5890.
[11] Polglase, Brown, and Smith, *J. Biol. Chem.*, 1953, **199**, 105.
[12] See, *e.g.*, Trautman, Schumaker, Harrington, and Schachman, *J. Chem. Phys.*, 1954, **22**, 555.
[13] Cori, *Makromol. Chem.*, 1956, **20**, 169.
[14] See, *e.g.*, Kinell and Rånby in " Advances in Colloid Science," Vol. III, Interscience, Publ. Inc., New York, 1950.
[15] *E.g.*, Meyer and Jeanloz, *Helv. Chim. Acta*, 1943, **26**, 1784.
[16] Staudinger, *Makromol. Chem.*, 1948, **2**, 88.
[17] Bridgman, *J. Amer. Chem. Soc.*, 1942, **64**, 2349.
[18] Illingworth, Larner, and Cori, *J. Biol. Chem.*, 1952, **199**, 105.

PRINTED IN GREAT BRITAIN BY RICHARD CLAY AND COMPANY, LTD.,
BUNGAY, SUFFOLK.